

Copyright  
by  
Rachel E. Aisner  
2010

**The Thesis Committee for Rachel E. Aisner  
Certifies that this is the approved version of the following thesis:**

**Patch-reef and ramp interior facies architecture of the Early Albian  
Mural Limestone, Southeastern Arizona**

**APPROVED BY  
SUPERVISING COMMITTEE:**

---

Charles Kerans

---

Robert Loucks

---

Ronald Steel

**Patch-reef and ramp interior facies architecture of the Early Albian  
Mural Limestone, Southeastern Arizona**

**by**

**Rachel E. Aisner, B.A.**

**Thesis**

Presented to the Faculty of the Graduate School of

The University of Texas at Austin

in Partial Fulfillment

of the Requirements

for the Degree of

**Master of Science in Geological Sciences**

**The University of Texas at Austin**

**December 2010**

## **Acknowledgements**

Throughout my academic career at the University of Texas at Austin, many people have contributed to the successful completion of my Masters degree. I am very grateful for the economic and academic support I received through the Jackson School of Geosciences (JSG), Reservoir Characterization Research Laboratory (RCRL), and the American Association of Petroleum Geologists (AAPG). Financial support through these groups in research assistantships, fellowships, and grants has been fundamental for my research. Through coursework, field trips, integrated research, meetings, and technical resources provided by these groups I have had the opportunity to enhance my geologic skills. Thanks to JSG students Selin, Sean, Nabil, Moodie, Travis, Daniel, Safiya, and Jose for their assistance in the field. Special thanks to Philip Guerrero for his gentle reminders to turn in all of my forms.

I would like to express my utmost gratitude to my advisor, Charlie Kerans, whose tutoring and receptiveness to new ideas have allowed me to develop a strong knowledge base of the carbonate systems that I am truly passionate about and to study a fascinating and unique area for my graduate research. It has been an honor to work with him. Thanks to my committee members Bob Loucks and Ron Steel who have provided their insights and guidance despite their busy schedules.

Several people at the BEG and RCRL have contributed to the completion of my thesis project both in the field and in the office. Thanks to my field assistants Charlie Harman, Molly Kent, and Cari Sadler - I couldn't have tackled Grassy Hill without them! Thanks to James Donnelly, Kenneth Edwards, Nathan Ivicic, and Josh Lambert at the CRC for their assistance with processing field data. Additional thanks to Joseph El-Azzi, Chuck Garza, Ruben Reyes, and Joseph Yeh for their technical support and assistance

with lidar-related troubleshooting. I would also like to acknowledge the distinguished RCRL research scientists, students, and sponsors who have contributed to this project through discussions and guidance: Dave Hunt, Xavier Janson, Patrick Lehman, Jerry Lucia, Ryan Phelps, Chris Zahm, and Laura Zahm. Additional thanks to Sammy Jacobo for making sure I turned in my paperwork properly.

I cannot write these acknowledgements without mentioning the geological community back home. It is there where my interest in geology and carbonates developed through work, classes, workshops, and other activities with the West Texas Geological Society, Permian Basin Section SEPM, Southwest Section AAPG, and UTPB. I would like to thank David Crass, Tim Dunn, and Tommy Lent at CrownQuest Operating for giving me the opportunity to explore my geologic interests at work. Lyn Canter, Dave Entzminger, Debra Rutan, Emily Stoudt, Mark Sonnenfeld and Ron Young saw potential in me and have been a continuous source of encouragement during this journey.

Last and certainly not least, I would like to thank my friends and family for moral support and discussions. Thanks to Jess, Cari, Jennifer and Stefan for being there. Many thanks to my mom who has always told me I can do whatever I set my mind to.

December 3, 2010

## **Abstract**

### **Patch-reef and ramp interior facies architecture of the Early Albian Mural Limestone, Southeastern Arizona**

Rachel E. Aisner, M.S.Geo.Sci.

The University of Texas at Austin, 2010

Supervisor: Charles Kerans

The Mural Limestone, located in the Mule Mountains to the northeast and southeast of Bisbee, Arizona provides an exceptional outcrop analog for time-equivalent productive reservoirs in the Albian Glen Rose patch-reef play of the Maverick Basin. The Mural Limestone is exposed in a number of folds and east-dipping fault blocks in the Grassy Hill and Paul Spur localities in the Mule Mountains and represents a remnant of a south-facing distally-steepened carbonate ramp that prograded into the Chihuahuan Trough in Albian time. This study documents the detailed facies architecture and sequence stratigraphic setting of a multicyclic patch-reef and its associated ramp interior facies at the Paul Spur and Grassy Hill localities, respectively.

Small mud-dominated coral-algal buildups (~5 m thick) and tabular biostromes (up to 1.5 m thick) consisting of rudist floatstones are common in the bedded ramp interior carbonates at the Grassy Hill locality in the Mule Mountains 10 km landward of the Paul Spur reef. Buildups in this area are flanked by weakly-cyclic and well-bedded skeletal mud- and grain-dominated packstones. At the Paul Spur locality, Mural facies consist of a 10-35 m thick patch-reef with four distinct reef communities: microbial-*Microsolena* framestone, algal-*Actinastrea* boundstone, branching coral-skeletal framestone and caprinid-requienid floatstone. Measured reef dimensions show a distinct windward-leeward margin with reef frame facies extending ~70 m from the margin and extensive leeward rudstone debris and grainstone shoal facies extending a distance of 870 m. Reef and backreef shoal facies exhibit low preserved porosity but petrographic analysis of backreef grainstones shows that primary porosity and permeability was present. These extensive reservoir-prone shoals may be a suitable reservoir target similar to flank rudstones and grainstones of the Maverick Basin reefs.

Three aggradational to retrogradational cycles of reef growth are evident at the Paul Spur locality. Retrogradational stacking is consistent with that of time-equivalent Lower Glen Rose patch-reefs in the Maverick Basin of Texas, which suggests a eustatic driver for stratigraphic architecture along the Bisbee/Comanche shelf. Backstepping of reef frame facies in Cycle 3 is interpreted to be time-equivalent to patch-reef development at the Grassy Hill locality.

## Table of Contents

List of Tables .....	ix
List of Figures .....	x
1. Introduction.....	1
Maverick Basin patch-reefs .....	1
Geologic setting .....	3
Previous work .....	6
2. Data and Methods .....	11
3. Depositional setting of ramp interior .....	13
Facies .....	13
Depositional model .....	34
Cyclicality.....	42
4. Characterization of Paul Spur Reef.....	44
Facies .....	44
Outcrop reconstruction and facies dimensions from ground-based lidar .....	70
Depositional model .....	79
Stratigraphic succession and depositional history .....	85
Stratigraphic framework .....	91
5. Discussion.....	94
Stratigraphic setting .....	94
Stratigraphic drivers.....	94
Implications for reservoir characterization .....	96
6. Conclusions.....	97
Appendix A: Measured section data .....	100
References.....	154
Vita.....	161

## **List of Tables**

Table 1. Grassy Hill ramp interior facies.....	15
Table 2. Paul Spur patch-reef facies .....	45
Table 3. Paul Spur facies thicknesses .....	76
Table 4. Lateral extents of Paul Spur facies. ....	77

## List of Figures

Figure 1. Location of study area .....	4
Figure 2. Tectonic and paleogeographic setting of the Mural Limestone. ....	5
Figure 3. Stratigraphic framework of the Mural Limestone. ....	8
Figure 4. Previous depositional model of the Paul Spur patch-reef .....	10
Figure 5. Measured section locations.....	12
Figure 6. Grassy Hill facies 1: Mollusk siliciclastic sandstone .....	16
Figure 7. Grassy Hill facies 3 and 4: Arenaceous skeletal-algal MDP/Miliolid- peloid WS.....	19
Figure 8. Grassy Hill facies 5: Bedded peloid-foraminifer-mollusk-skeletal MDP/GDP .....	21
Figure 9. Burrow styles in bedded MDP/GDP .....	22
Figure 10. Grassy Hill facies 6: <i>Orbitolina</i> -mollusk-peloid GS.....	24
Figure 11. Grassy Hill facies 7: Chondrodont FLT .....	26
Figure 12. Grassy Hill facies 8: Rudist FLT.....	28
Figure 13. Rudist associations .....	29
Figure 14. Grassy Hill facies 10: Branching coral-skeletal FMST.....	30
Figure 15. Grassy Hill facies 11 and 12: Rudist-coral RS/Echinoid- <i>Orbitolina</i> - mollusk WS.....	33
Figure 16. Depositional model of ramp interior .....	36
Figure 17. Vertical facies associations: restricted marine .....	37
Figure 18. Vertical facies associations: bedded shallow subtidal.....	39
Figure 19. Vertical facies associations: rudist buildups and coral patch-reefs .....	40
Figure 20. Stratal geometry of bedded ramp interior at Section GHAS.....	41

Figure 21. Grassy Hill ramp interior facies architecture.....	43
Figure 22. Paul Spur patch-reef facies architecture.....	46
Figure 23. Paul Spur facies 1 and 2: Echinoid- <i>Orbitolina</i> -mollusk WS/ <i>Orbitolina</i> -skeletal RS .....	49
Figure 24. Outcrop facies mapping Sections A-F.....	51
Figure 25. Paul Spur facies 3: Microbial- <i>Microsolena</i> FMST .....	52
Figure 26. Paul Spur facies 4: Algal- <i>Actinastrea</i> BNDST .....	54
Figure 27. Syndepositional fractures .....	55
Figure 28. Paul Spur facies 5: Bored Algal- <i>Actinastrea</i> FLT .....	57
Figure 29. Paul Spur facies 6: Rudist coral RS.....	58
Figure 30. Outcrop facies mapping Sections G-J .....	59
Figure 31. Paul Spur facies 7: Echinoid-mollusk-peloidal GDP .....	61
Figure 32. Paul Spur facies 8: Branching coral-skeletal FMST .....	62
Figure 33. Outcrop facies mapping Sections K-L .....	63
Figure 34. Outcrop facies mapping Sections M-Q.....	64
Figure 35. Paul Spur facies 9: Caprinid-requienid FLT .....	66
Figure 36. Paul Spur facies 10: Caprinid-requienid RS.....	67
Figure 37. Paul Spur facies 11: <i>Orbitolina</i> -skeletal GS .....	69
Figure 38. Orthoimagery map with lidar data coverage and structural elements removed in reconstruction.....	71
Figure 39. Structural reconstruction steps .....	73
Figure 40. 2D facies and structural reconstruction results.....	74
Figure 41. Depositional model of the Paul Spur patch-reef.....	80
Figure 42. Windward margin facies and forereef debris facies .....	81
Figure 43. Vertical succession of windward margin facies .....	82

Figure 44. Backreef debris beds.....	84
Figure 45. Depositional processes and modern analog.....	85
Figure 46. Stratigraphic architecture of Paul Spur locality.....	86
Figure 47. Indicator facies, Cycles 1 and 2.....	90
Figure 48. Indicator facies, Cycles 2 and 3.....	91
Figure 49. Local and regional stratigraphic framework.....	93

## **1. Introduction**

Cretaceous carbonate shelf systems, including patch-reef complexes, host some of the world's most prolific and complex oil and gas reservoirs (Burchette and Wright, 1992; Cook, 1979; Scott, 2004). Carbonate reservoirs are difficult to characterize in the subsurface, as wireline-log and seismic data commonly lack the resolution necessary to delineate facies-controlled systems and predict their spatial extents. Outcrop studies, where a clear link between facies geometry and stratigraphic context can be established, provide much of our understanding. Such studies have been conducted in uppermost Albian reef and grainstone complexes in areas of central and south Texas (Lozo et al., 1949; Kerans, 2002; Kerans et al., 2008), but little is known of the lower Albian interval that is time equivalent to productive patch-reef complexes in the Maverick Basin and circum-Gulf of Mexico regions. This outcrop-based study documents the detailed facies architecture and stratigraphic setting of a time-equivalent reef and its associated shelf facies in southeastern Arizona that may provide new insights into the facies distribution and reservoir quality of patch-reef reservoirs such as those in the Maverick Basin.

### **MAVERICK BASIN PATCH-REEFS**

The Maverick Basin patch-reefs have been studied by numerous authors (Scott, 2004; Scott et al., 2007; Aconcha, 2008). The most recent study was conducted by Aconcha (2008) in which he used an integrated subsurface dataset (3D seismic, well logs and core) to characterize a subset of Maverick Basin patch-reefs in a 15x15 km (~9x9 mi) area within the Chittim Gas Field in Maverick County, Texas. The reef complex is

comprised of four producing units that are contained within the highstand (HST) and transgressive (TST) systems tracts of 3rd-order sequences 6-8 of Loucks and Kerans (2003), with the most productive units exhibiting a retrogradational stacking pattern in sequence 7 (Aconcha, 2008). Loucks and Kerans (2003) and Aconcha (2008) developed a schematic depositional model of individual patch-reefs from data from two cores and identified gas-bearing units from neutron-density crossover. The best porosity development lies within capping lime rudstone shoal facies where original porosity may have been as high as 45% (Loucks and Kerans, 2003). Within the study area, 26 wells produced gas with each well draining one patch-reef. During the first stages of field development one out of thirteen wells in the study area was completed, but with the advent of seismic technology the success-failure ratio improved to one out of three (Aconcha, 2008). Overall, individual reefs showed an initial potential of 15 to 2800 million cubic feet per day (MCFD) with cumulative production ranging from 0.2 to 6 billion cubic feet (BCF) since 1970 (Aconcha, 2008). Over half of the completed wells have produced less than 1.0 BCF. The largest Glen Rose reef in the Maverick Basin has produced over 30 BCF (Scott, 2004).

The Chittim gas field is one example of a variably-productive carbonate field that demonstrates the limits of subsurface data interpretation. Production trends cannot be easily predicted with even clear high-resolution seismic data and wireline-logs, as smaller-scale factors such as facies heterogeneity are a likely reason for poor productivity. It is therefore important to investigate time-equivalent outcrop analogs in detail, especially for individual one-well reservoirs, in order to understand and predict

facies heterogeneity, reservoir quality, and ultimately well placement within the reservoirs.

## **GEOLOGIC SETTING**

The Mural Limestone is exposed in a number of folds and east-dipping fault blocks in the Mule Mountains at the Grassy Hill and Paul Spur localities of southeastern Arizona, to the northeast and southeast of Bisbee in southeastern Arizona (Figure 1). The Mural Limestone is underlain by siliciclastics of the Morita Formation (Aptian) and overlain by marginal marine to fluvial siliciclastics of the Cintura Formation (Albian). These three formations, combined with the basal Glance Conglomerate (Aptian), comprise the Bisbee Group (Scott, 1987) (Figure 2A).

The Mural Limestone represents a shelfal remnant of a south-facing carbonate distally-steepened ramp that prograded into the Chihuahua Trough in Early Albian time; exposures of coalesced patch-reefs representing a well-defined shelf margin are located in Sonora, Mexico (Warzeski, 1983). The Chihuahua Trough formed as a result of extensional tectonics associated with rifting of the early Gulf of Mexico during the Late Jurassic (Bilodeau, 1982, Figure 2B). A combination of thermal subsidence associated with deposition of Mural carbonates in the study area. During this time, intrashelf basins on the Comanche Shelf in south Texas, including the Maverick Basin, formed as a result of differential subsidence (see Figure 2A). Mural carbonates were subsequently buried by marginal marine to fluvial siliciclastics of the Cintura Formation during Middle and Late Albian time. During the Late Cretaceous, the Mural Limestone was uplifted by extensive folding and thrust faulting associated with Laramide compressional tectonics (Hayes,

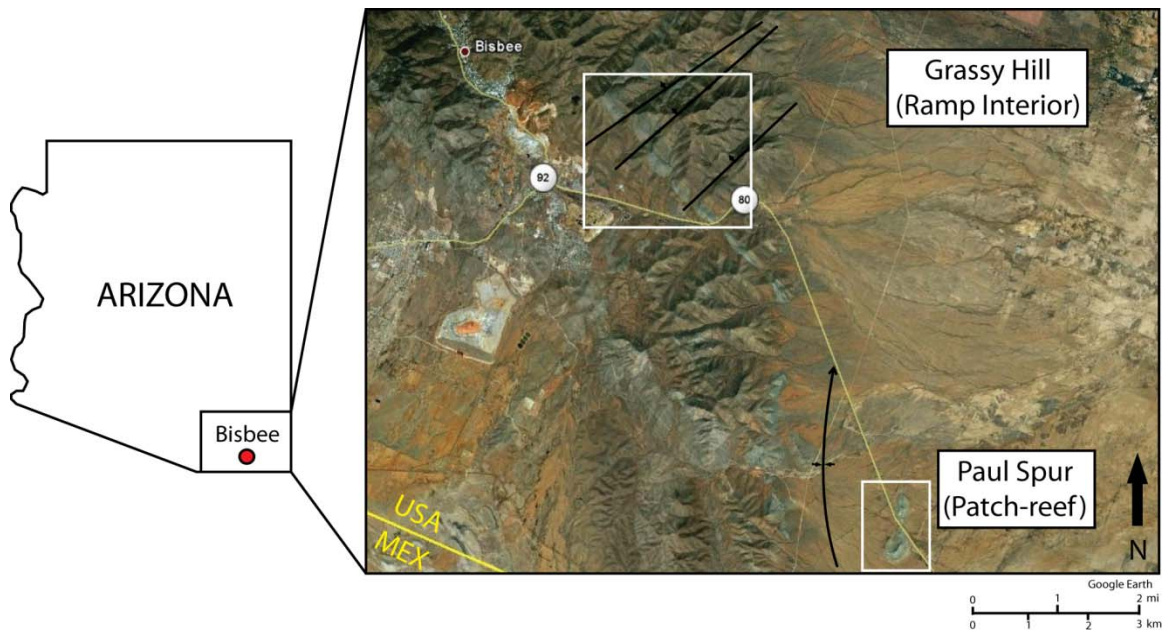


**Figure 1.** Location of study area showing the present-day structure of the Mule Mountains near Bisbee, AZ. The Mural Limestone is exposed in east-dipping normal faults at the Grassy Hill locality and in north to south plunging folds at the Paul Spur locality. Individual studies conducted in the Mural Limestone (gray) are highlighted in white. The Grassy Hill study was conducted in a linear transect 5 km long, and the Paul Spur study was conducted in a linear transect 1.7 km long.

1970); the Paul Spur patch-reef is exposed in one of the northwest to southeast-trending synclinal folds of Laramide origin (See Figure 1).

Three major lithostratigraphic components of Mural Limestone are exposed in the study area: (1) The Lower Mural (100-132 m thick), consisting of intercalated carbonates, siltstones, sandstones and shales, (2) a middle massive buildup-bearing subdivision of the Upper Mural (~27 m thick), and (3) and overlying medium to thick-bedded division of the Upper Mural (30-40 m thick) composed of carbonates and sandstones (Hayes, 1970; Warzeski, 1987). The middle massive and bedded carbonates contain abundant coral-algal patch-reefs and rudist buildups, which are the focus of this study. This middle unit is exposed in a NW-SE linear trend of approximately 13 km from NNW to SSE with

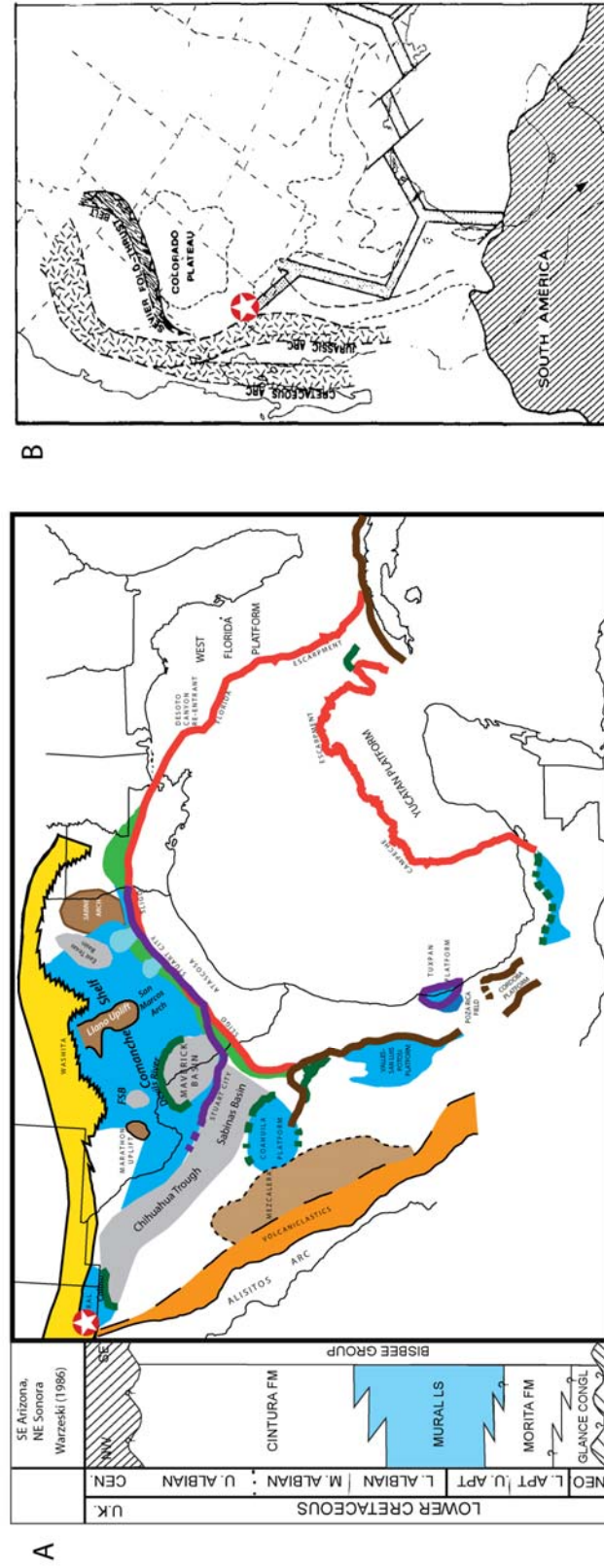


**Figure 2.** A) General stratigraphy and paleogeography of southern North America during Early Albian time (Modified from Winker and Buffler (1988), Goldhammer and Johnson (2000), McFarlan and Menes (1991)) showing the tectonically quiescent time when the Mural Limestone ramp interior and patch-reef facies were deposited. During the same period, Lower Glen Rose patch-reefs developed in the intrashelf sag basins on the Comanche Shelf to the east. B) Mesozoic tectonic setting during Late Jurassic to Early Cretaceous time (adapted from Bilodeau, 1982) showing the formation of the Chihuahua Trough by extensional rifling of the Gulf of Mexico.

patch-reefs up to 30 m thick in the southernmost extents (Scott, 1979). The present-day arid climate, minimal vegetation cover, and relatively simple post-depositional tectonics make this area well-suited for detailed outcrop study.

## **PREVIOUS WORK**

Stoyanow (1949) was the first to place the Mural Limestone in the lower Cretaceous system based on ammonite assemblages. Warzeski (1983) assembled a stratigraphic chart of the Mural Limestone in southeastern Arizona and northeastern Sonora and correlated it to adjacent systems based on the field studies of Stoyanow (1949), Hayes (1970), Scott (1979), Rose (1972), and others (Figure 3A). Correlation was based on the biostratigraphic assemblages of ammonites and pelagic microfossils (Warzeski, 1987). Warzeski (1987) suggested that the Mural Limestone represents one large-scale (possibly 2nd order) transgressive-regressive supersequence bounded above and below by time-transgressive surfaces, and that the transgressive patch-reef-bearing lower section of the Upper Mural Member is time-equivalent to the Lower Glen Rose Formation in south Texas. The upper section of the upper Mural carbonate cycles are equivalent to upper Glen Rose, and represent the regressive phase of Mural deposition (Warzeski, 1987). Scott (1987) suggested that the lower Mural member is time-equivalent to south Texas transgressive deposits of the Pine Island Shale (Pearsall Formation) based on ammonite and benthic and planktonic foram assemblages. In that study, Scott also suggested that the upper Mural Limestone includes the Aptian-Albian boundary.

The most recent stratigraphic studies of the Mural Limestone are by Lawton et al. (2003) and Gonzalez-Leon et al. (2007). Lawton et al. (2003) studied the Mural Limestone in northeastern Sonora, Mexico, and characterized the control of eustasy, sediment supply, and tectonics on bank evolution. They proposed that global eustatic sea-level fluctuations were the main control on Mural sedimentation and stratigraphic geometries in that study area. Gonzalez-Leon et al. (2007) described geochronologic -  $^{206}\text{Pb}/^{238}\text{U}$  data, biostratigraphy, and cyclicity of locally defined members of the Mural Limestone in central Sonora, and correlated these members to biozones in central Texas (see Figure 3A). They concluded that the Mural Limestone is composed of three third-order transgressive-regressive cycles with lowstand, transgressive, and highstand systems tracts, and that these cycles correlate to the Hammett/Cow Creek, Hensel, and Glen Rose 2 depositional cycles defined by Scott et al., (2007) in central Texas. No effort has been made to extend these correlations into southeastern Arizona.

Scott and Warzeski (1993) divided the Mural Limestone in Arizona and Sonora, Mexico into two depositional sequences. In Sonora, the first sequence is composed of transgressive Lower Mural carbonates and shales and an aggradational-progradational lower section of the Upper Mural Limestone buildup-bearing shelf carbonates; the second sequence is composed of a regressive upper section of Upper Mural Limestone shelf carbonates and Cintura Formation sandstones. Important bounding surfaces, sequence boundaries and maximum flooding surfaces were defined based on depositional facies and biostratigraphy within five marker ledges (Scott and Warzeski, 1993). Time lines



Key depositional facies of Aptian-Albian patch-reefs have been identified in the Mural Limestone in Arizona (Scott, 1979), Sonora, Mexico (Warzeski, 1983), and in the Maverick Basin of Texas (Loucks and Kerans, 2003; Aconcha, 2008). Scott (1979) characterized biotic constituents, key facies, ecology, and the depositional environments of patch-reefs in both the Mule Mountains and Paul Spur. He determined that the reefs are coral-algal dominated and proposed an alternative depositional model to those of rudist-dominated reefs that are prevalent in the Early Cretaceous (e.g. Perkins, 1974) (Figure 4). Scott was the first to provide a detailed carbonate facies interpretation in southeastern Arizona for carbonate reservoir analog research and facies prediction.

Scott (1979) proposed five depositional environments in upper Mural patch-reefs with mappable facies and microfacies. The facies and depositional environments are as follows: coral-stromatolite-rudist boundstone (reef core), rudist-coral fragment packstone (reef flank), peloid-oid grainstone (shoal), mollusk-miliolid-*Orbitolina* wackestone (open lagoon), and ostracod-mollusk-skeletal-algal wackestone (restricted lagoon). Warzeski (1983) identified similar facies in his dissertation study in northeastern Sonora, Mexico. Loucks and Kerans (2003) and Aconcha (2008) identified similar reef core and flank facies in the Maverick Basin, Texas.

Coral-algal reef buildups formed during the Early Albian transgression in Arizona. Scott (1979) interpreted high- and low-energy components of patch-reef cores, with well-developed rudist complexes on the lee sides (low-energy) of the reefs. Overall, these reefs were interpreted as developing in a more open-marine setting than those of the mid-shelf patch-reefs of the Glen Rose in central Texas because of a more diverse

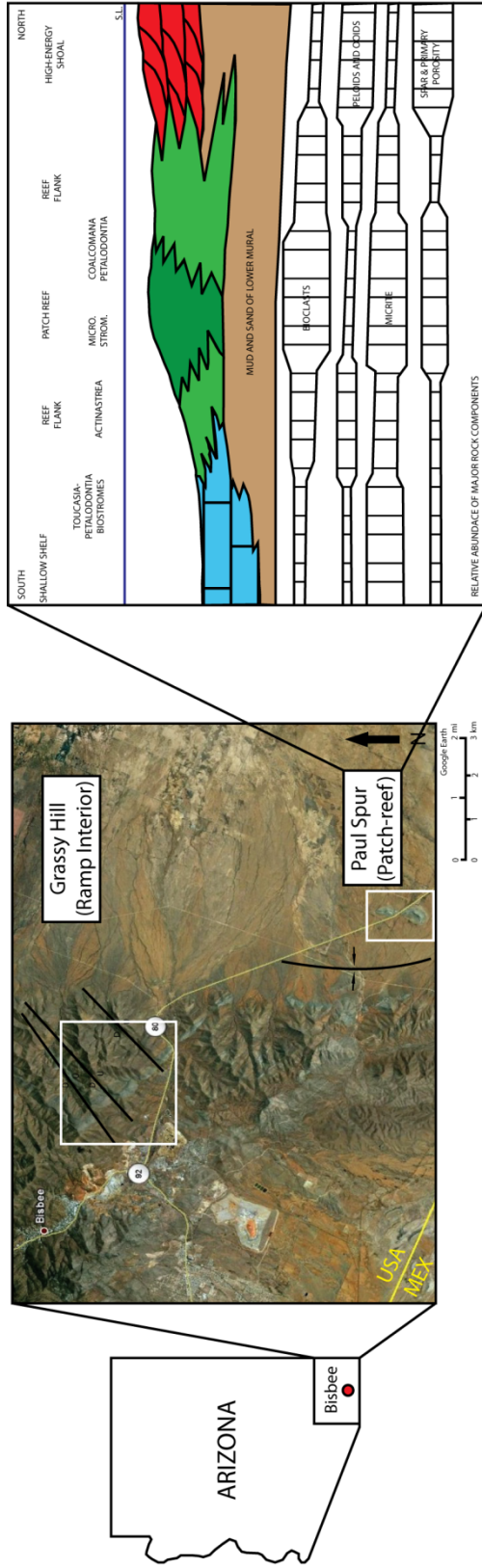


**Figure 4.** Depositional model of the Paul Spur patch-reef from Scott (1979) showing four basic facies associations: Lower Mural Limestone, patch-reef, reef flank, high energy shoal, and shallow shelf. Distribution of major rock components are illustrated in the diagram below the depositional model. This depositional model differs from that of the abundant high-energy rudist-dominated reefs in the Cretaceous (Loucks and Kerans, 2003) and is analogous in facies composition to the coral-algal gas producing patch-reefs in the Maverick Basin.

assemblage of open marine fauna (corals) and general lack of grainy infill.

Scott (1979) interpreted reef flank skeletal packstones as somewhat high-energy with the presence of abraded grains. Wackestone facies were interpreted as open lagoon, low-energy environment (benthic foraminifera, miliolids, caprinids, toucasids), and low-energy, restricted environment (ostracods, nerinid gastropods). Scott (1979) observed interbedding of wackestone and sandstone facies to the north and implied a record of salinity and temperature fluctuations in this nearshore environment, possibly due to minor sea-level fluctuations.

Peloid-oid grainstone facies are restricted to the southwest section of the Mule Mountains. This facies has been interpreted as both an ooid shoal complex discrete from patch-reef systems (Warzeski, 1987), and as a backreef sand apron (Scott, 1979). Its relation to patch-reefs is obscured due to faulting, but is thought to be laterally equivalent (Scott, 1979). Scott published one photomicrograph of this facies that showed predominantly peloidal and skeletal grains, none of which are shown to have extensive carbonate coating. The geometry of the grainstone bodies is discussed further in Section 4 of this study.

## **2. Data and Methods**

This field-based study employed a combination of standard field techniques and use of digital outcrop characterization using ground-based light detection and ranging (lidar). Six section locations at Grassy Hill were selected from orthoimagery from GoogleEarth® and photomosaics within a 5 km transect (Figure 5A). Section locations were not chosen in outcrops GHB and GHC because of their proximity to mining

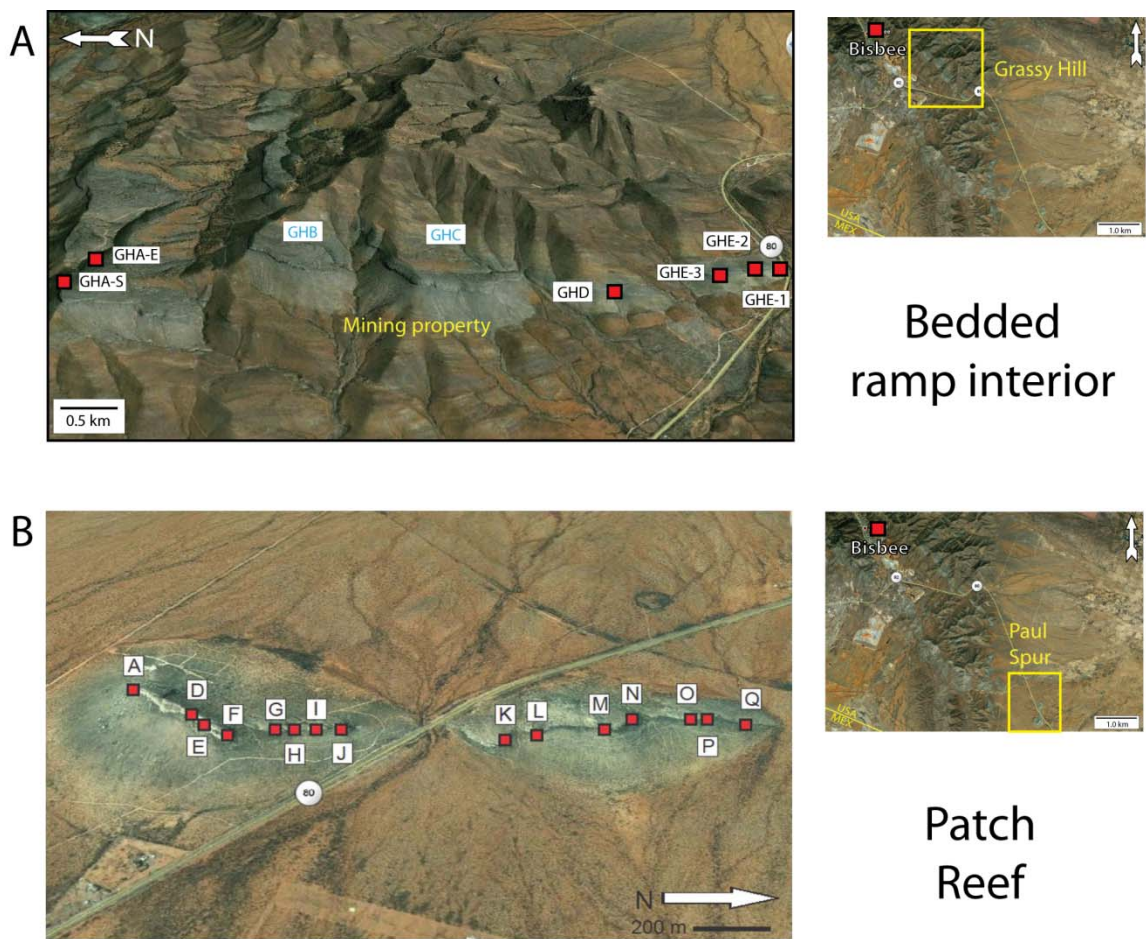


**Figure 5.** A) Section locations at the Grassy Hill locality in the Mule Mountains near Bisbee, AZ. These sections document bedded ramp interior facies composition and geometry. Sections were measured at variable spacing within a 5 km transect. Outcrops GHB and GHC lack measured section data because of the proximity to mining property. B) Section locations at the Paul Spur patch-reef locality are approximately 9 km southeast of the bedded ramp interior outcrops. Sections were measured at 30-100 m spacing within a 1.7 km transect.

property and limited accessibility from back roads. Measured sections at Grassy Hill provided sufficient data to delineate shelf facies and construct a depositional setting for the patch-reef at Paul Spur. Fifteen measured sections within a 1.7 km transect at Paul Spur were chosen at regularly spaced intervals ranging from 30-100 m (Figure 5B). Ground-based lidar data were collected at Paul Spur with an Optech, Inc. ILRIS-3D

scanner and covered the 1.19 km<sup>2</sup> area of reef exposure (see Figure 5B).

Facies mapping was conducted on photomosaics at Paul Spur. Reef frame facies were defined by presence and abundance of macrofauna, lime mud and growth fabric. Petrographic analysis of 115 thin sections was conducted to qualitatively enhance facies definitions and determine reservoir quality of reef frame facies and grainstones by estimating allochem percentage and primary porosity using a percent composition chart. Thin sections were impregnated with blue epoxy and were left unstained, uncovered and unpolished. Ten grainstone samples were collected from the 0.6 km grainstone facies transect at Paul Spur north for porosity and permeability plug analysis.

Stratigraphic surfaces were mapped on photomosaics and were determined by facies offsets using the methodology of Read et al. (1995). Stratigraphic surfaces, strike and dip data and measured section trajectories were digitally mapped with a Trimble® real-time kinematic global positioning system (RTK-GPS) and portable Nomad® systems for calibration with lidar data. Finally, all outcrop and digital data were combined to construct a 2D reef reconstruction in order to ascertain original facies associations, dimensions and depositional dips and geometries. Reef reconstruction was conducted in InnovMetric Polyworks® and Adobe Illustrator software packages.

### **3. Depositional setting of ramp interior**

#### **FACIES**

Mural Limestone ramp interior carbonates are exposed in an oblique dip-parallel outcrop belt approximately 5 km long in the Mule Mountains north of Bisbee, AZ, here referred to as the Grassy Hill locality (see Figure 1). The goal of this study is to develop a

depositional model for the Mural Limestone in the interior portion of the ramp from just seaward of the siliciclastic shoreline to patch-reef facies at Paul Spur, which are discussed in Section 4. Twelve depositional facies within three ramp interior sub-environments were identified for the Upper Mural Limestone from measured section and thin section data based on bedding, sedimentary and trace fossil structures and faunal associations. The depositional facies for Grassy Hill are described below, as they would be observed in an interpreted depositional model from landward (north) to seaward (south). These facies are summarized in Table 1.

#### **Facies 1: Mollusk siliciclastic sandstone**

**Description:** Thin- to medium-bedded (up to 1 m thick) sandstone weathers light tan to orange and is comprised of > 50% fine-grained quartz with grain sizes ranging from 130-230  $\mu\text{m}$ . Turritellid (cerithid) gastropods (15%) and bivalves (10%) are the dominant fauna (Figure 6A). Peloids (15%), green algae (5%), ostracods (2%) and oysters (1%) are also present. There is a small component of lime mud (1%). Some exposures of mollusk sandstone display cross-lamination (Figure 6B). Mollusk siliciclastic sandstone is heavily iron-stained, which is evident in both outcrop and thin section. Mollusk siliciclastic sandstone is typical of Lower Mural Limestone facies (Hayes, 1970; Scott, 1979; Warzeski, 1987), but may have been present in now covered intervals in the uppermost Upper Mural Limestone that are interbedded with wavy-laminated lime mudstone (facies 2) and peloid-milioid wackestone (facies 4).

Ramp interior facies (Grassy Hill)									
Facies	Composition				Color	Bedding		Depositional Environment	
	Quartz	Lime mud	Peloids	Skeletal Grains		Thickness	Character		
1	Mollusk siliciclastic sandstone	>50%	1%	15%	cerithid gastropods (15%) bivalves (10%) green algae (5%) ostracods (2%) oysters (1%)	light tan to orange	30 cm - 1m	massive to recessive weathering, cross-laminae	marginal marine
2	Wavy-laminated mudstone	?	95%	0%	mollusks (5%)	mottled light and medium blue-gray	10 - 60 cm	massive to fissile weathering, wavy laminae	restricted marine
3	Arenaceous algal-skeletal mud-dominated packstone	15%	20%	15%	mollusks (30%) <i>Lithocodium/Bacarella</i> (10%) dasyclads (5%) echinoids (3%) foraminifera (2%)	medium gray	10 - 50 cm	massive, cliff-forming	restricted marine
4	Miliolid-peloid wackestone/mud-dominated packstone	0%	25-50%	15%	miliolids (10%) mollusks (5%) other benthic foraminifera (<1%)	medium gray	10 cm - 1m	massive, cliff-forming	restricted marine
5	Peloid-foraminifer-mollusk-skeletal mud- and grain-dominated packstone	0%	8-25%	20%	mollusk/rudist fragments (20%) foraminifera, including <i>Orbitolina</i> (5%) echinoids (10%) <i>Lithocodium/Bacarella</i> (10%) grain aggregates (5%)	light to medium gray	15 cm - 1m	massive, cliff forming tabular beds, burrowed	shallow subtidal, moderate to localized high energy, bedded
6	<i>Orbitolina</i> -mollusk-peloid grainstone	0%	0%	40%	mollusk/rudist fragments (30%) <i>Orbitolina</i> (15%) echinoids (5%) coral fragments (5%) foraminifera (2%) dasyclads (2%)	light gray	10 cm - 1m	massive, cliff forming tabular beds, cross beds (?)	shallow subtidal, high energy, backreef shoal, tidal?
7	Chondrodont floatstone	0%	45%	5%	chondrodonts (35%) capritid/ucasid fragments (10%) <i>Orbitolina</i> (5%) echinoids (5%)	medium gray	15 - 25 cm	massive, tabular and laterally extensive	shallow subtidal, muddy, biostrome
8	Rudist floatstone	0%	17%	0%	to ucasids (30%) capritids (25%) radiolites (5%) mono pleurids (2%) nondescript mollusk fragments (20%) echinoids (1%)	light gray	1 - 5 m	massive, cliff-forming	shallow subtidal, low-relief buildups
9	Rudist rudstone	0%	10%	0%	requienids (40%) capritids (30%) mono pleurids (10%) radiolites (10%)	blue-gray to red -brown	2.7 - 3.5 m	massive to nodular	rudist buildup flank
10	Branching coral-skeletal framestone	0%	10%	0%	branching coral (20%) massive coral (15%) stromatoporoids (15%) <i>Lithocodium/Bacarella</i> (10%) capritids (5%) bivalves (3%) echinoids (2%) matrix fragments (20%)	light to medium gray and light tan	up to ~6 m	massive, cliff-forming	shallow subtidal patch-reef
11	Rudist-coral rudstone	0%	10%	0%	coral (20%) to ucasids (20%) capritids (10%) radiolites (10%) serpulid worm tubes (10%) <i>Lithocodium/Bacarella</i> (10%) echinoids (5%) red algae (2%) mono pleurids (2%) oysters (1%)	light gray to tan	50 cm - 1m	massive to nodular	shallow subtidal buildup/reef flank
12	Echinoid- <i>Orbitolina</i> -mollusk wackestone	0%	60%	0%	nondescript skeletal fragments (25%) mollusk (10%) <i>Orbitolina</i> (5%)	dark gray	20 - 60 cm	recessive-weathering	open subtidal ramp

**Table 1.** Depositional facies of the ramp interior carbonates at the Grassy Hill locality.



**Figure 6.** A) Mollusk siliciclastic sandstone (facies 1) is common in the Lower Mural Limestone. It is comprised of > 50% quartz and contains a low-diversity faunal assemblage of bivalves and cerithid gastropods. B) Localized cross-laminae are observed in facies 1 at Section GHE3. Preservation of cross-laminae may indicate low biologic activity (Enos, 1983) or persistent high-energy conditions in the marginal marine environment.

**Depositional environment:** High siliciclastic content and a depauperate low-diversity marine faunal assemblage are characteristic of a marginal marine/shoreline environment close to a basement source terrain, as is found in the central and southern lagoons of the modern Belize platform (Purdy and Gischler, 2003). The presence of thin-shelled turrillid (?) cerithid gastropods indicates an environment with slightly elevated salinity levels that are common in marginal marine environments (Fursich, 1993). Furthermore, preservation of cross-laminae may suggest an environment where biologic activity was scarce (Enos, 1983) or where a persistent high-energy level existed. The former interpretation is favored because of the fine-grained size of the quartz grains.

## **Facies 2: Wavy-laminated lime mudstone**

**Description:** Mottled light and medium blue-gray wavy-laminated mudstone comprises thin (10 cm) to thick (60 cm) beds of 95% lime mud with 5% non-descript mollusk fragments. In thin section, very fine mollusk debris is present but sparse. Burrows are locally common. Wavy-laminated mudstone overlies and is overlain by miliolid-peloid wackestone (facies 4) and bedded peloid-foraminifer-mollusk-skeletal mud-dominated packstone (facies 5).

**Depositional environment:** Wavy-laminated mudstone was likely deposited in a restricted lagoon environment in the intertidal zone. This interpretation is supported by lack of fauna and proximity to restricted marine facies observed in measured section, including miliolid-peloid wackestone.

## **Facies 3: Arenaceous algal-skeletal mud-dominated packstone**

**Description:** Medium-gray smooth weathering medium (10 cm) to thick (50 cm) beds of arenaceous algal-skeletal mud-dominated packstone are comprised of well-sorted fine-grained (120-135  $\mu\text{m}$ ) quartz grains (15%), mollusks, including gastropods (30%) and peloids (15%) (Figure 7A). Grains are commonly coated with *Lithocodium/Bacinella* (10%), a problematic micro-encruster. Round dasycladacean green algae fragments range up to 1 mm in diameter and are common (5%). Echinoids (3%), other foraminifera, including miliolids (2%) and intraclasts (1%) are minor components. Matrix is composed of 30% lime mud. In thin section, former aragonitic shell walled mollusks contain micrite rims and some examples are coated with *Lithocodium/Bacinella*. This facies is devoid of

sedimentary structures. No preserved macroporosity is present; allochem molds of mollusks are replaced with equant calcite spar. Arenaceous algal-skeletal mud-dominated packstone is probably analogous to the sandy ostracod-mollusk-skeletal-algal packstone facies of Scott (1979) and the skeletal algal-mollusk-echinoid packstone facies of Warzeski (1987) that were documented in the upper-most Upper Mural Limestone. While there are some occurrences of this facies at Sections GHAE, GHD and GHE3 where it is associated with mollusk siliciclastic sandstone (facies 1) and wavy-laminated lime mudstone (facies 2), it is most prevalent near the bases of these sections within Lower Mural strata.

**Depositional environment:** The presence of dasycladacean green algae, gastropods, and miliolids indicate a shallow-water and well-lit shelf environment (Wilson, 1975, p. 27, 72; Enos, 1983; Buitron et al., 1995). Dasycladacean green algae are commonly found in 3 – 5 m of water depth of varying salinity (Wilson, 1975, p. 72). The presence of miliolids indicates restricted marine conditions (Warzeski, 1983; Hartshorne, 1989) provided that the tests were not washed in from adjacent peloid-miliolid wackestone facies. In any case, adjacency to facies 1 and 2, combined with a low-diversity faunal assemblage suggests that the marine environment may have been normal to slightly restricted.

#### **Facies 4: Miliolid-peloid wackestone/mud-dominated packstone**

**Description:** Smooth-weathering medium gray miliolid-peloid wackestone forms continuous thin to medium beds < 1 m thick. Miliolid-peloid wackestone is comprised

dominantly of lime mud (25-50%) with peloids (15%) and miliolid foraminifera (10%). Mollusks (5%) and other foraminifera (< 1%) are accessory allochems. Miliolid-peloid wackestone is poorly sorted (150-400  $\mu\text{m}$ ) with large (~2 mm) *Orbitolina* foraminifera (Figure 7B). Micrite rims on mollusk fragments are common. There is no present macroporosity observed; allochem molds are filled with equant calcite spar. Pressure-resolution seams are common. Miliolid-peloid wackestone is intercalated with wavy-laminated lime mudstone (facies 2) and arenaceous algal-skeletal mud-dominated packstone (facies 3). It is also associated with thin to medium beds of rudist floatstone at Section GHAS.

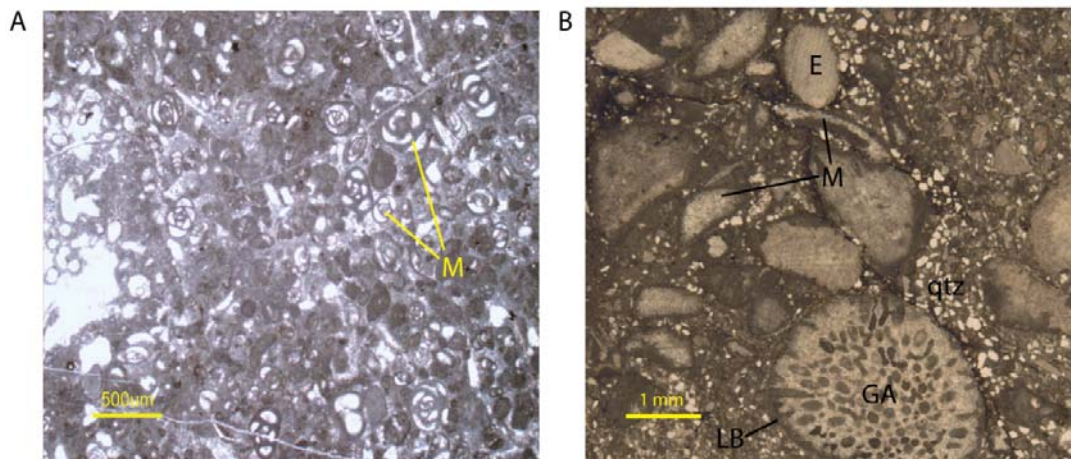


**Figure 7.** Restricted marine facies of the ramp interior at Grassy Hill. A) Arenaceous algal-skeletal mud-dominated pack-stone (facies 3) consists of mollusk (M) fragments and fine-grained quartz (qtz), with minor echinoid (E) and green algal (GA) fragments. *Lithocodium/Bacinella* (LB) encrustation is common. B) Miliolid-peloid (M) wackestone to mud-dominated packstone (facies 4) is found above the massive cliff-forming beds at all sections.

**Depositional environment:** A high abundance of peloids and miliolid foraminifera indicates an inner ramp restricted lagoon environment in close proximity to

the paleo-shoreline (Warzeski, 1983; Hartshorne, 1989). Miliolid-rich facies are characteristic of Lower Cretaceous restricted carbonate inner ramp environments in Texas (Loucks, 1977; Scott and Kidson, 1977; Hillgartner et al., 2003) and the Aptian Shuaiba Formation of the Middle East (Alsharan, 1995; Hillgartner et al., 2003).

**Facies 5: Peloid-foraminifer-mollusk-skeletal mud- and grain-dominated packstone**

**Description:** Light to medium gray smooth-weathering mud- and grain-dominated packstones (Figures 8A, 8B) form medium (15 cm) to massive (> 1 m) beds that are peloid-rich (20%) with an abundance of mollusks including caprinid and toucasid rudists (15%). Foraminifera, including planispiral, biserial, and *Orbitolina* (15%) and echinoids (10%) are common. *Orbitolina* foraminifera exhibit a high aspect ratio (conical). Skeletal grains are commonly coated with *Lithocodium/Bacinella* (10%); multiple coated grains make grain aggregates (5%). Red algae is a minor component (<1%).

Bedded peloid foraminifer mollusk skeletal mud-dominated packstone is poorly-sorted, with grain sizes ranging from 100 µm to > 2 mm. Matrix is composed of 25% lime mud. Burrowing is visible in mud-dominated packstone facies in outcrop (Figure 9A) and at least two types of burrows are identified: 1) large (up to 5 cm-wide) silicified burrows that are primarily associated with bedding planes (Figure 9B) and were identified by Scott and Warzeski (1993) as *Thalassinoides* and 2) prevalent 3 cm-wide 3D burrow networks characterized by mottled texture in outcrop (Figure 9C). Characteristic features for specific burrow types were not identified in this study. Peloid-

foraminifer-mollusk-skeletal mud-dominated packstone facies at the Grassy Hill sections are otherwise devoid of sedimentary structures. In thin section, micrite rims are common on mollusk fragments. Syntaxial overgrowth cements are common on echinoids. These facies do not contain abundant porosity; primary porosity is occluded with equant calcite (see Figure 8B). Bedded peloid-foraminifer-mollusk-skeletal mud-dominated packstone is associated with the lower-energy facies at Grassy Hill, including miliolid-peloid wackestone (facies 4) and rudist floatstone (facies 8).

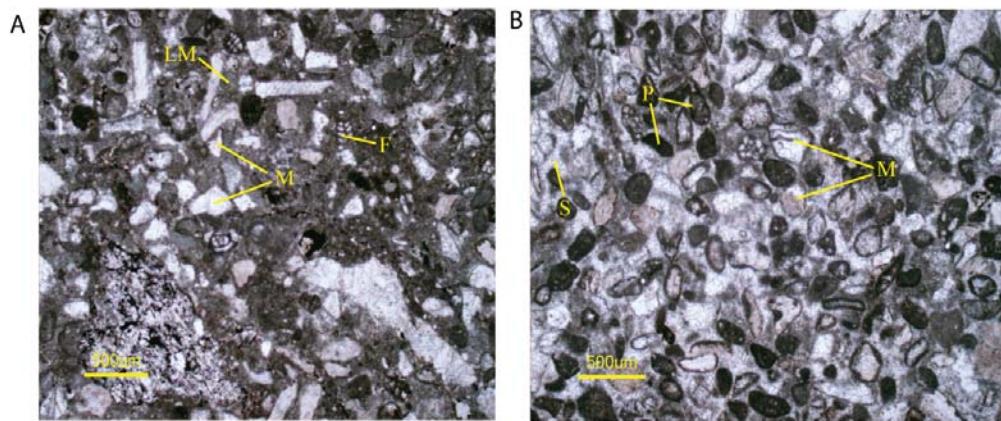


**Figure 8.** Bedded facies of the ramp interior carbonates at Grassy Hill (facies 5). A) Peloid-foraminifer-mollusk-skeletal mud-dominated packstone, with abundant foraminifera (F) and mollusks (M) in lime mud (LM) matrix. B) Peloid-foraminifer-mollusk-skeletal grain-dominated packstone consists of well-sorted and well-rounded grains of peloids (P), mollusks (M) and foraminifera with interparticle pore spaces filled with calcite spar (S).

Bedded peloid-foraminifer-mollusk-skeletal grain-dominated packstone is well-sorted, with well-rounded grains 175-250  $\mu\text{m}$  (see Figure 8B). Lime mud is present (~8%) but the majority of interparticle pore space is filled with equant calcite spar. Although secondary porosity may be observed locally, it is not characteristic and leached grains are also filled with calcite spar. Peloid-foraminifer-mollusk-skeletal grain-dominated packstones are associated with high-energy facies such as *Orbitolina*-mollusk-

peloid grainstone (facies 6), rudist-coral rudstone (facies 11) and caprinid-dominated floatstones (facies 8).

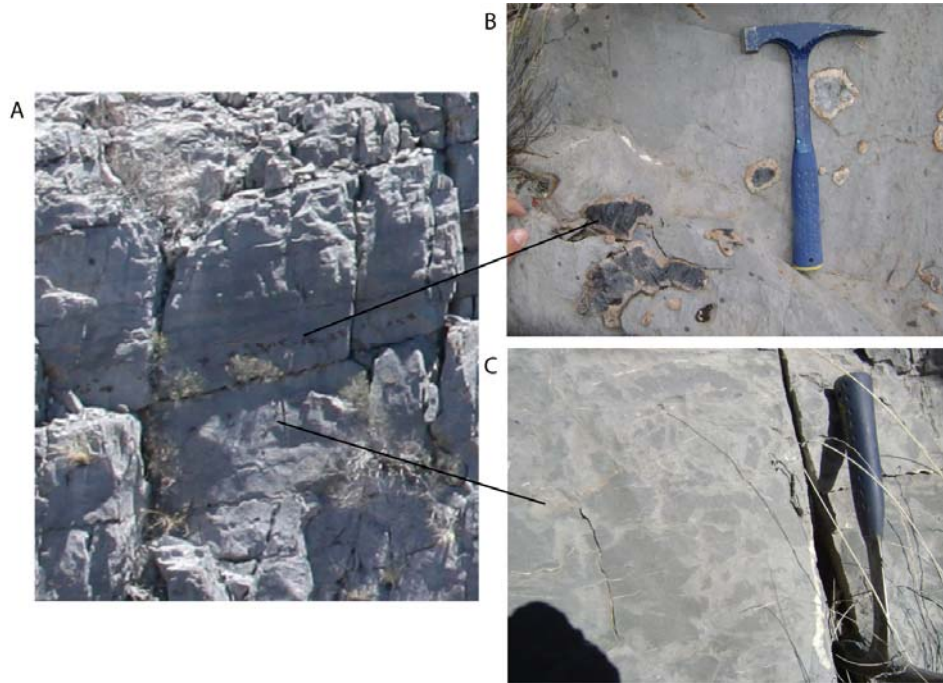


**Figure 9.** A) Burrow styles common in bedded peloid-foraminifer-mollusk-skeletal mud-dominated packstone (facies 5) at Grassy Hill near Section GHAE, B) Large silicified burrows are oriented parallel to bedding planes. C) Small centimeter-scale burrows weather lighter than surrounding matrix.

**Depositional environment:** Burrowed skeletal mud- and grain-dominated packstones are prolific in shallow-water subtidal environments (Wilson and Jordan, 1983). The presence of *Lithocodium /Bacinella*, conical morphology of *Orbitolina* and abundant burrowing suggest well-oxygenated and well-lit conditions (Schmid and Leinfelder, 1996; Vilas et al., 1995). Micritization and encrustation by *Lithocodium/Bacinella* of grains within the mud-dominated packstone facies indicates a moderate-energy environment (Bebout and Loucks, 1974; Enos, 1983), while well-sorted

grains within the grain-dominated facies indicates areas of localized high wave energy. Analogous bioclastic are documented in the Lower Cretaceous of Texas (Scott & Kidson, 1977; Loucks and Kerans, 2003) and the Middle East (Burchette and Britton, 1985; Alsharan, 1995; Hillgartner et al., 2003).

#### **Facies 6: *Orbitolina*-mollusk-peloid grainstone**

**Description:** Light gray to buff smooth-weathering *Orbitolina*-mollusk-peloid grainstone comprises medium to massive beds 10 cm-1 m thick. *Orbitolina*-mollusk-peloid grainstone is comprised primarily of peloids (40%), mollusks, including locally abundant caprinid and toucasid rudist fragments (30%) and *Orbitolina* foraminifera (15%) (Figure 10A). Accessory allochems include echinoids (5%), locally abundant coral (5%), other foraminifera (2%) and dasycladacean green algae (2%). In thin section, peloid and skeletal grains are medium- to coarse-grained (400-600  $\mu\text{m}$ ) and well-sorted (Figure 10B). *Orbitolina* are conical and are up to 2 mm in diameter. Micrite rims on former aragonitic mollusk fragments are common. These grains, as well as *Orbitolina* and coral fragment cavities are filled with equant calcite spar cement. Syntaxial calcite overgrowth is common on echinoid plates. Skeletal grains are heavily abraded. *Orbitolina*-mollusk-peloid grainstone grades laterally into and overlies chondrodont floatstone (facies 7), rudist floatstone (facies 8), branching coral-skeletal framestone (facies 10) and rudist-coral rudstone (facies 11). It is intercalated with bedded peloid foraminifer mollusk skeletal mud-dominated and grain-dominated packstone (facies 5). Localized *Orbitolina*-rich grainstones are constrained to Sections GHAS, GHAE and

GHD and are associated with facies 8 (Figure 10C).

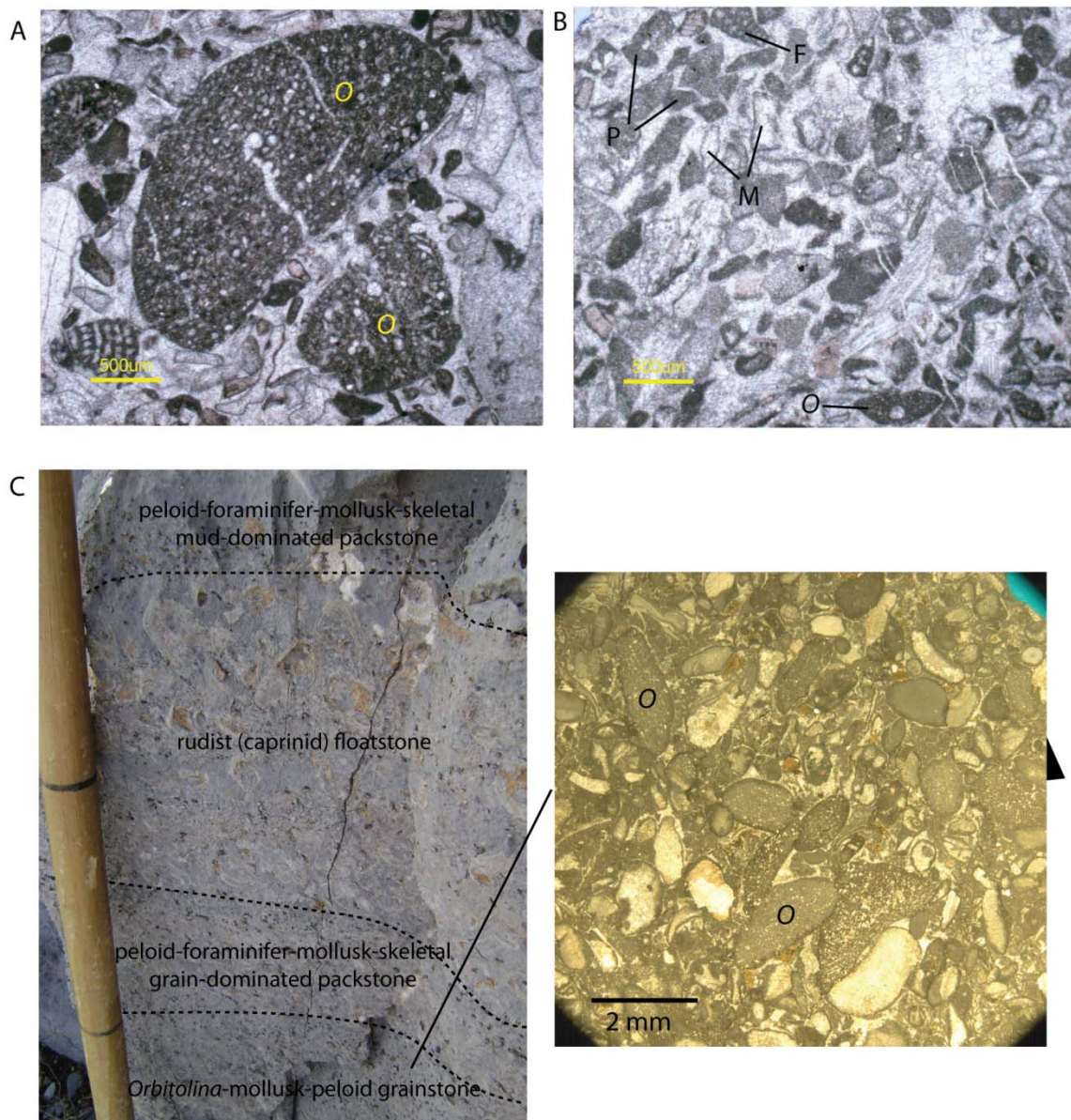


**Figure 10.** *Orbitolina*-mollusk-peloid grainstone (facies 6) contains A) large *Orbitolina* foraminifera and B) well-sorted peloid (P) and skeletal fragments, including mollusks (M) and biserial foraminifera (F). C) *Orbitolina*-mollusk-peloid grainstone are locally *Orbitolina*-rich and are associated with peloid-foraminifer-mollusk-skeletal grain-dominated packstone with large fragments of caprinid rudists and caprinid-rich rudist floatstone.

### **Facies 7: Chondrodont floatstone**

**Description:** Medium gray massive and smooth-weathering floatstone is comprised of horizontally-oriented chondrodonts (35%) within a muddy lime matrix (45%). Accessory allochems include caprinid and toucasid rudist fragments (10%), peloids (5%), *Orbitolina* (5%) and echinoids (5%). Chondrodont floatstone occurs in 15-25 cm-thick beds. Horizontally-oriented chondrodonts are up to 10 cm in length and weather dark gray to black. Chondrodonts are sparsely encrusted with microbial micrite; other encrusting organisms such as *Lithocodium/Bacinella* are not present. Matrix is composed of echinoid-*Orbitolina*-mollusk wackestone. *Orbitolina* foraminifera exhibit conical morphology. There is no preserved macroporosity. Chondrodont floatstone is present at Section GHD and Sections GHE1-3 at the southern extent of the Grassy Hill locality. In some locations, it underlies rudist floatstone (facies 8) (Figure 11), but also occurs as separate biostromes 20 cm to 70 cm thick within bedded peloid-foraminifer-mollusk mud-dominated packstone (facies 5). Chondrodont floatstone is also associated with miliolid-peloid wackestone (facies 3) at Section GHAS.

**Depositional environment:** *Orbitolina* are conical and therefore indicate a clear shallow water depositional environment (Vilas et al., 1995). Heavily abraded and well-sorted skeletal grains with little to no mud content are evidence of exposure to constant wave agitation above fair-weather wave base (Flügel, 2004, p. 90, 354). Grainstone facies at Grassy Hill are primarily associated with small branching coral and rudist buildups and back-buildup debris rudstones and therefore suggests that the grainstones represent a

small-scale high-energy debris shoal similar to that observed at the Paul Spur patch-reef described in Section 4 of this study.

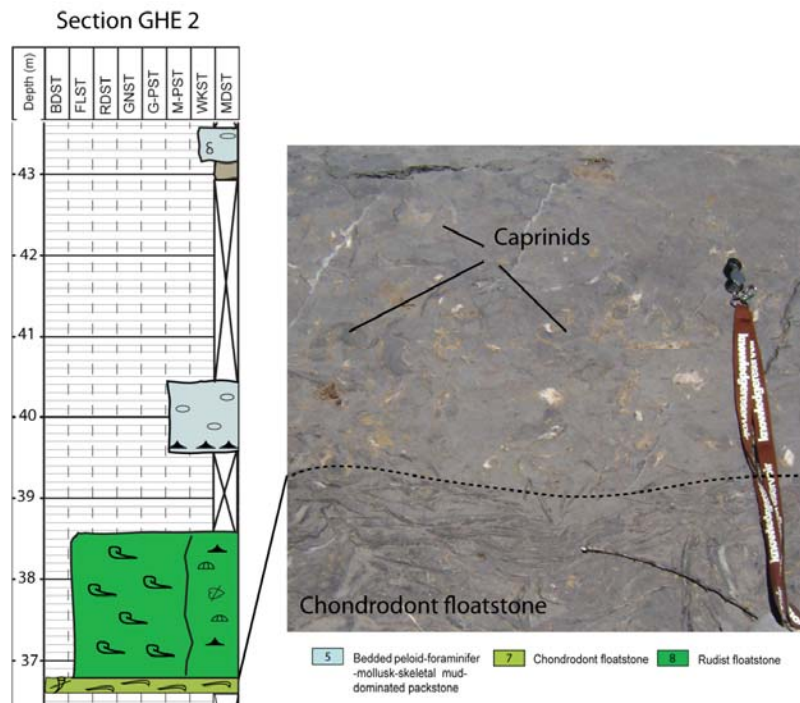


**Figure 11.** Chondrodont floatstone (facies 7) is present in the shallow subtidal facies belt at Grassy Hill, where it is commonly associated with rudist floatstone. Chondrodonts lie within an echinoid-*Orbitolina*-mollusk wackestone matrix.

**Depositional environment:** An abundance of lime mud and presence of open marine fauna such as echinoids indicates that chondrodont floatstone was deposited in a shallow-water subtidal depositional setting with relatively low wave-energy, likely below fair-weather wave base. Chondrodonts likely lived in expansive muddy substrates as they do on the northern margin of the Maverick Basin (Kerans, 2002). Individual chondrodont beds were traced 0.5 km at the GHE outcrop.

### **Facies 8: Rudist floatstone**

**Description:** Light gray smooth-weathering rudist floatstone comprises small

mound communities 1-5 m high with whole shells of tucasids (40%) (Figure 12A), caprinids (30%), radiolitids (5%) and less common, some monopleurids (2%). Non-descript mollusk fragments (5%) and echinoids (<1%) are minor components. Matrix is comprised of echinoid-mollusk wackestone to grain-dominated skeletal packstone matrix. Rudists are commonly encrusted with serpulid worm tubes and dark laminated micritic crusts of either microbial or red algal origin. Encrusting green algae are common. Geopetal structures are filled with dark grey lime mud and equant calcite spar. Rudist floatstone overlies branching coral-skeletal framestone (facies 10) and chondrodont floatstone (facies 7). It is flanked by bedded peloid-foraminifer-mollusk-skeletal mud-dominated packstone (facies 5). At Section GHAS it is also associated with miliolid-peloid wackestone (facies 4) and rudist rudstone (facies 9).

**Depositional environment:** Lower Cretaceous caprinid and tucasid rudists are common in the shallow-water ramp interior (Wilson, 1975, p. 320; Hartshorne, 1989; Scott et al., 1990, Alsharan, 1995). Caprinid rudists occur predominantly in high-energy settings, while tucasids are a low-energy form (Ross and Skelton, 1993; Kerans, 2002). Wilson (1975, p. 322) furthermore reported that both caprinid and tucasid rudists are tolerant of restricted marine environments where they are found in association with abundant miliolid foraminifera. Consequently, caprinid and tucasid rudists appear to have inhabited a number of environments on the ramp interior at Grassy Hill: 1) low-energy, open marine environments at Sections GHAE, GHE1 and GHE2 where caprinids and tucasids form buildups up to 4 m in relief that are associated with facies 5 (Figure 13A), 2) higher-energy marine environments at Sections GHAS, GHD, and GHE3, where

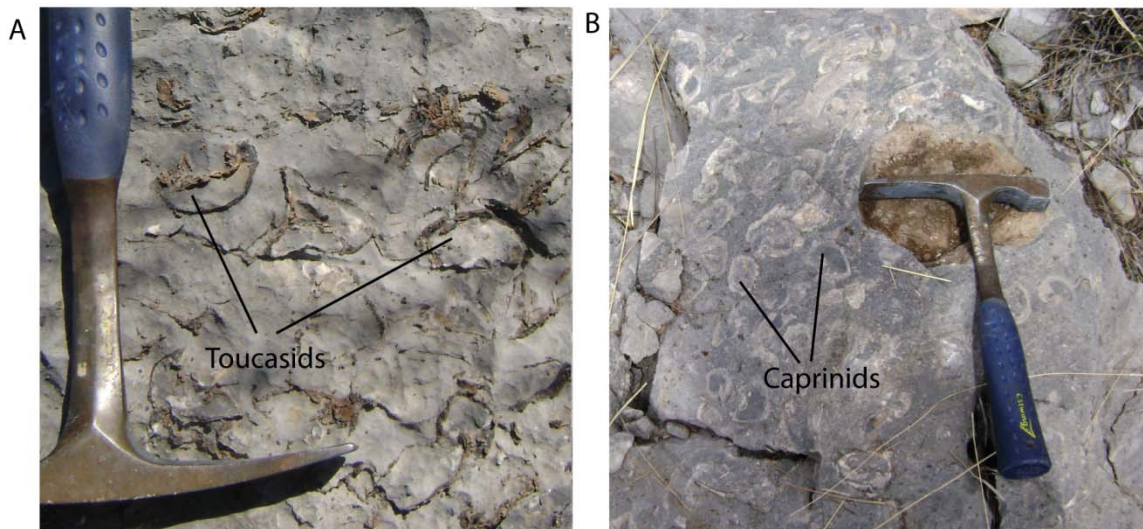


**Figure 12.** Rudist floatstone (facies 8) types are common in the shallow subtidal ramp setting at Grassy Hill. Although radiolitid and monopleurid rudists are present, the dominant rudist types are the A) toucasids and B) caprinids.

caprinid-dominated buildups lie in a coarser matrix and are associated with facies 6 and 10 comprised of rudist and other skeletal debris (Figure 13B) and 3) restricted environments in the middle to upper sections of Sections GHAS, GHD, and GHE2 where toucasid-dominated buildups are associated with facies 4 (Figure 13C).

**Facies 9: Rudist rudstone**

**Description:** Mottled-weathering blue-gray to red-brown rudist rudstone is composed of fragments of requienid (40%), caprinid (30%), monopleurid (10%) and radiolitid (10%) rudists within a poorly-sorted (fine to coarse) peloidal-skeletal wackestone to grain-dominated packstone matrix. Matrix allochems include other mollusks, echinoids, and rare *Orbitolina*. Requierid rudist fragments are up to 10 cm in diameter and are dark “root beer” brown. Geopetal structures are variably oriented and are filled with gray-blue

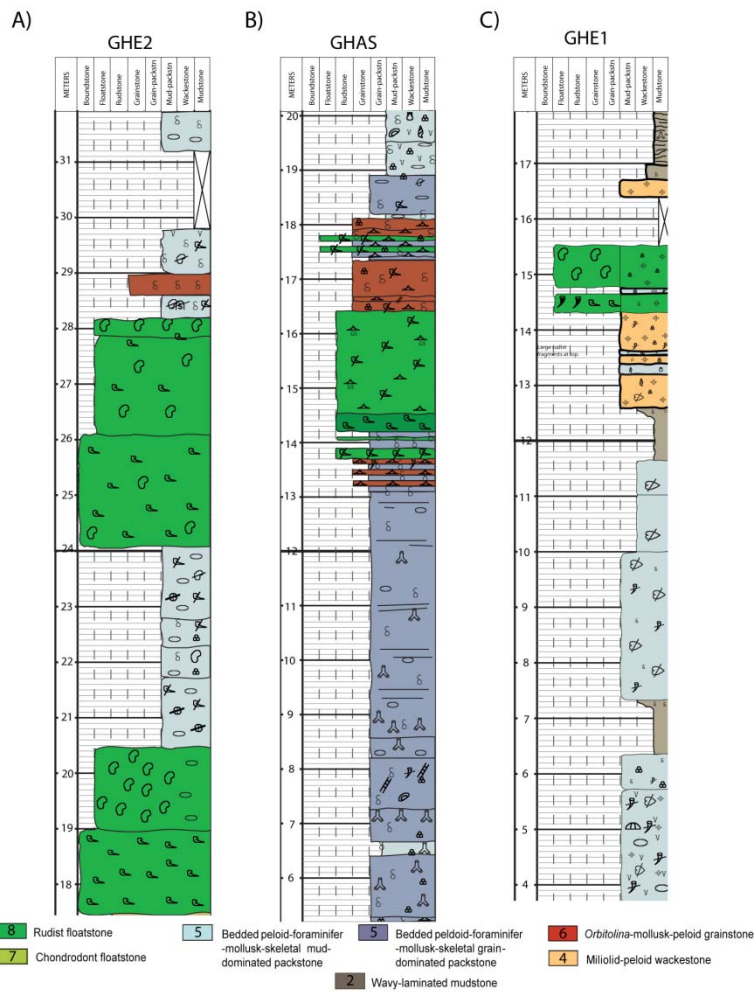


**Figure 13.** Rudist floatstones (facies 8) are found in various depositional settings in the ramp interior at Grassy Hill. A) At Section GHE2, rudist floatstone forms relatively thick buildups and consists of muddy peloidal matrix. These buildups are associated with a low-energy subtidal depositional environment similar to facies interpreted by Wilson (1975), Hartshorne (1989), Scott et al. (1990), Alsharan (1995) and Kerans (2002). B) At Section GHAS, rudist floatstones form buildups with moderate relief within *Orbitolina*-peloidal-skeletal grainstone (facies 6) beds. Caprinids are prolific in this higher-energy environment. C) At Section GHE 1 rudist floatstone forms relatively thin buildups within miliolid-peloid wackestone (facies 4) and consists mostly of toucasids. Toucasids are tolerant of higher salinities associated with restricted lagoon settings (Wilson, 1975, p. 320).

smooth-weathering lime mud and blocky calcite. Rudist fragments are commonly encrusted with dark, micritic laminite of possible microbial origin. This facies lacks

evidence of early cementation, although equant calcite fills preexisting moldic pore space. Rudist rudstone overlies rudist floatstone (facies 8) at Section GHAS and likely grades laterally into the buildup located to the south of this section.

**Depositional environment:** This facies is interpreted as rudist colony debris that was washed beds by moderate wave energy (Scott, 1979), likely between storm and fair-weather wave base. Fragmented rudist and skeletal fragments in a poorly-sorted skeletal matrix further suggests a relatively lower-energy depositional setting.

### **Facies 10: Branching coral-skeletal framestone**

**Description:** Branching coral-skeletal framestone is comprised of whole branching corals (20%) (Figure 14A), massive corals (15%) (Figure 14B) and

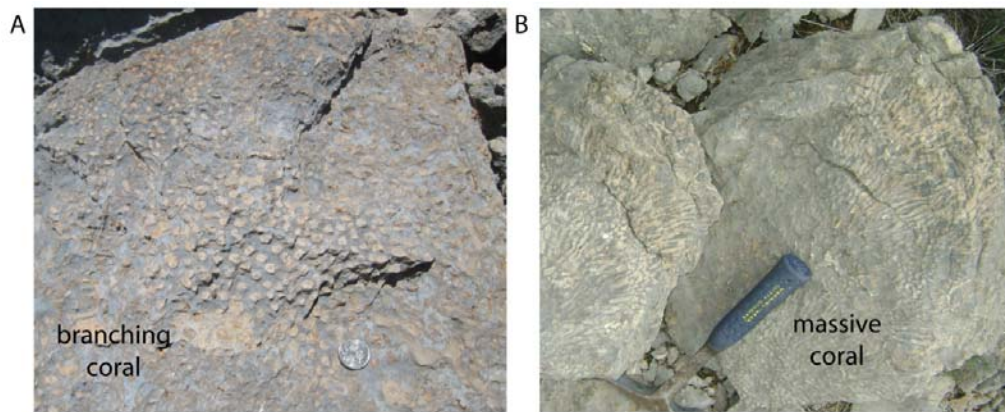


**Figure 14.** Corals found within branching coral-skeletal rudstone include A) branching corals and B) massive corals. Branching corals exhibit a finger-like colony structure, as in A), while others are more columnar with branches up to 3 cm in diameter. Corals are encrusted with *Lithocodium/Bacinella*. These corals were excellent bafflers that were able to trap fine-grained sediments.

stromatoporoids (15%) encrusted with *Lithocodium/Bacinella* (10%). Accessory allochems include whole tests of caprinid rudists (5%), echinoids (2%) and bivalves

(3%). Matrix is comprised of skeletal grain-dominated packstone (20%). Branching corals with branches up to 3 cm wide weather light tan. Corals are encrusted with *Lithocodium/Bacinella*, which are in turn bored by lithophagid bivalves. Recumbent caprinid rudists are rare to common with preserved geopetal structures in original position. Internal sediment fill is composed of skeletal mud-dominated packstone. Preserved macroporosity is not present; allochem molds in the matrix and internal sediment are filled with equant calcite spar. Branching coral-skeletal framestone grades laterally to the north into coral rudist rudstone and is flanked by bedded peloid-foraminifer-mollusk-skeletal mud-dominated packstone. This facies is present at Section GHE2 and to the northwest of Section GHAE where it forms massive beds ~ 6 m in relief. This facies is capped by rudist floatstone (facies 8) and rudist-coral rudstone (facies 10) at both locations.

**Depositional environment:** The presence of in-situ branching and massive corals suggests that they thrived in low to moderate wave energy but well-lit conditions (Vilas et al., 1995). Fine-grained skeletal fragments and lime mud were trapped by corals and stromatoporoids that served as baffles to moderate wave activity. Shoaling into wave-base is indicated by the presence of the capping rudist community that lies within a skeletal rudstone matrix (See Appendix A, Section GHE2, 8-15 m).

### **Facies 11: Rudist-coral rudstone**

**Description:** Smooth to nodular-weathering rudist-coral rudstone (Figure 15A) is comprised of large coral (20%), toucasid (10%) and caprinid (10%) fragments. Toucasids

measure 5 cm - 10 cm in length, weather dark brown, and are commonly iron-stained. Radiolitid fragments (10%) are common and monopleurid fragments are rare (2%). Also present are serpulid worms (10%), *Lithocodium/Bacinella* (10%), Radiolitids (10%), echinoids (5%), red algae (2%), and oysters (1%). Oysters are bored; borings are filled with lime mud. A small component of lime mud (10%) matrix is comprised of skeletal lithoclastic grain-dominated packstone. Rudist-coral rudstone forms the top cliff-forming beds at Sections GHE2, GHE3 and GHD. In thin-section, equant calcite spar is common within allochem molds. Microfractures cross-cut the rudstone fabric and are filled with equant calcite. Rudist-coral rudstone overlies and grades laterally into branching coral-skeletal framestone (facies 9) and rudist floatstone (facies 8) to the south and *Orbitolina*-mollusk-peloid grainstone (facies 6) to the north at Sections GHE2 and GHE3.

**Depositional environment:** Rudstone facies are interpreted as reef-derived debris from branching coral-skeletal framestone patch-reef facies (facies 9) that were washed leeward into beds by wave energy (Scott, 1979). The presence of very poorly sorted fragments of corals and rudists, as well as other mollusks, echinoderms, and benthic foraminifera support this interpretation.

### **Facies 12: Echinoid-*Orbitolina*-mollusk wackestone**

**Description:** Gray, discontinuous, wavy-laminated lime echinoid-*Orbitolina*-mollusk wackestone forms medium (20-60 cm) beds that are less indurated and weather recessively; laminae are commonly iron-stained. Echinoid-*Orbitolina*-mollusk wackestone is comprised of nondescript fine-grained skeletal hash (25%), mollusk

fragments (10%) and *Orbitolina* foraminifera (5%) floating within a lime mud matrix (Figure 15B). In thin section, skeletal fragments are poorly sorted (100-600  $\mu\text{m}$ ). *Orbitolina* are up to 4 mm in diameter and exhibit a low aspect-ratio (disk-like). Minor constituents include coral fragments (2%), echinoid fragments (2%) and biserial and planispiral foraminifera. Bivalves with originally aragonitic shell walls have been leached and subsequently replaced with equant calcite cement with no evidence of micritization. Some echinoid plates exhibit syntaxial overgrowth of calcite cement. Original macroporosity is not preserved; former aragonitic mollusk fragments have been replaced with equant calcite spar. Echinoid-*Orbitolina*-mollusk lime wackestone is associated with low-energy bedded peloid foraminifer mollusk skeletal mud-dominated packstone (facies 5).

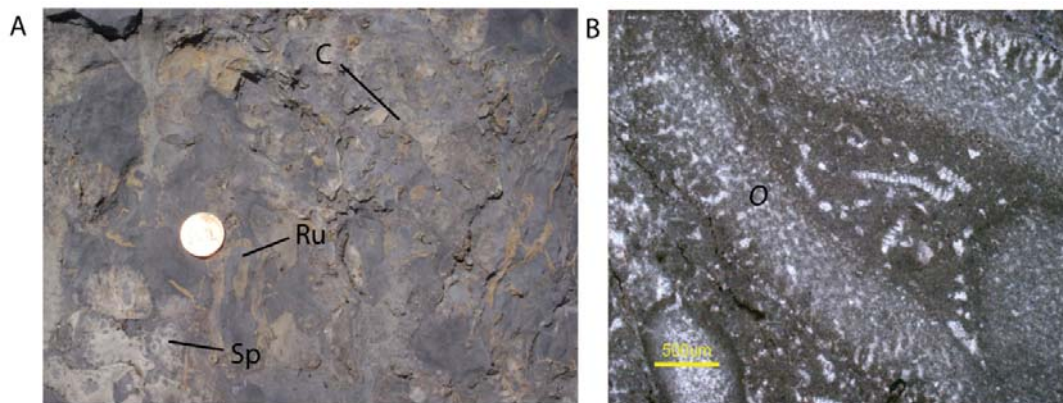


**Figure 15.** A) Rudist-coral rudstone is interpreted as reef-derived debris facies from underlying branching coral-skeletal framestone (facies 9) patch-reef facies. Large fragments of corals (C) and rudists (Ru) are encrusted with dark rinds of *Lithocodium/Bacinella* and serpulid (Sp) worm colonies. B) Echinoid-*Orbitolina*-mollusk wackestone is comprised of large *Orbitolina* (O) > 2mm in diameter floating in a lime mud matrix and is characteristic of an open subtidal ramp setting.

**Depositional Environment:** Depositional environment is interpreted as open subtidal ramp and lower reef flanks, below fair-weather wave base (Scott, 1979; Vilas et

al., 1995; Aconcha, 2008). Petrographic evidence for a deeper-water environment relative to that of the aforementioned facies includes high abundance of carbonate mud and poor sorting, and disk-like morphology of *Orbitolina* benthic foraminifera (Vilas et al., 1995). Immenhauser and Scott (2002) documented similar facies in the Albian shelf carbonates in the Wadi el Assyi platform, Oman based on *Orbitolina* morphology. *Orbitolina*-rich shallow shelf facies are documented in the Aptian Shuaiba platform (Burchette and Britton, 1985; Alsharan, 1995), Aptian off-reef low energy shelf carbonates of SE Spain (Vilas, et al., 1995) and the Maverick Basin of Texas (Loucks and Kerans, 2003). This facies is analogous to Scott's (1979) mollusk-miliolid-*Orbitolina* wackestone.

#### **DEPOSITIONAL MODEL**

The ramp interior facies at the Grassy Hill locality are defined by four main architectural components, including small coral-algal patch-reefs, rudist bioherms comprised of tucasids and/or caprinids, *Orbitolina*-mollusk-peloid grainstones and capping thin- to medium-bedded peloid-miliolid wackestones. These components and their associated facies are divided into three ramp interior subenvironments based on vertical facies associations as well as previous work by Scott (1979) and Warzeski (1983, 1987). The ramp interior subenvironments are 1) nearshore/semirestricted lagoon 2) peloid-oid shoal and 3) shallow subtidal ramp. A depositional model for the ramp interior setting is illustrated in Figure 16 and defines the overall environment in which large patch-reefs like the Paul Spur reef (see Section 4 of this study) may have developed in the area. Restricted lagoon facies include facies 1 and 4 of the Lower Mural Limestone (Figure 17A) (Hayes, 1970; Scott, 1979; Warzeski, 1983, 1987), in addition to facies 2 and 3 of

the Upper Mural Limestone (Figure 17B). These facies associations are best observed at the base of Section GHE3 and in Section GHD. Although no shoreline indicator is present for this study, it is likely that, based on analogous faunal assemblages in the Stuart City Trend in Texas and the El Abra Formation in northern Mexico, lagoonal facies accumulated in low-energy conditions in ~ 6 m of water (Bebout and Loucks, 1974; Enos, 1974). Semirestricted lagoonal facies at Section GHD also include peloid-miliolid grainstone and miliolid-rich chondrodont floatstone and toucasid-rich rudist floatstone. Grainstone fabrics may have been common in areas of varied local topography or higher wave energy around tidal channels (Bebout and Loucks, 1974).

Peloid-oid shoals are common carbonate ramp settings and are located close to the paleoshoreline (Read, 1995). The peloid-oid grainstone shoal facies is defined as a massive-weathering cross-bedded tabular grainstone comprised of peloids, transported caprinid fragments, micritized grains and coated grains (Scott, 1979). This facies is 31 m thick at Section 7923 (Scott, 1979) and is in close proximity to Section GHAS of this study. Cross-bedded peloid-oid grainstone is not documented at Section GHAS; however, it is possible that this facies exists in Mural carbonates south of Section GHAS and north of Section GHD where access to the outcrop for this study was not granted. If present, the peloid-oid grainstone shoal facies would have provided a physical barrier to current flow that allowed for semirestricted lagoonal facies accumulation (Scott, 1979; Warzeski 1987) observed at GHAS, GHD and GHE3 in this study.

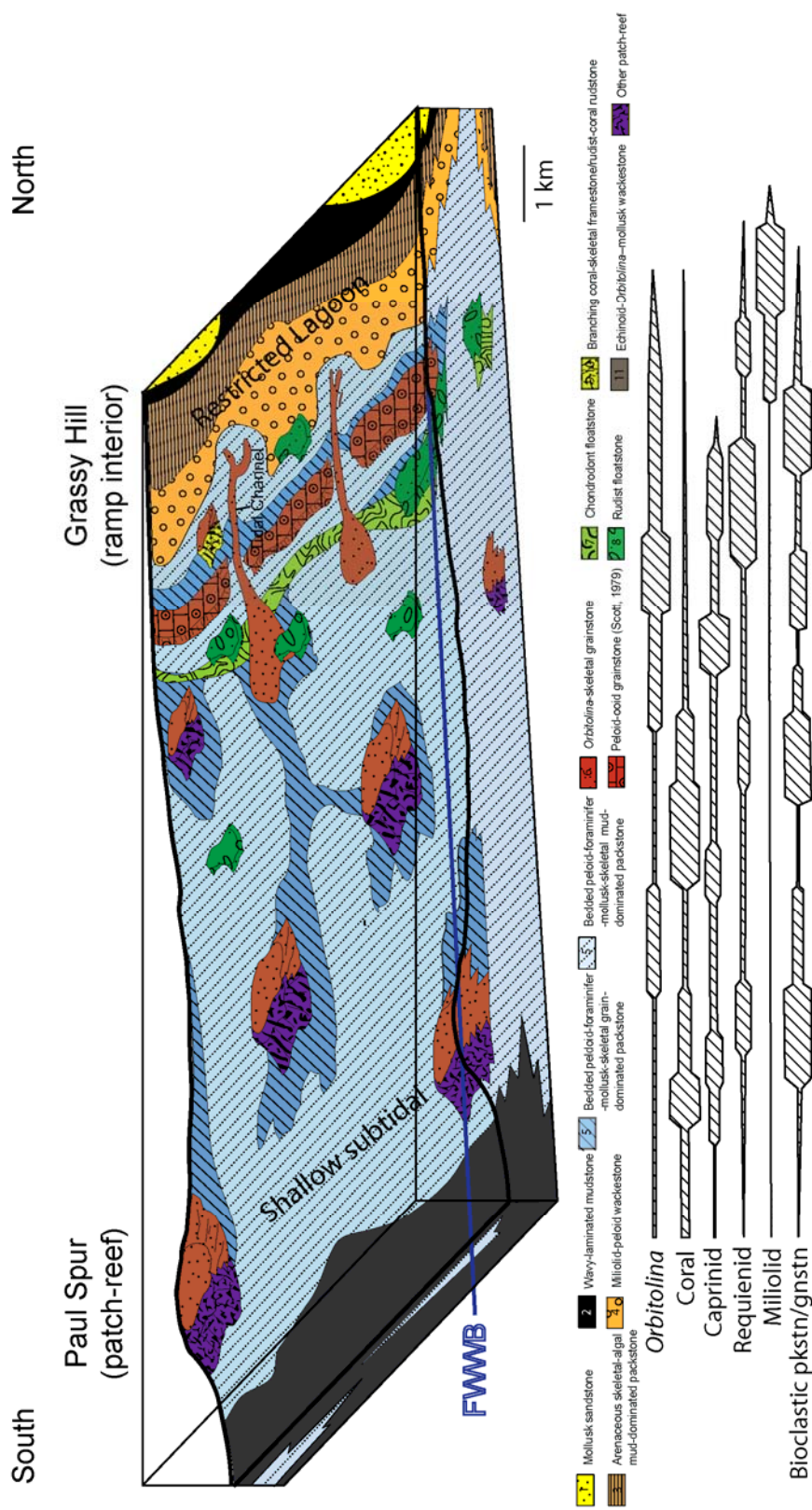


**Figure 16.** Facies and interpreted depositional environments of the Mural Limestone ramp interior at the Grassy Hill and Paul Spur patch-reef study areas, southeastern Arizona. The conceptual model spans at 15 km transect that represents a depositional dip profile from north to south. Lateral facies associations are based on vertical relationships in measured sections. The Grassy Hill facies are interpreted to be deposited in a marginal marine/restricted lagoon, ooid shoal and shallow-water subtidal ramp-interior setting. Large coral patch-reefs (~30 m thick), such as the one studied at the Paul Spur locality, are constrained to the shallow subtidal only. Smaller (~6 m) coral patch-reefs are present updip at the Grassy Hill locality. Caprinid-requienid buildups with moderate (up to 5 m) relief are prevalent in the shallow subtidal setting and smaller scale caprinid-requienid buildups (1-2 m) are associated with restricted marine miliolid-peloid wackestone facies.

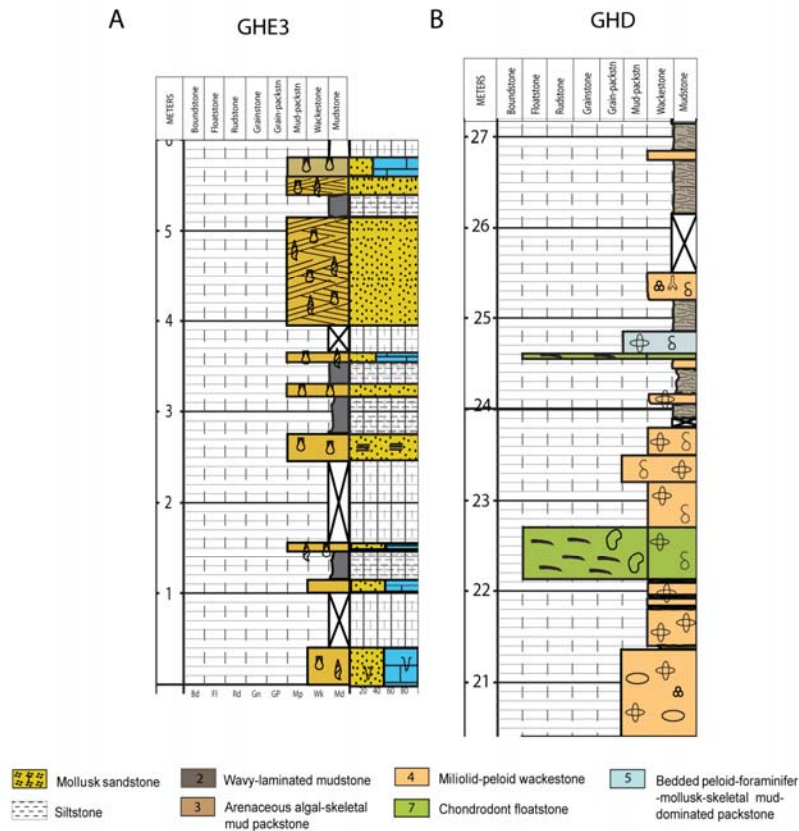


**Figure 17.** Restricted lagoon facies of the ramp interior at the Grassy Hill locality. A) The facies at GHE3 are typical of Lower Mural marginal marine sediments (Hayes, 1970; Scott, 1979; Warzeski, 1983, 1987) but some also occur in the upper-most Upper Mural Limestone (Scott, 1979; Warzeski, 1987). These facies are comprised of interbedded mollusk siliciclastic sandstone (facies 1), siltstone and arenaceous algal-skeletal mud-dominated packstone (facies 5). B) Facies at Section GHD are representative of a restricted lagoon environment rich in miliolids and interbedded with wavy-laminated mudstone (facies 2). While no algal structures were identified in the mudstone, the lack of fauna and association with miliolid-peloid wackestone (facies 4) suggests that this facies is in close proximity to the paleo-shoreline.

Shallow subtidal ramp facies include chondrodont and rudist floatstones, bedded peloid-foraminifer-mollusk-skeletal mud- and grain-dominated packstones, *Orbitolina*-skeletal grainstone, echinoid-*Orbitolina*-mollusk wackestone, and patch-reef boundstones and rudstones. The most prolific facies are well-bedded peloid-foraminifer-mollusk-skeletal mud- and grain-dominated packstones; these facies comprise the first 13 m of

Section GHAS (Figure 18) and individual beds are 0.3 m to 4.8 m thick. Burrows are common in mud-dominated packstones (see Figure 9), some of which have been described by Scott and Warzeski (1993) as *Thalassinoides*.

Chondrodont floatstone (facies 7) and rudist floatstone (facies 8) form buildups 0.5 m to 7 m thick are commonly associated with peloid-foraminifer-mollusk-skeletal mud- and grain-dominated packstones (facies 5). These buildups are present in all measured sections but are prolific at section GHE2 where they form relatively thick buildups over a small coral patch-reef (Figure 19). Section GHE2 is located in a downdip (southern) position relative to other sections at Grassy Hill where normal marine shallow subtidal facies are prevalent throughout the section. This area likely provided sufficient accommodation for relatively thick rudist buildups to stack above the preexisting coral patch-reef. A large rudist buildup ~ 7 m thick is located to the south of Section GHAS and is identified based on stratal geometry of flank beds and surrounding bedded packstone (Figure 20). Flank beds are exposed in an oblique-strike section and dip to the northeast and southwest. Preservation of the bedded rudstones suggests that the buildups accumulated below fair-weather wave base.

On the seaward side of shallow subtidal middle ramp, branching and massive corals, as well as stromatoporoids and rudists formed patch-reefs and associated debris rudstones and grainstones. Small patch-reefs are documented at Section GHE2 (see Figure 19) and near Section GHAE below the semi-restricted lagoonal facies. The patch-

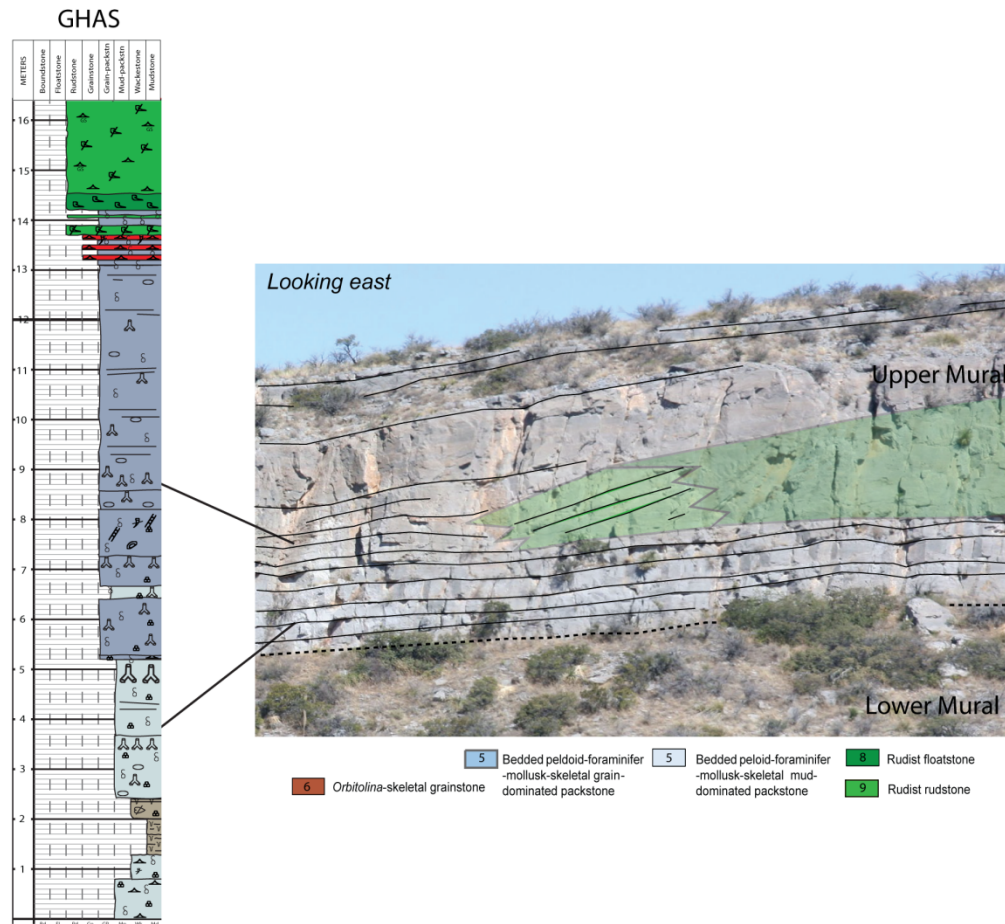


**Figure 18.** Composite section GHAS showing vertical facies associations of ramp-interior facies. The majority of this outcrop is composed of well-bedded peloid-foraminifer-mollusk-skeletal mudstone and grain-dominated packstone (facies 5) and is associated with rudist floatstone (facies 8) buildup and rudist rudstone (facies 10) flank facies (green). These facies are the cliff-forming limestones. The top of this section is comprised of thin- to medium-bedded miliolid-peloid wackestones intercalated with wavy-laminated mudstone (facies 2), arenaceous algal-skeletal mud-dominated packstones (facies 3), and minor mollusk siliciclastic sandstone (facies 1). These facies comprise the relatively recessive and partially covered beds at the top of the photo. The boundary between the Lower Mural and Upper Mural facies is indicated by the dashed line.

reef at GHE2 measures 6 m in relief, but is likely not fully exposed due to high-angle dips (~73 degrees) and faulting. The matrix of this patch-reef is comprised of skeletal-

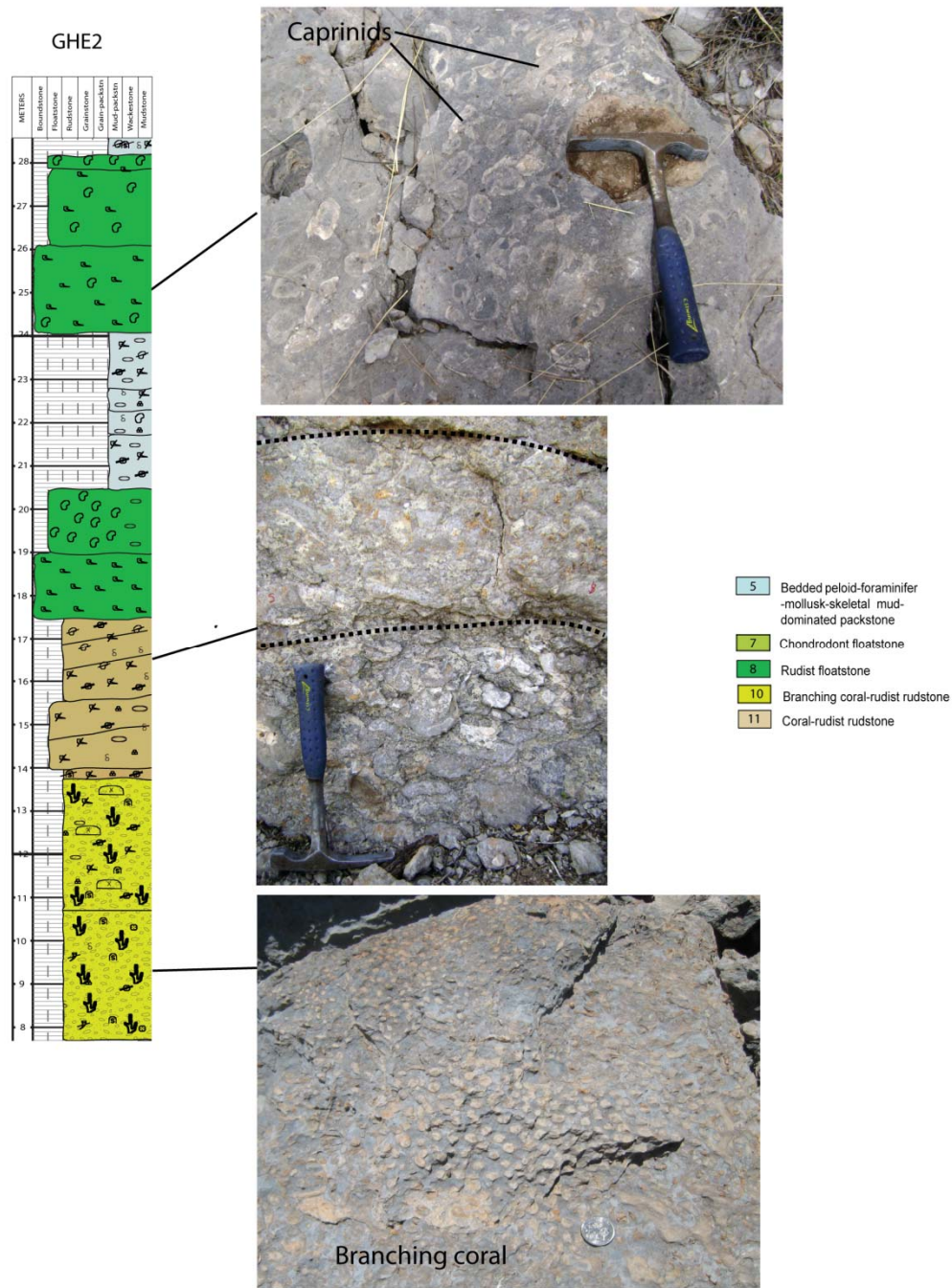


**Figure 19.** Rudist floatstone (facies 8) buildups up to 5 m in relief at Section GHE2. These buildups overlie a massive bed of branching coral-skeletal framestone (facies 10) and rudist-coral rudstone (facies 11) that are interpreted to be a small patch-reef and associated debris facies. The coral patch-reef may have provided antecedent topography for preferential nucleation of the rudist buildups.

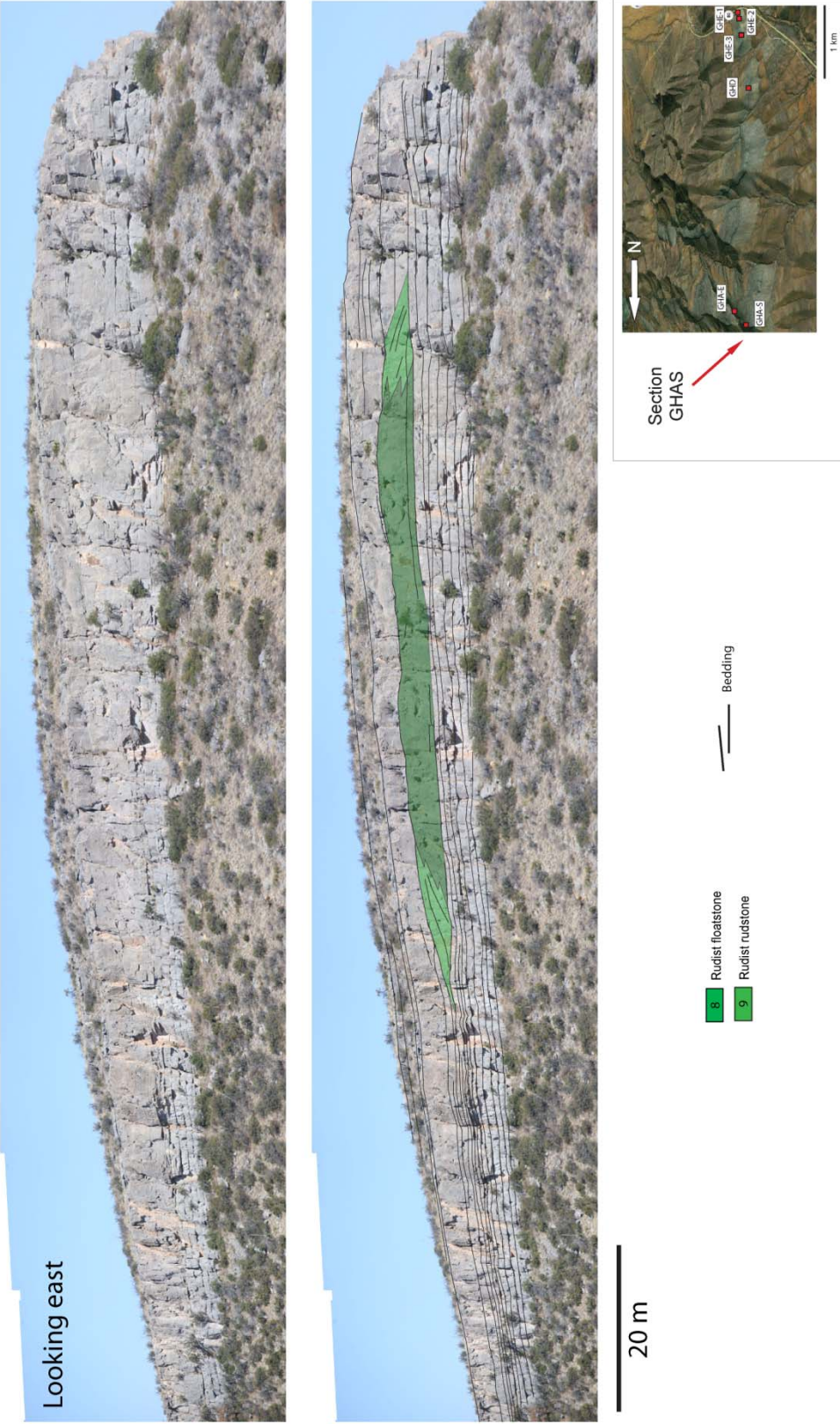


**Figure 20.** Stratigraphic geometry of bedded ramp interior carbonates at the Grassy Hill GHAS outcrop. Well-bedded peloid-foraminifer-mollusk-skeletal mud- to grain-dominated packstones (facies 5) comprise the majority of the stratal architecture. Bedding is predominantly horizontal. A rudist buildup measures ~ 7 m high and is outlined in green. This buildup is exposed in an oblique-strike section where both build-up and debris facies are observed. Debris facies are identified by flank beds that dip away

peloidal mud-dominated packstone. The patch-reef is overlain with rudist-coral debris rudstone (see Figure 15A) that is correlated to Section GHE3 to the north (Figure 21). This lateral facies transition suggests leeward (north) transport of reef-derived debris. A similar capping rudist-coral rudstone is present at the patch-reef to the northwest of Section GHAE. *Orbitolina*-mollusk-peloid grainstone is locally abundant above rudist floatstone buildups at Sections GHE3, GHAS and GHAE (see Figure 21) and may indicate shoaling into fair-weather wave base. Patch-reefs and associated rudist floatstone buildups are assumed to persist seaward to the Paul Spur patch-reef locality (see Figure 16). The environments of the Paul Spur patch-reef are addressed in Section 4.

#### **CYCLICITY**

A subregional cross-section depicting 2D facies architecture is shown in Figure 21. While vertical and lateral facies associations reveal complex facies architecture, there is little evidence of well-developed cyclicity within the measured sections. This is a common phenomenon in peak greenhouse settings such as the Cretaceous where low-amplitude sea-level fluctuations prevent updip (peritidal) cycles from deepening and downdip (subtidal) cycles from shoaling to sea-level (Read, 1995). The result is a series of amalgamated subtidal cycles that are difficult to delineate and correlate (Read, 1995). The sections at Grassy Hill exhibit this type of weakly-cyclic to non-cyclic character. Thus, only the large-scale accommodation trends such as the aggradational/progradational systems tracts proposed by Scott and Warzeski (1993) are observable for the Grassy Hill outcrops in this study. Three cycles are proposed for the area (see Figure 21).

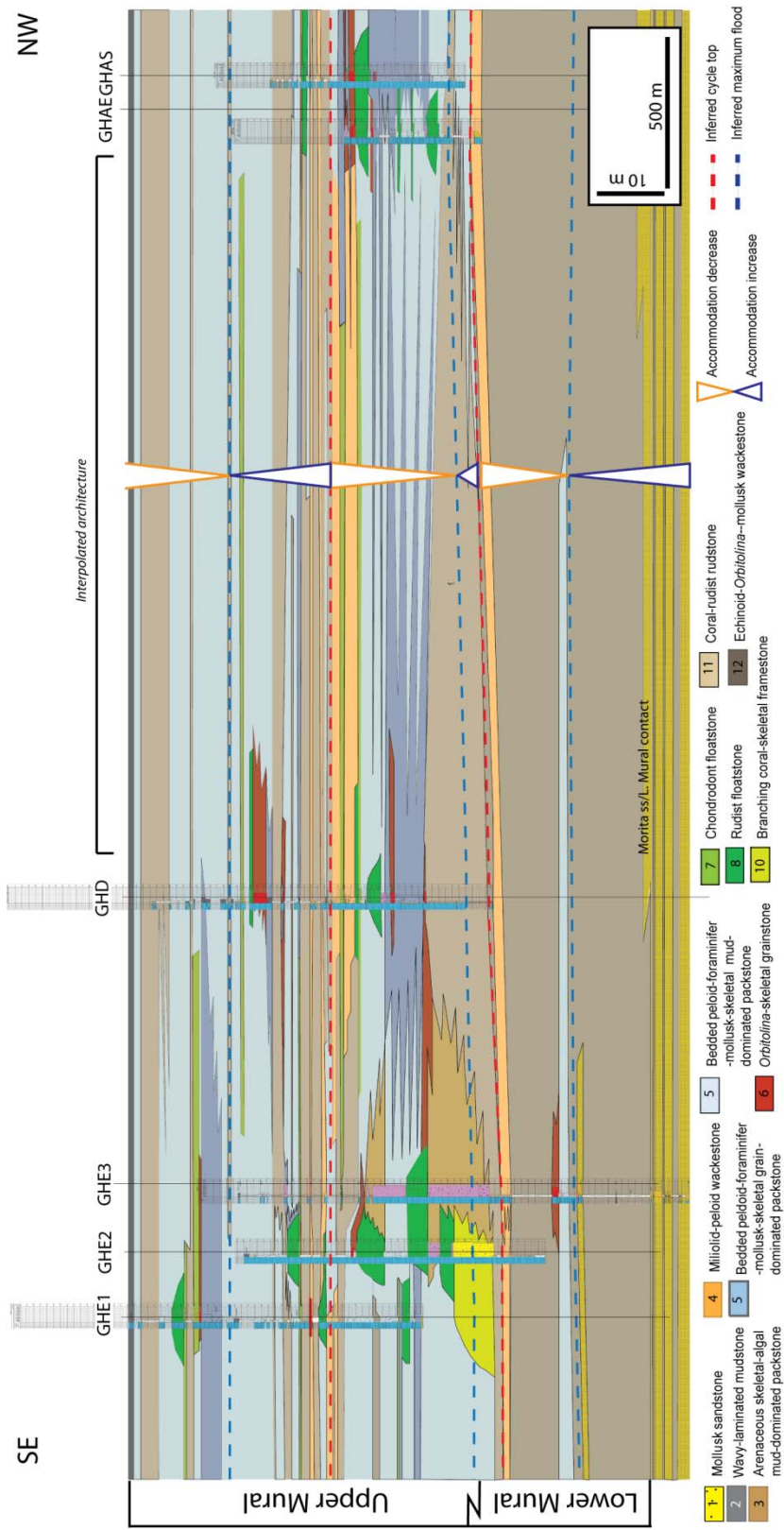


**Figure 21.** Facies architecture of the Mural Limestone ramp interior at the Grassy Hill and Paul Spur patch-reef study areas, southeastern Arizona. The conceptual model spans a 5 km transect and represents a depositional dip profile from north to south. The Grassy Hill facies are interpreted to be deposited in marginal marine/restricted lagoon, ooid shoal, and shallow subtidal setting. Marginal marine/restricted lagoonal facies include facies 1-4. Ooid shoal facies were identified by Scott (1979) and are located between Sections GHAEGHAS and GHD where outcrop access for this study was not granted. Shallow subtidal facies consist of facies 5-11, and include small coral-algal patch-reefs, and rudist buildups (facies 8). Facies 8 is found in various settings: Relatively thick rudist floatstones are associated with facies 5, particularly where they stack above facies 10 at Section GHE2. facies 8 is also found in higher energy settings where they are associated with facies 6. Relatively thin rudist floatstone buildups are found in restricted lagoon settings where they are associated with facies 4. The Grassy Hill facies are overall weakly-cyclic; three Upper Mural cycles are proposed for the entire section.

## 4. Characterization of Paul Spur Reef

### FACIES

The focus of work at Paul Spur was to document the lateral facies heterogeneity and vertical stacking patterns of a well-exposed Early Albian patch reef analogous to producing equivalents in the Maverick Basin. Fifteen sections were measured at 50 m to 200 m spacing at the Paul Spur reef (Figure 22). Additionally, detailed mapping of the patch-reef revealed cyclicity similar to that of patch reefs in the Maverick Basin previously studied by Loucks and Kerans (2003) and Aconcha (2008). Furthermore, lateral and vertical facies distributions are complex and reveal important relationships between reef frame and backreef debris aprons in terms of identifying reservoir quality and extent. Eleven depositional facies were identified in the reef based on faunal assemblages, energy regime and stratigraphic context (see Figure 22). The reef facies and their associated depositional environments are described in the following section, beginning with the basal facies of the older reef. These facies are summarized in Table 2.

#### **Facies 1: Echinoid-*Orbitolina*-mollusk wackestone**

**Description:** Echinoid-*Orbitolina*-mollusk wackestone forms beds 20-60 cm thick that are comprised of nondescript fine-grained skeletal hash (30%), mollusk fragments (10%) and *Orbitolina* foraminifera (5%) floating within a lime mud matrix (Figure 23A). In thin section, skeletal fragments are poorly sorted (100-600  $\mu\text{m}$ ). *Orbitolina* are up to 4 mm in diameter and exhibit a low aspect-ratio (disk-like). Mollusk fragments include oysters with well-preserved LMC shell wall microstructure and bivalves with former aragonitic

Patch-reef facies (Paul Spur)						
Facies	Compositor		Color	Bedding		Depositional Environment
	Lime mud	Dominant Aliochems		Thickness	Character	
1 Echinoid- <i>Orbitolina</i> -mollusk wackestone	55%	nondescript skeletal fragments (30%) mollusk (10%) <i>Orbitolina</i> (5%)	dark gray	20 - 60 cm	recessive-weathering	open subtidal ramp
2 <i>Orbitolina</i> -skeletal rudstone	5%	<i>Actinastrea</i> (20%) oyster (5%) echinoids (5%) intracrystals (5%) rudists (5%) <i>Orbitolina</i> (10%) other coral (5%)	light gray	1- 2.5 m	massive	subtidal shoal
3 Microbial- <i>Microsolena</i> framestone	30%	<i>Microsolena</i> (40%) microbialite (10%) other coral (10%) bivalves (5%) stromatolites (5%)	medium to dark gray	15 - 9.1m	massive no n-bedded	reef frame low to moderate energy below FWMB
4 Algal- <i>Actinastrea</i> boundstone	3%	<i>Actinastrea</i> (45%) <i>Lithocodium/Bacinella</i> (40%) microbialite (5%) caprinids (5%)	light gray to tan	2.1- 5.1m	massive no n-bedded	reef frame shallow wave-agitated setting within FWMB
5 Bored algal- <i>Actinastrea</i> floatstone	15%	<i>Actinastrea</i> (40%) <i>Lithocodium/Bacinella</i> (5%) litho phagid bivalves (20%) solitary coral (5%)	medium gray	1- 2 m	nodular, coarsening upward	shallow subtidal
6 Rudist-coral rudstone	10%	<i>Actinastrea</i> (25%) <i>Microsolena</i> (25%) <i>Lithocodium/Bacinella</i> (5%) requienids (5%) caprinids (10%) serpulid worm tubes (5%)	medium to light gray, tan	35 cm - 1m	nodular to massive	backreef debris apron between SWB and FWMB
7 Echinoid-mollusk peloidal grain-dominated packstone	10%	peleids (40%) mollusk fragments (25%) echinoids (5%) foraminifera (5%) coral (5%)	medium gray	50 - 70 cm	massive	shallow subtidal reef flank
8 Branching coral-skeletal framestone	10%	Branching coral (35%) <i>Actinastrea</i> (25%) <i>Microsolena</i> (5%) <i>Lithocodium/Bacinella</i> (5%) stromatolites (5%) caprinids (5%)	light gray to tan	14 - 4.6 m	massive no n-bedded	reef frame moderate energy
9 Caprinid-requienid floatstone	10-30%	requienids (40%) caprinids (30%) monopleurids (10%) radiolites (10%) <i>Lithocodium/Bacinella</i> (5%) serpulid worm tubes (5%)	medium gray	6.4 m	massive no n-bedded	capping reef frame moderate energy
10 Caprinid-requienid rudstone	10%	requienids (40%) caprinids (30%) monopleurids (10%) radiolites (10%)	blue-gray to red -brown	2.7 - 3.5 m	massive to nodular	backreef debris apron between SWB and FWMB
11 (Silicified) <i>Orbitolina</i> -skeletal grainstone	0%	mollusks (30%) <i>Orbitolina</i> (5%) echinoids (10%) foraminifera (2%)	light to medium gray	1m?	massive	backreef shoal within FWMB

Table 2. Summary of the depositional facies at the Paul Spur patch-reef.

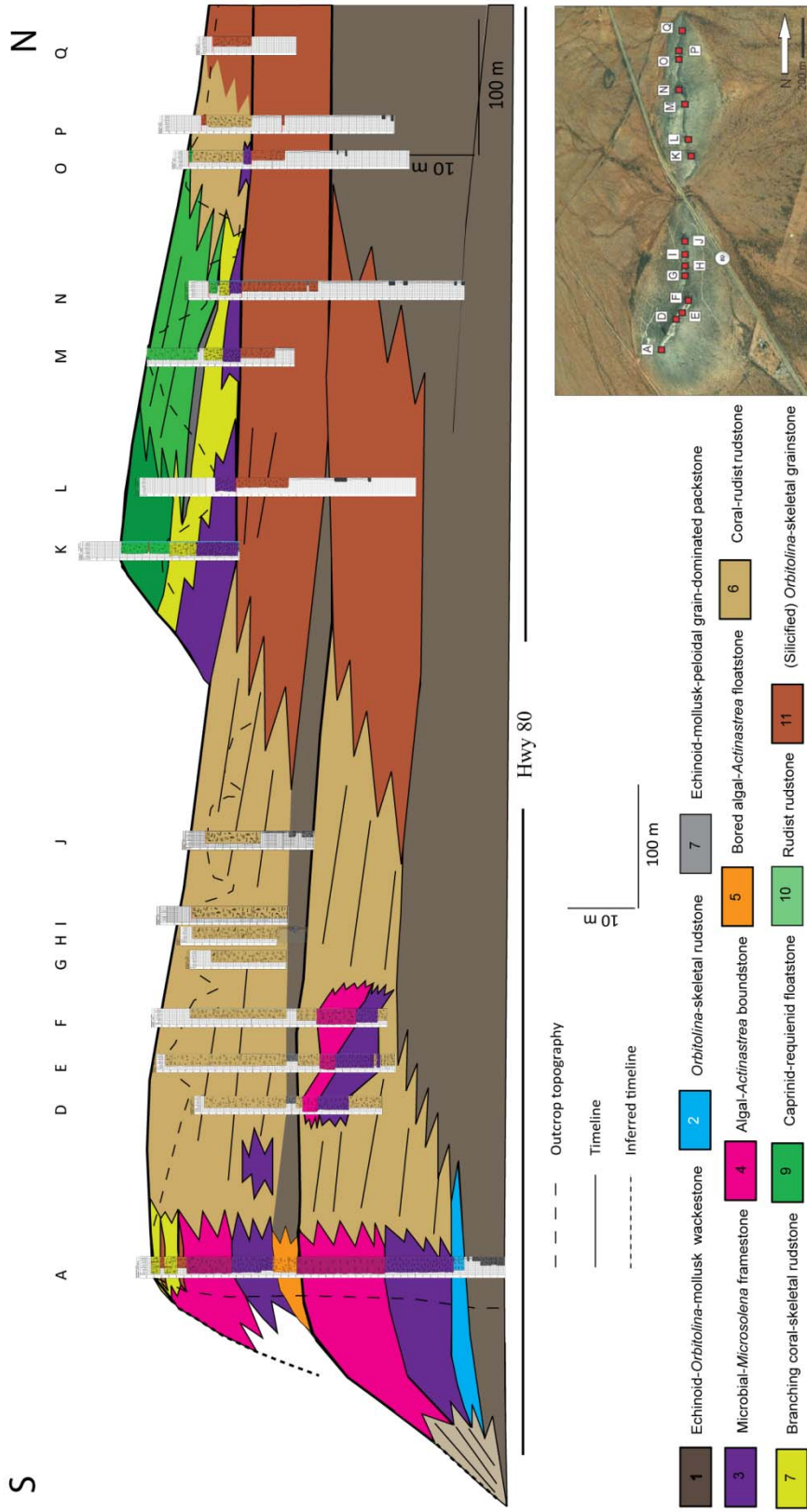


**Figure 22.** Section locations at Paul Spur with cross-section and facies distributions from measured section data and facies mapping.

shell walls have that have been leached and subsequently replaced with equant calcite. Some echinoid plates exhibit syntaxial overgrowth of calcite cement. Minor constituents include coral fragments (2%), echinoid fragments (2%) and biserial and planispiral foraminifera. Original moldic porosity is occluded with equant calcite spar. Echinoid-*Orbitolina*-mollusk lime wackestone is overlain by *Orbitolina*-rudist-coral rudstone at Sections A-F (Figure 23B); a second medium (~30 cm) bed is intermittently exposed within the rudist-coral rudstone facies at these locations (Figure 24). It grades laterally to and is overlain by *Orbitolina*-skeletal grainstone (facies 2) at Sections M-P.

**Depositional Environment:** Depositional environment is interpreted as open subtidal ramp and lower reef flanks, below fair-weather wave base (Scott, 1979; Vilas et al., 1995; Aconcha, 2008). Petrographic evidence for a deeper-water environment relative to that of subsequent facies includes high abundance of carbonate mud and poor sorting, and disk-like morphology of *Orbitolina* benthic foraminifera (Vilas et al., 1995). Immenhauser and Scott (2002) documented similar facies in the Albian shelf carbonates in the Wadi el Assyi platform, Oman based on *Orbitolina* morphology. *Orbitolina*-rich shallow shelf facies are documented in the Aptian Shuaiba platform (Burchette and Britton, 1985; Alsharan, 1995), Aptian off-reef low energy shelf carbonates of SE Spain (Vilas, et al., 1995) and the Maverick Basin of Texas (Loucks and Kerans, 2003). This facies is analogous to Scott's (1979) mollusk-miliolid-*Orbitolina* wackestone.

#### **Facies 2: *Orbitolina*-rudist-coral rudstone**

**Description:** Light grey *Orbitolina*-rudist-coral rudstone forms a thick (~1 m) to massive (2.5 m) bed comprised of *Actinastrea* fragments coated with

*Lithocodium/Bacinella* (20%), oysters (15%), echinoids (10%), large (up to ~2 cm) rudist fragments, including monopleurids, requienids and caprinids (15%) and flat *Orbitolina* foraminifera (10%) (see Figure 23B). Intraclasts are common (15%). Lime mud is present between grains (<5%) and is preferentially dolomitized and iron-stained; otherwise, grains are cemented with equant calcite and syntaxial cements are common on echinoid fragments. Original moldic porosity is occluded with equant calcite spar. *Orbitolina*-rudist-coral rudstone overlies and grades laterally to the north into echinoid-*Orbitolina*-mollusk wackestone (facies 1) and echinoid-mollusk-peloidal grain-dominated packstone (facies 7) to the west. It is overlain by microbial-*Microsolena* framestone (facies 3) and rudist-coral rudstone (facies 6) at Sections A-F (see Figure 24).

**Depositional Environment:** The depositional environment is interpreted as a discontinuous subtidal shoal that served as the nucleus upon which the pioneer *Microsolena* reef community (described below) was established. Subtidal shoals are common nucleation points for patch-reef development (James, 1983). The presence of flat *Orbitolina* with skeletal rudstone suggests that deeper-water *Orbitolina* sourced from underlying echinoid-*Orbitolina*-mollusk wackestone were re-worked into the shoal environment during a period of marine transgression. The shoal substrate was likely stabilized by algae, echinoids, and other encrusting biota to form a stable substrate for patch-reef nucleation (James, 1983).

### **Facies 3: Microbial-*Microsolena* framestone**

**Description:** Massive to nodular-weathering blue-gray framestone (Figure 25A) is

comprised predominantly of platy *Microsolena* corals (40%) with encrusting microbialite (10%) (Figure 25B) in a lime mud matrix (30%). Associated allochems

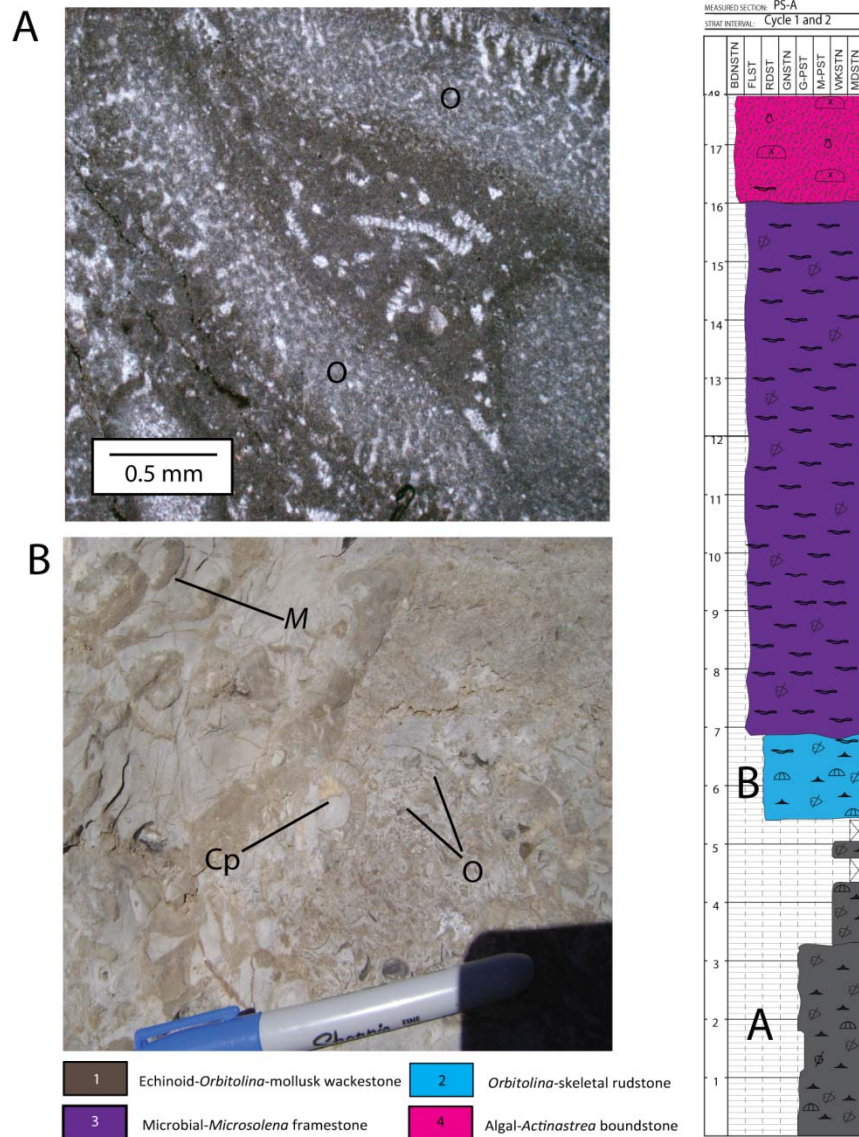


**Figure 23.** Photomicrographs of basal Paul Spur facies at Section A. A) Echinoid-*Orbitolina* (O)-mollusk wackestone (facies 1) forms medium to thick beds and is indicative of an open-marine ramp depositional environment. B) *Orbitolina*-skeletal rudstone (facies 2) with small, flat reworked *Orbitolina* (O), *Microsolena* (M), and caprinids (Cp) is interpreted as a shoal upon which the Paul Spur patch-reef nucleated.

include branching and solitary corals (10%), thin-shelled lithophagid bivalves (5%) and boring sponges (Rigby and Scott, 1981). *Microsolena* corals weather dark gray are capped with light gray faintly-laminated stromatolites (Scott, 1979). Stromatolitic laminations are less than 1 mm thick. Both corals and stromatolites are moderately bored by thin-shelled bivalves; borings measure ~1cm in length and are filled with light grey mud. Voids within the *Microsolena* frame are filled with fine-grained bioclastic sediment or lime mud. Original macroporosity is not observed. Microbial-*Microsolena* framestone overlies *Orbitolina*-skeletal rudstone (facies 2) at Section A and is underlain by algal-*Actinastrea* boundstone (facies 4) at Sections A-F (See Figure 24). It overlies *Orbitolina*-skeletal grainstone (facies 11) and underlies branching coral-rudist framestone (facies 8) at Sections K-O (Figure 25C).

**Depositional environment:** This facies is interpreted as a deeper, quieter depositional environment based on the platy morphology of *Microsolena* corals and presence of associated delicate branching corals and boring sponges (Rigby and Scott, 1981; Dupraz & Strasser, 2002), and high abundance of carbonate mud, internal bioclastic sediment and/or clay. A homogenous assemblage of encrusting cyanobacterial stromatolites and microbialites may also be indicative deeper water, where these organisms are adapted to low light intensities. Paucity of phototrophic encrusting organisms such as blue green algae and *Lithocodium/Bacinella* (Schmid and Leinfelder, 1996) further support this interpretation. It may be concluded based on the aforementioned observations, that, the *Microsolena* community thrived below fair weather wave base. Similar deep- water pioneering microsolenid communities have been

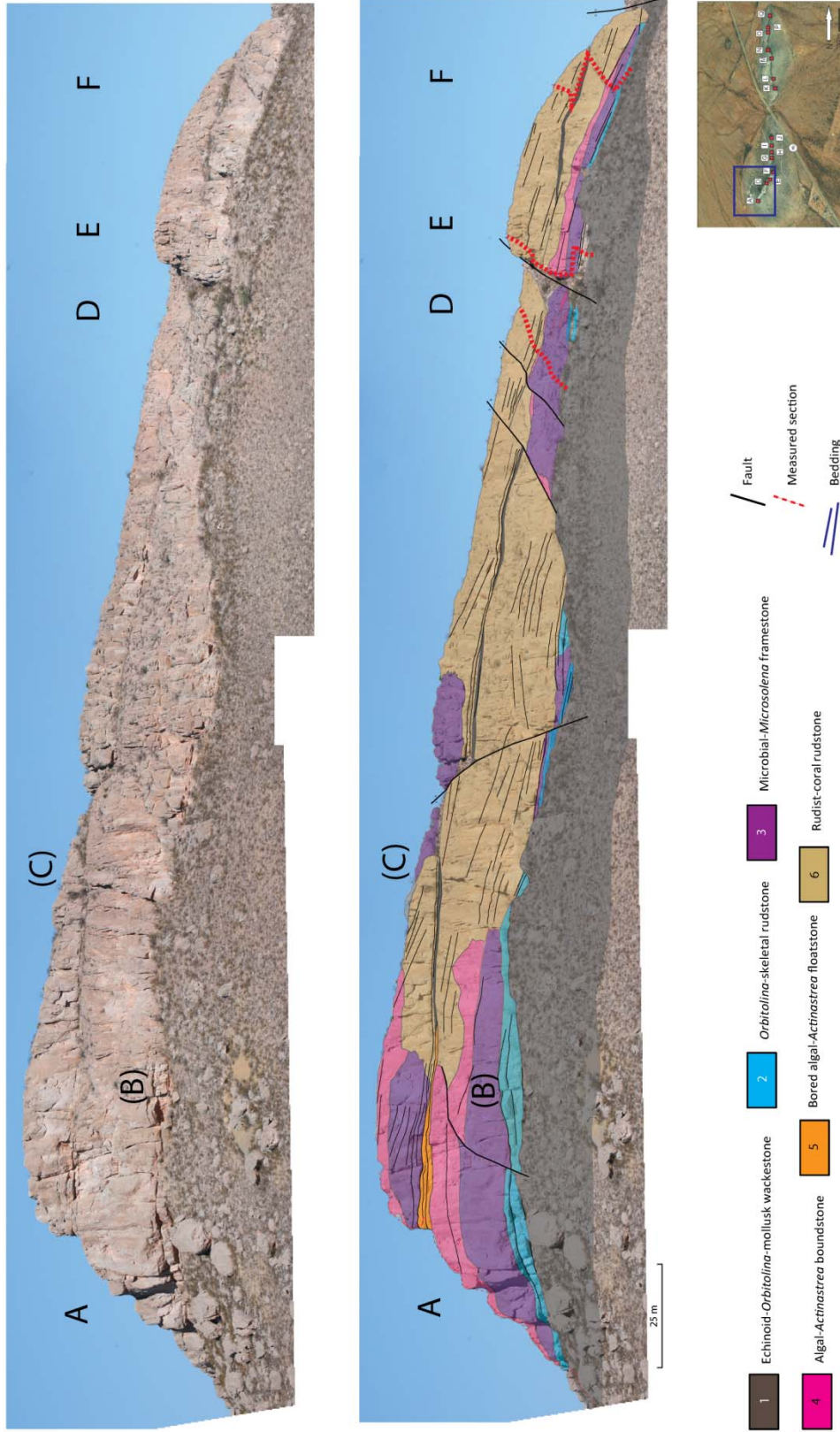


**Figure 24.** Uninterpreted and interpreted sections at Paul Spur Sections A-F. Coral framestones and boundstones (facies 3 and 4) are dominant at Section A. The majority of the outcrop is composed of rudist-coral rudstone debris (facies 6). A thin bed of echinoid-*Orbitolina*-mollusk wackestone (facies 1) spans the entirety of the outcrop above facies 4, 5, and 6 and separates two stages of reef growth.

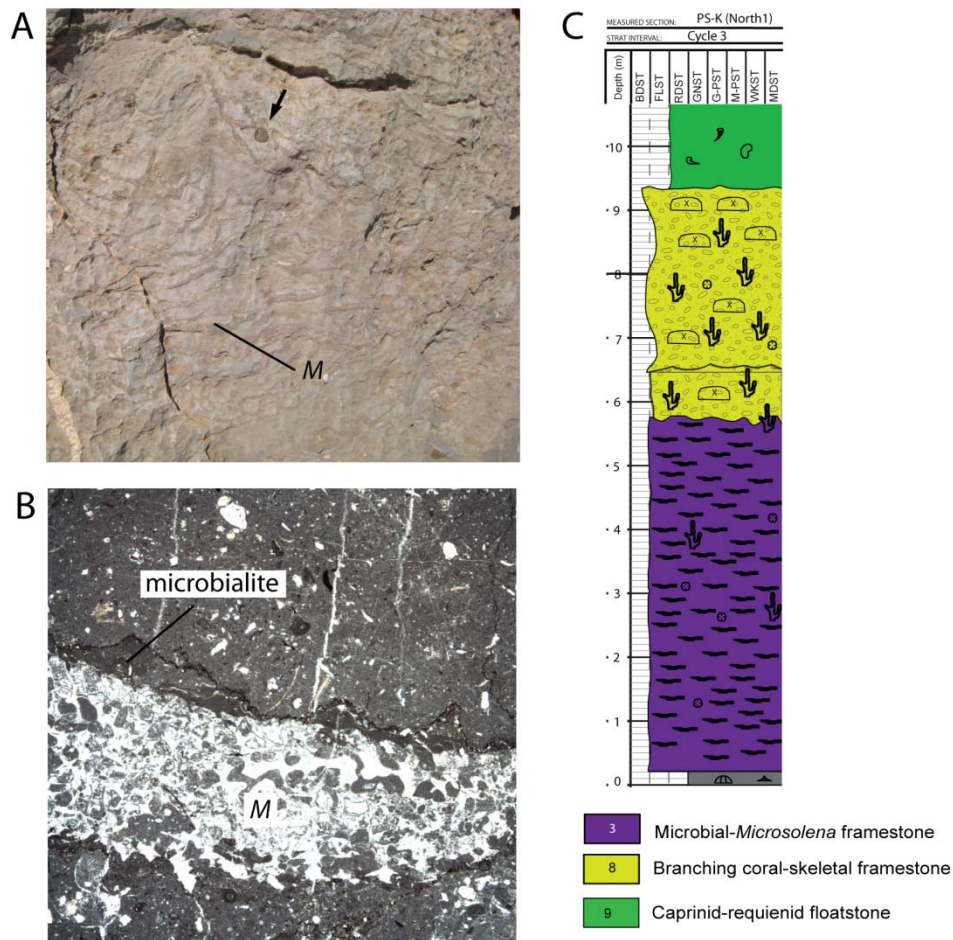


**Figure 25.** A) Microbial-*Microsolena* framestone (facies 3) showing platy morphology of dark gray *Microsolena* (M) corals. B) *Microsolena* are encrusted with cryptic microbialite, which appears darker than surrounding lime wackestone matrix. Microbial-*Microsolena* framestone is interpreted to be a pioneering coral community that thrived in relatively deep water at Paul Spur. Similar microsolenid coral colonies are documented in Early Cretaceous patch-reefs in eastern Spain (Götz et al., 2005) and in Late Jurassic (Oxfordian) platforms of central Europe (Insalaco, 1995; Dupraz & Strasser, 2002), C) In addition to Section A, microbial-*Microsolena* framestone is present at Section K (shown) and Sections L-O.

documented in eastern Spain (Götz et al., 2005) and in upper Jurassic (Oxfordian) platforms of central Europe (Insalaco, 1995; Dupraz & Strasser, 2002).

#### **Facies 4: Algal-*Actinastrea* boundstone**

**Description:** Algal-*Actinastrea* boundstone weathers light tan and forms a massive bed at Section A (Figure 26A). This facies is comprised primarily of *Actinastrea* massive corals (45%) that are 10-30 cm in length (Figure 26B) and heavily encrusted with dark gray rinds of *Lithocodium aggregatum* and *Bacinella irregularis* (45%). Accessory allochems include caprinids (5%), microbial micrite (5%), echinoids (2%) and monopleurids (1%). Encrusting biota are diverse and consist of flat to domal encrusting algae (?), including *Lithocodium/Bacinella* (Figure 26C) and green algae (?) which are in turn encrusted with dark, micritic and structureless organisms of possible microbial origin. Lime mud is a minor component (3%). As this facies consists of prolific binding organisms, there is little primary porosity observed. Coral septa and other allochem molds are occluded with equant calcite spar. Microdigitate stromatolites are present but rare. Small syndepositional fractures ~30 cm long by ~6 cm wide are oriented normal to the reef margin. Large meter-scale syndepositional fractures are also common. The fractures are filled with cemented brown coarse skeletal grain-dominated packstone to grainstone (Figure 27). Algal-*Actinastrea* boundstone is restricted to Section A where it overlies microbial-*Microsolena* framestone (facies 2) and grades laterally into high-energy rudist-coral rudstone (facies 6) to the north (see Figure 24). It is overlain by bored algal-*Actinastrea* floatstone (facies 5) (see Figure 26C).

**Depositional environment:** The algal-*Actinastrea* boundstone facies represents a discrete coral community that overlies microbial-*Microsolena* framestone. This facies is interpreted as residing in clear, shallow, and wave-agitated waters based on

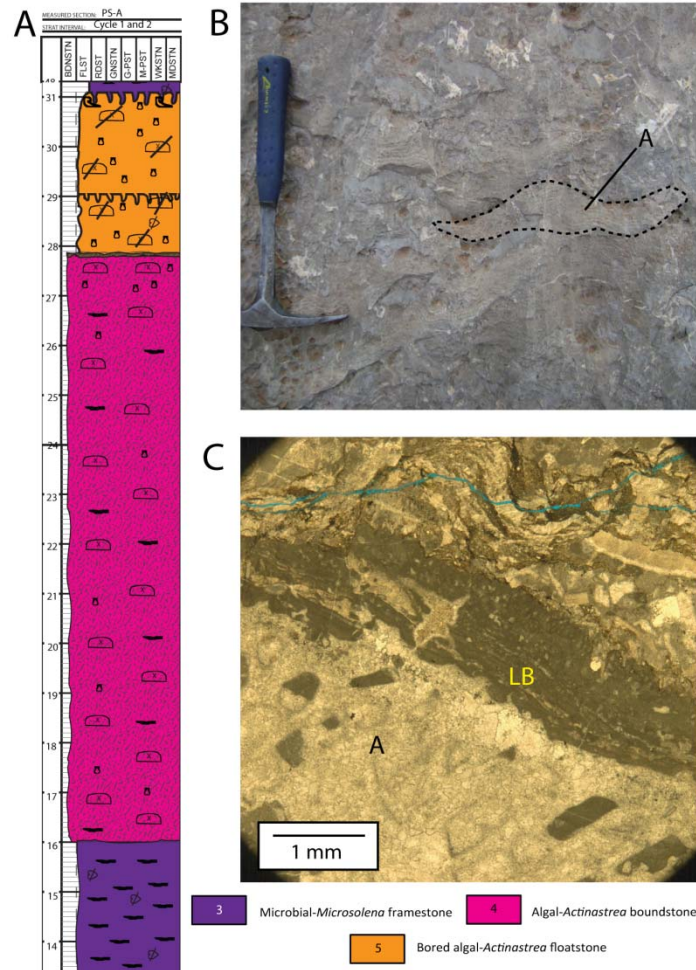


**Figure 26.** A) Algal-*Actinastrea* boundstone (facies 4) is most prevalent at Section A. B) Algal-*Actinastrea* (A) boundstone exhibits a domal morphology, C) *Actinastrea* (A) are encrusted with *Lithocodium/Bacinella* (LB).

massive/encrusting morphology of *Actinastrea* and an abundant and diverse assemblage of encrusting organisms with little internal sediment infill or mud. Phototrophic encrusting organisms such as *Lithocodium/Bacinella* provide the best evidence for shallow well-lit conditions (Dupraz & Strasser, 2002). The presence of syndepositional

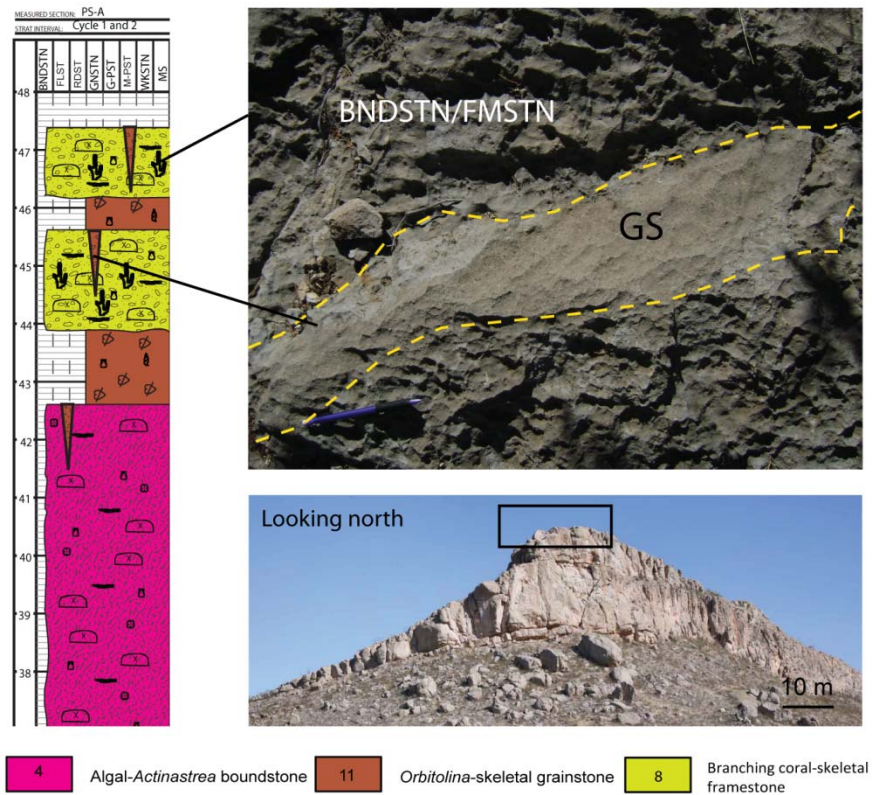


**Figure 27.** An example of a syndepositional fracture located at the top of the Paul Spur reef is outlined in yellow. The fractures are oriented normal to the reef margin and are filled with coarse cemented *Orbitolina*-skeletal grainstone (facies 10). Syndepositional fractures are indicators of early marine lithification resulting from organic binding and/or cementation of the margin that is associated with wave-agitated settings (Frost and Kerans, 2010).

fractures indicates early marine lithification from encrustation/binding and cemented grainstone infill (Frost and Kerans, 2010) typically associated with high wave-energy settings.

### **Facies 5: Bored Algal-*Actinastrea* floatstone**

**Description:** Nodular-weathering light to dark gray floatstone is comprised primarily of large (4-30 cm) *Actinastrea* (40%) that are encrusted with *Lithocodium/Bacinella* (15%) and bored by lithophagid bivalves (20%) (Figure 28).

Solitary corals (5%) and echinoids (5%) are present but rare. Matrix near the base is predominantly burrowed light blue-gray lime mud (15%) and coarsens upward to skeletal grain-dominated packstone. Iron-staining is associated with burrowed/nodular weathering. *Orbitolina* are not present. Preserved macroporosity is not observed. Bored algal-*Actinastrea* floatstone overlies algal-*Actinastrea* boundstone (facies 4) and is overlain by microbial-*Microsolena* framestone (facies 2) (see Figure 26A). It grades laterally to the north into echinoid-*Orbitolina*-mollusk wackestone (facies 1) (See Figure 24). This facies is constrained to Section A.

**Depositional environment:** The presence of extensive boring indicates that this facies represents a marine hardground unconformity (Shinn, 1969). Extensive boring of reef frame fragments indicates higher rates of bioerosion and therefore low carbonate productivity (Stearn and Scoffin, 1977). This facies represents flooding on the windward patch-reef margin concomitant to flooding on the leeward (north) margin that is represented by echinoid-*Orbitolina*-mollusk wackestone (facies 1) (Figure 28B).

#### **Facies 6: Rudist-coral rudstone**

**Description:** Nodular-weathering rudist-coral rudstone is characterized by large *Microsolena* (25%), *Actinastrea* (25%) and rudist (15%) fragments in skeletal lithoclastic grain-dominated packstone matrix (Figure 29A). Recumbent requienids (10%) and caprinids (10%) are common; monopleurids are rare (1%). Accessory allochems include serpulid worm tubes (10%), *Lithocodium/Bacinella* (15%), echinoids (3%), red algae

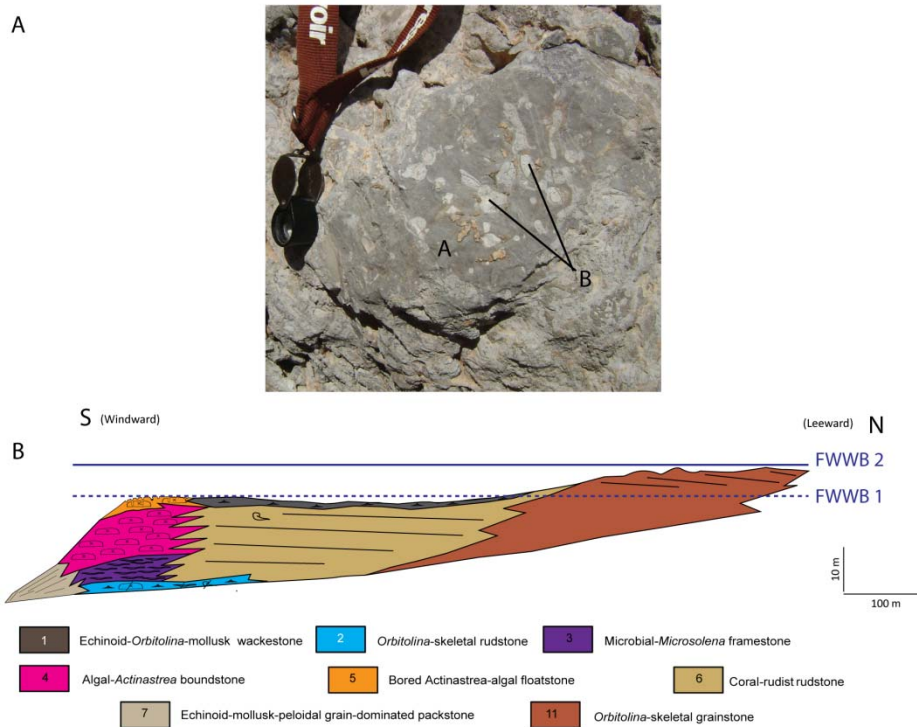


**Figure 28.** A) Bored (B) algal-*Actinastrea* (A) floatstone (facies 5) overlies algal-*Actinastrea* boundstone (facies 4) and underlies microbial-*Microsolena* framestone (facies 4) at Section A. Abundant borings are indicative of slow sedimentation rates (Stearn and Scoffin, 1977) that are commonly associated with platform drowning. B) Schematic diagram showing drowning and subsequent bioerosion from boring bivalves on the reef margin, which is represented by facies 5 floatstone (south), and coeval deposition of open ramp echinoid-*Orbitolina*-mollusk wackestone (facies 1) on the leeward margin (north).

(1%), oysters (1%). Lime mud is a minor component (10%). *Actinastrea* coral fragments show abundant boring and encrustation with *Lithocodium/Bacinella* (Figure 29B), and in some cases with red algae. Rudists are bored and encrusted with serpulid worm tubes, red algae, and laminated microbial micrite. Equant calcite spar is common within allochem molds; otherwise no primary porosity is observed. Microfractures cross-cut the rudstone fabric and are also filled with equant calcite. Rudist-coral rudstone overlies and grades laterally to the south into algal-*Actinastrea* boundstone (facies 4) and microbial-

*Microsolena* framestone (facies 3) at Section A (see Figure 24) and comprises the majority of facies at Sections D – F. It is the only facies present at Sections G-J (Figure 30) and is also present at Sections O-P.

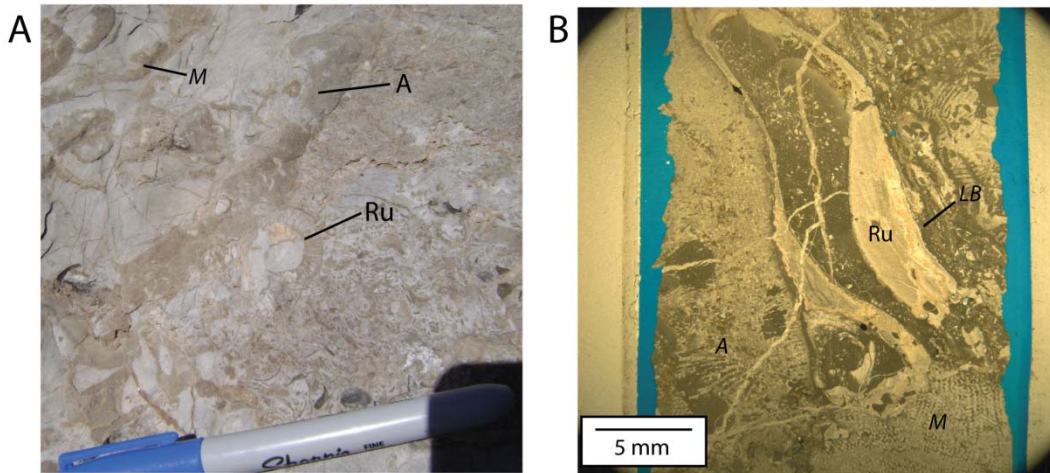


**Figure 29.** A) Outcrop photograph of rudist-coral rudstone (facies 6) showing fragments of *Microsolena* (M), *Actinastrea* (A) and rudists (Ru). B) Corals and rudists are encrusted with *Lithocodium/Bacinella* (LB). Facies 6 forms the outcrops at Sections D-J and is also present at Sections O-P.

**Depositional environment:** Rudstone facies are interpreted as reef-derived debris that is washed to the north into beds by predominantly wave energy (Scott, 1979). The presence of large coral and rudist fragments, as well as other mollusks, echinoderms, and benthic foraminifera support this interpretation. Paleo-water depth was likely between storm and fair weather wave base, as deposition of reef-derived debris is commonly attributed to storm-generated currents (Ball, 1967; Hubbard et al., 1990).

### **Facies 7: Echinoid-mollusk-peloidal grain-dominated packstone**

**Description:** Echinoid-skeletal packstone forms medium beds to the southwest of Section A. It is comprised predominately of peloids (40%), mollusk fragments (25%) and

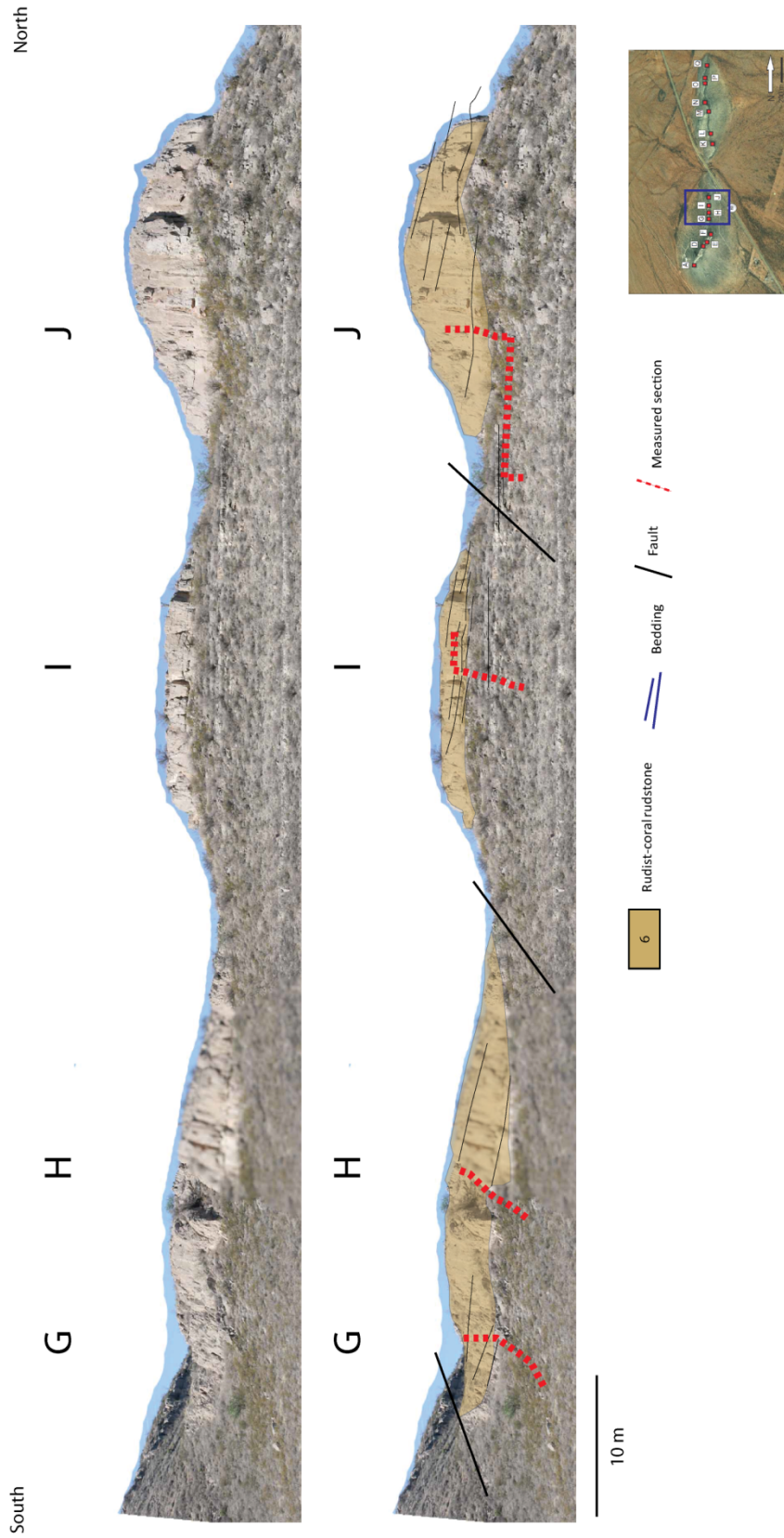


**Figure 30.** Uninterpreted and interpreted sections at Paul Spur Sections G-J just south of Highway 80. All outcrops are comprised of reef debris facies 6. Distinct landward-dipping beds indicate deposition in the leeward direction. Whole caprinid rudists are loosely distributed on top of the sections and may be preserved in growth position. This outcrop is a continuation of bedded reef debris facies from the top section of Figure 11.

echinoids (15%) in a lime mud (10%) matrix (Figure 31A). Peloids may be fragments of *Lithocodium/Bacinella*. Biseriate foraminifera (5%) and coral fragments (5%) are present; coral fragments are often difficult to identify in thin-section. Syntaxial overgrowth cements are common on echinoids. This facies is present to the southwest of Section A where it grades laterally to the east into *Orbitolina*-rudist-coral rudstone (facies 2), microbial-*Microsolena* framestone (facies 3) and algal-*Actinastrea* boundstone (facies 4) (Figure 31B).

**Depositional environment:** Echinoid-mollusk-peloidal grain-dominated packstone is interpreted as reef flank debris facies between storm and fair weather wave base (Scott, 1979).

### **Facies 8: Branching coral skeletal framestone**

**Description:** Branching coral-skeletal framestone is comprised of large in-situ branching corals (35%) up to 60 cm tall, as well as *Actinastrea* (25%) and *Microsolena* (15%) corals (15%) that are both in-situ and within a rudstone matrix. Thin, delicate dendritic corals weather dark gray with fronds a few millimeters wide; larger branching corals weather light tan and have branches up to 3 cm wide (Figure 32A). Corals are encrusted with *Lithocodium/Bacinella* (10%), which is in turn bored. Fragments of dark gray-weathering *Microsolena* with capping laminated blue gray stromatolites (5%) are up to 5 cm in length. Caprinids (5%) are common. Preserved macroporosity is not observed. Branching coral-skeletal framestone overlies microbial-*Microsolena* framestone (facies 3) (Figure 32B) at Sections K-O where its distribution is volumetrically significant

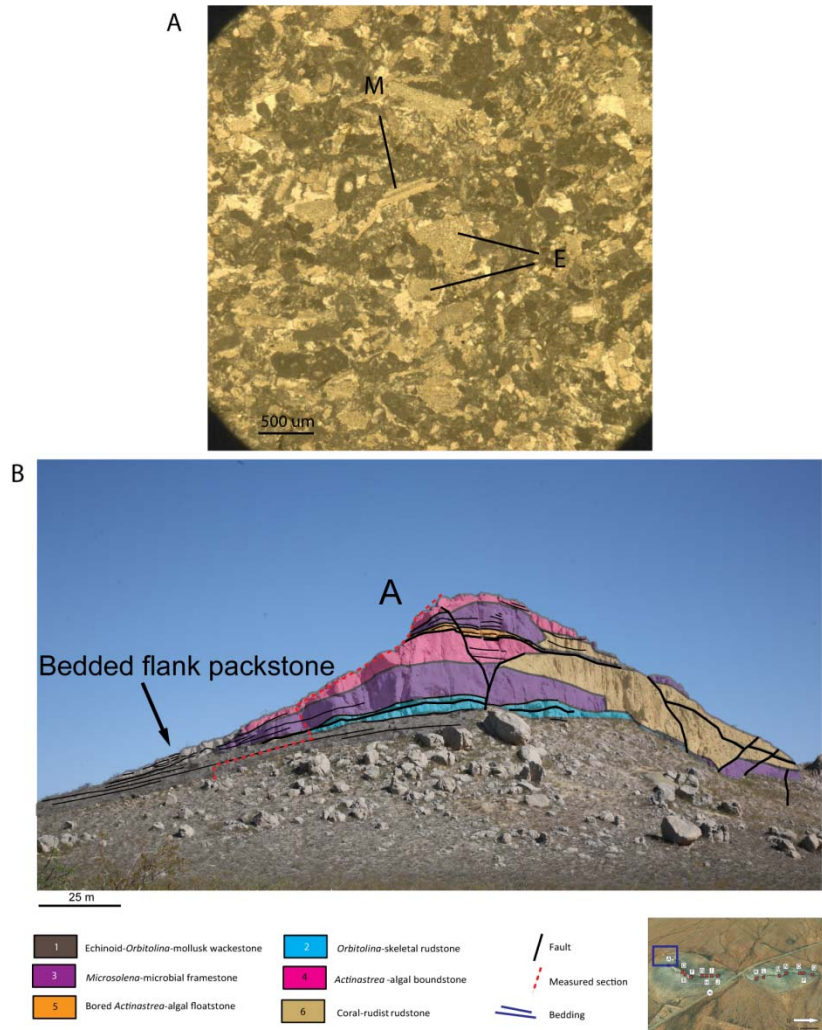


**Figure 31.** A) Echinoid-mollusk-peloidal grain-dominated packstone (facies 7) contains abundant echinoid (E) and mollusk (M) fragments. B) This facies comprises the reef flank beds to the southwest of Section A where it grades laterally into *Orbitolina*-rudist-coral rudstone, microbial-*Microsolena* framestone and algal-*Actinastrea* boundstone.

33 and 34); it is also present as a minor facies component at Section A where it overlies algal-*Actinastrea* boundstone (facies 4) (see Figure 24). Branching coral-skeletal framestone overlies and grades laterally into (silicified) *Orbitolina*-skeletal grainstone (facies 11) at Sections K-O and underlies caprinid-requienid floatstone (facies 9) and caprinid-requienid rudstone (facies 10) at Section M (see Figs. 33 and 34).

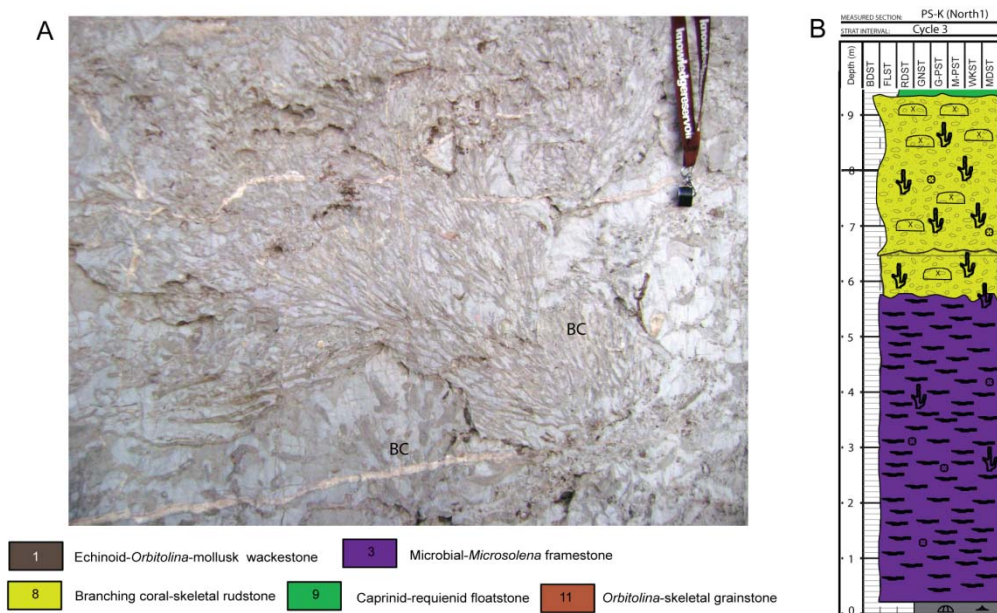


**Figure 32.** A) Branching coral-skeletal framestone (facies 8) contains a diverse assemblage of corals, including different species of branching corals (shown), solitary corals and localized requienid colonies. B) This facies is overlain by capping caprinid-requienid floatstone (facies 9) at Section K.

**Depositional environment:** This facies represents a new stage in reef development that occurred upon antecedent topography formed by the reef crest of the stratigraphically older patch-reef. The presence of delicately branching corals in a muddy matrix with *Lithocodium/Bacinella* suggests that this reef thrived in low to moderate wave energy but well-lit conditions (Dupraz & Strasser, 2002). A rudstone matrix composed of fragmented microbial-*Microsolena* framestone and algal-*Actinastrea* boundstone facies sourced from the stratigraphically older reef is present throughout the section and suggests that this reef may have been subject to intermittent storm deposits that are common in modern settings (Ball, 1967; Baines et al. 1974; Scoffin, 1993; Hughes, 1999).

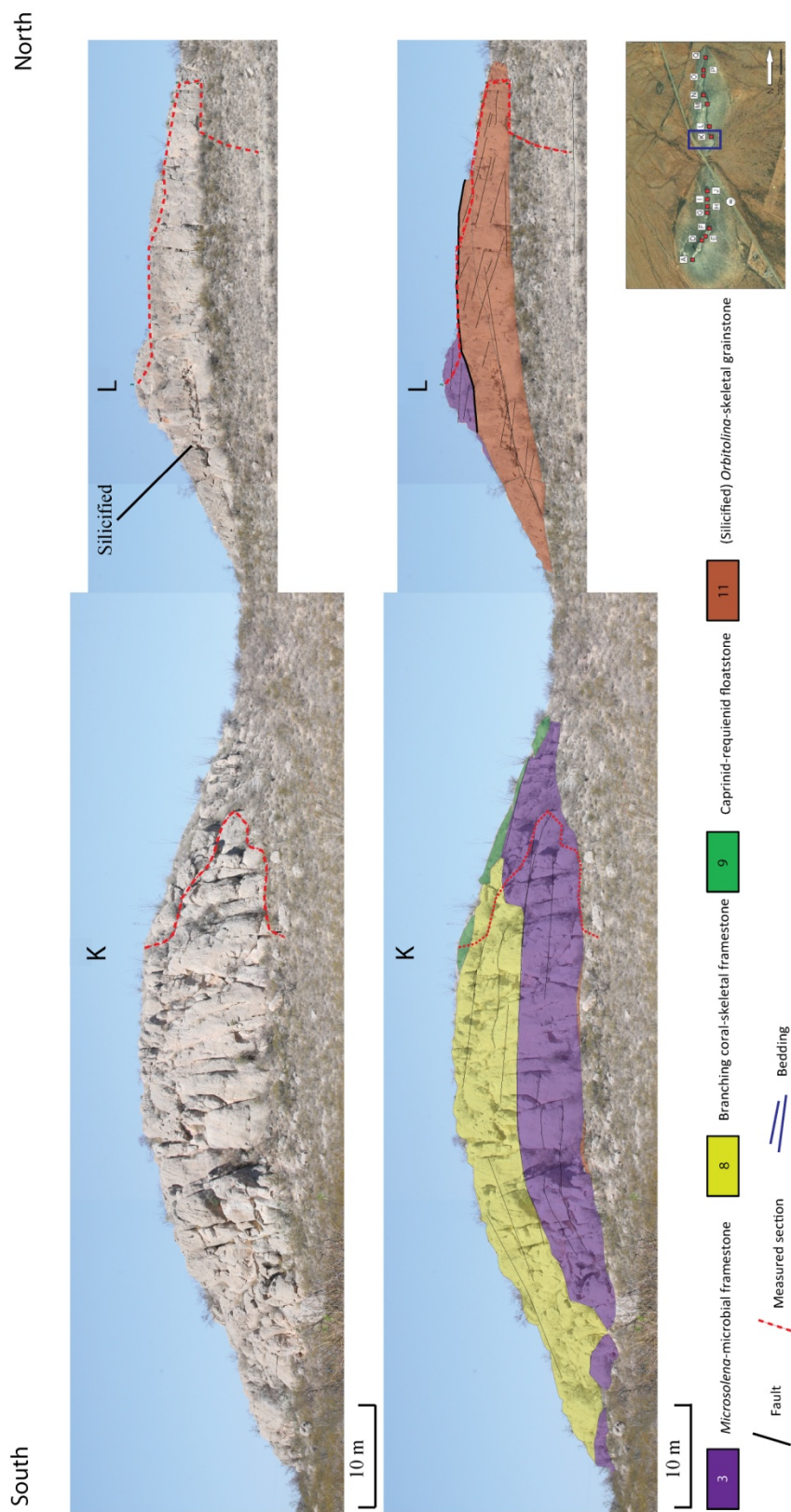


**Figure 33.** Uninterpreted and interpreted sections at Sections K and L. Section K is comprised of a microbial-*Microsolena* framestone (facies 3), branching coral-skeletal framestone (facies 8), and rudist floatstone reef frame (facies 9) that nucleated upon reef debris rudstones from the reef at Sections A-J. The *Microsolena* reef base is correlated to Section L where it overlies back-reef grainstones (facies 11) derived from the reef at Sections A-J. Silicified *Orbitolina*-skeletal grainstone (facies 11) weathers dark gray and is best observed at Section. The overall vertical facies stacking pattern observed at Section L suggests the presence of a younger phase of reef growth than those observed at Sections A-J.

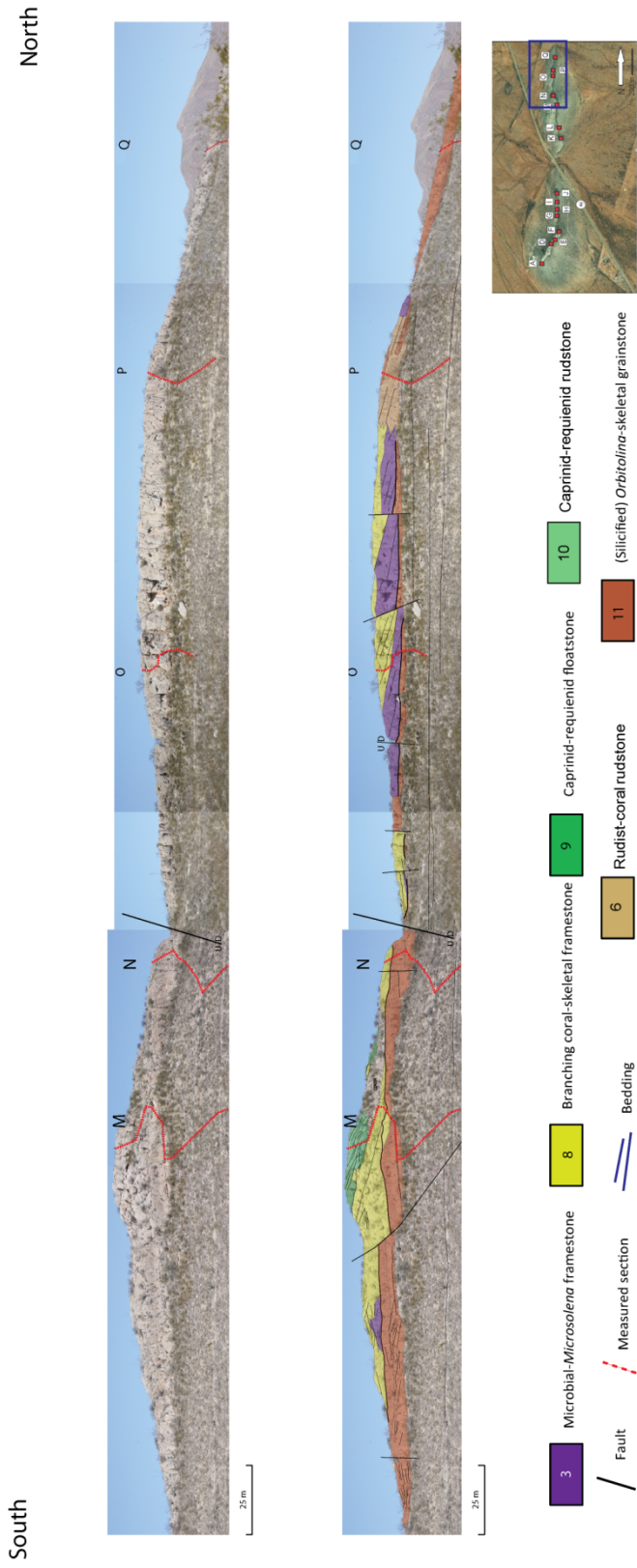


**Figure 34.** Uninterpreted and interpreted photopan at Sections M-Q. Section M and N exhibit the same vertical stacking facies patterns as those found in Sections K and L. The top of Section M is comprised of caprinid-requienid floatstone (facies 9) and caprinid-requienid rudstone (facies 10). Facies 10 is well-bedded with beds that dip to the north. Note that *Orbitolina*-skeletal grainstone (facies 11) spans the entirety of the outcrop and dips into the subsurface; it is the most laterally extensive of all facies documented at Paul Spur.

### **Facies 9: Caprinid-requienid floatstone**

**Description:** Light to medium gray smooth weathering caprinid-requienid floatstone comprises the capping reef community at Section K (Figure 35A). This facies contains a diverse assemblage of rudists, including large requienids (40%) (Figure 35B), caprinids (30%) (Figure 35C), monopleurids (10%) and radiolitids (10%) (Figure 35D). Rudists float in an echinoid-mollusk wackestone to grain-dominated packstone matrix and are commonly encrusted with *Lithocodium/Bacinella* (Figure 35E), serpulid worm tubes and dark gray microbialite. Encrusting green algae are present but rare. Geopetal structures are preserved and cavities are occluded with equant calcite spar. The various rudist groups are well-developed on the dip slope at Section K where they overlie branching coral-skeletal framestone (facies 8) and grade laterally into caprinid-requienid rudstone (facies 10) to the north (See Figure 34).

**Depositional environment:** Caprinid-requienid floatstone represents the capping reef community at Paul Spur. The abundance of carbonate mud as seen in thin section suggests that the rudist colonies likely thrived where they were protected from high energy wave activity. Additionally, a change from a coral-dominated reef community to a rudist-dominated reef community suggests that local environmental controls such as increased nutrient supply at Paul Spur favored heterotrophic communities (Hallock and Schlager, 1986; Hofling and Scott, 2002).

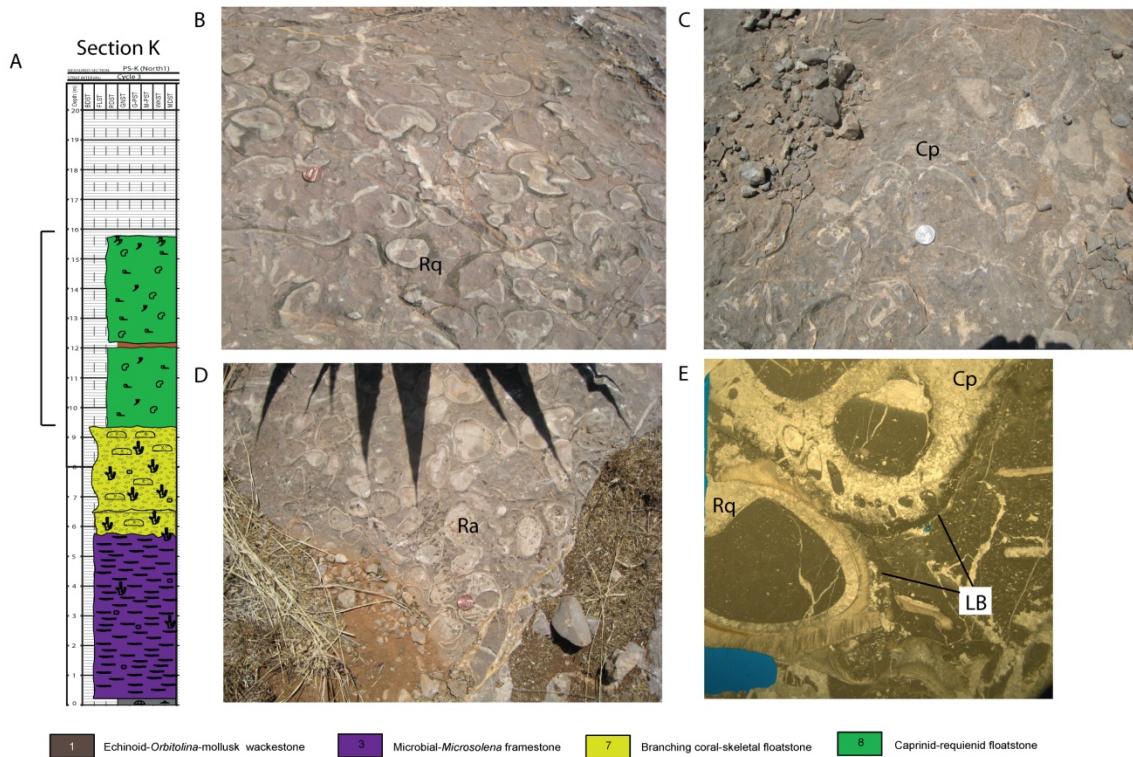


**Figure 35.** A) Caprinid-requienid floatstone (facies 9) forms the capping reef community at Section K. It is comprised predominantly of B) colonies of large requienid rudists (Rq) and C) caprinid rudists (Cp). D) Colonies of in-situ elevator rudists such as radiolitids (Ra) are also present. E) Caprinids (Cp) and requienids (Rq) float in a lime wackestone to packstone matrix and are commonly encrusted with *Lithocodium/Bacinella* (LB).

### Facies 10: Caprinid-requienid rudstone

**Description:** Mottled-weathering blue-gray to red-brown caprinid-requienid rudstone (Figure 36A) is composed of fragments of requienid (40%), caprinid (30%), monopleurid (10%) and radiolitid (10%) rudists within a poorly-sorted (fine to coarse) peloidal-skeletal wackestone to grain-dominated packstone matrix. Matrix allochems include other mollusks, echinoids, and rare *Orbitolina*, and calpionellids. Requienid rudist fragments are up to 10 cm in diameter and are dark “root beer” brown. *Actinastrea*

coral fragments are up to 15 cm in diameter. Meter-scale rudstone beds are visible in outcrop at Section M and dip ~8 degrees to the north (Figure 36B). Geopetal structures are variably oriented and are filled with gray-blue smooth-weathering lime mud and blocky calcite. Rudist fragments are commonly encrusted with dark, micritic laminite of possible microbial origin. This facies lacks evidence of early cementation, although equant calcite fills preexisting moldic pore space. Caprinid-requienid rudstone grades laterally to the south into caprinid-requienid floatstone (facies 9) (see Figure 34).

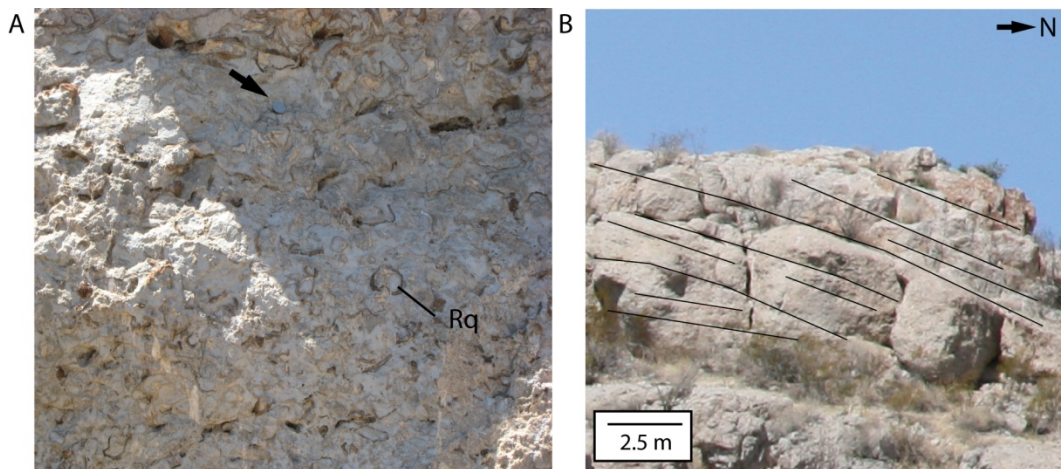


**Figure 36.** A) Caprinid-requienid rudstone (facies 10) is comprised of large fragments of requienid (Rq) and caprinid rudists at Section M. B) Thick beds of rudstone are derived from caprinid-requienid floatstone (facies 9) from the south and dip ~8 degrees to the north. These landward-dipping beds are similar to those observed in rudist-coral rudstone debris facies at Sections A-F.

**Depositional environment:** This facies is interpreted as rudist colony debris that was washed leeward (north) into beds by moderate wave energy (Scott, 1979), likely between storm and fair-weather wave base. Fragmented rudist and skeletal fragments in a poorly-sorted skeletal matrix further suggests a lower-energy depositional setting.

### **Facies 11: (Silicified) *Orbitolina* skeletal grainstone**

**Description:** Massive and smooth-weathering light gray grainstone ranges from 3-6 m thick at Sections L-Q (Figure 37A) and is comprised of coarse-grained (750  $\mu\text{m}$  – 1 mm) skeletal fragments of mollusks (30%), *Orbitolina* (15%), echinoids (10%) and other foraminifera. Silicified skeletal fragments are common at the top 20 cm. *Orbitolina* exhibit a more conical shape than those observed in echinoid-*Orbitolina*-mollusk wackestone facies. Micrite rim on former aragonitic mollusk fragments is common. Syntaxial calcite overgrowth is common on echinoid plates. Faint, patchy isopachous bladed calcite rim cements are present on some grains, but overall there little evidence of early marine cementation and some primary porosity is preserved (Figure 37B). From porosity and permeability analysis, grainstone porosity is  $\sim 2\%$ ; the majority of primary porosity has been occluded with a later generation of calcite spar or quartz cement (Figure 37C). In partially-silicified *Orbitolina*-skeletal grainstone, a small percent (less than 5%) of euhedral quartz is present in interparticle pore space and leached grains (Figure 37D). *Thalassinoides* burrows measuring up to 5 cm wide are present at Sections P and Q and (Figure 37E). *Orbitolina*-skeletal grainstone and partially-silicified *Orbitolina*-skeletal grainstone are overlain by microbial-*Microsolena* framestone (facies 3) at Sections K-L (See Figure 33) and by rudist-coral rudstone (facies 6) at Sections O-P (See Figure 34).

**Depositional environment:** Grainstone facies are located in the northernmost part of the outcrop, and are interpreted as back reef shoals (Scott, 1979). *Orbitolina*

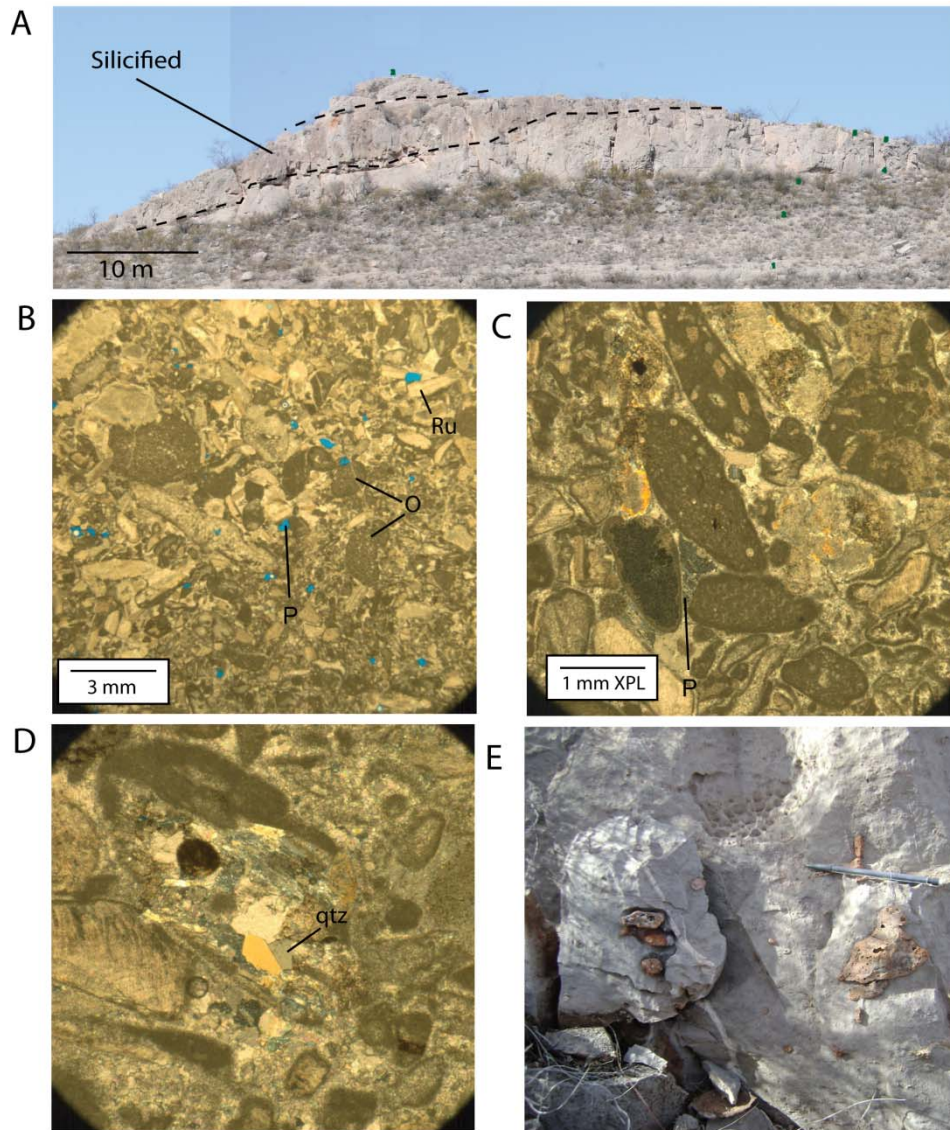


**Figure 37.** A) *Orbitolina*-skeletal grainstone (facies 11) comprises the majority of Section L and is also prevalent in Sections M-Q. In outcrop, silicified *Orbitolina*-skeletal grainstone weathers dark gray and lies above light gray *Orbitolina*-skeletal grainstone (nonsilicified). B) *Orbitolina*-skeletal grainstone is comprised of coarse-grained fragments of rudists (Ru), *Orbitolina* (O) and other skeletal grains. Primary porosity (P) is highlighted by blue epoxy and is estimated to be 2 percent, C) Further evidence of primary porosity (P) in thin-section shows poorly-developed rim cements with interparticle pore space occluded with a later generation of calcite spar, D) Evidence of permeability is seen where skeletal grains have been leached and partially replaced with euhedral quartz (qtz), E) Sedimentary structures include *Thalassinoides* burrows at Sections P and Q.

exhibit a tall, conical morphology, which indicates clear shallow-water conditions (Immenhauser and Scott, 2002). In thin section, heavily abraded and well-sorted skeletal grains with little to no mud are evidence for high-energy conditions. A transition from wackestone to grain-dominated packstone to grainstone in both thin section and measured section indicates an overall shoaling into fair-weather wave base.

### **OUTCROP RECONSTRUCTION AND FACIES DIMENSIONS FROM GROUND-BASED LIDAR**

Ground-based lidar (light detection and ranging) is a useful tool for delineating high-resolution stratigraphic geometry and structural context in three dimensions (Bellian et al., 2005; Bonaffe et al., 2007; Janson et al., 2007; Phelps et al., 2009). In the absence of a three-dimensional outcrop at Paul Spur, lidar data provide a basis for facies mapping and stratigraphic surface extrapolation on a robust digital outcrop model with accurate elevation data. Interpretations may then be used to develop a spatially correct 2D facies/stratigraphic reconstruction of the Paul Spur outcrop.

Data used for this study are: 1) xyz and intensity lidar data collected from a ground-based unit with ~2 – 10 cm resolution that includes the mapped cliff faces on the east side and the dip slopes on the west side (Figure 38A), 2) photo pan-based facies maps, 3) 15 high-resolution stratigraphic sections with lithofacies information, 4) strike and dip data, 5) RTK-GPS (real-time kinematic global positioning system) locations of stratigraphic sections and mappable surfaces.

The Paul Spur outcrop is exposed in the eastern limb of a southern-plunging syncline (Figure 38B). Structural dips range from 12 degrees at Section P to 44 degrees

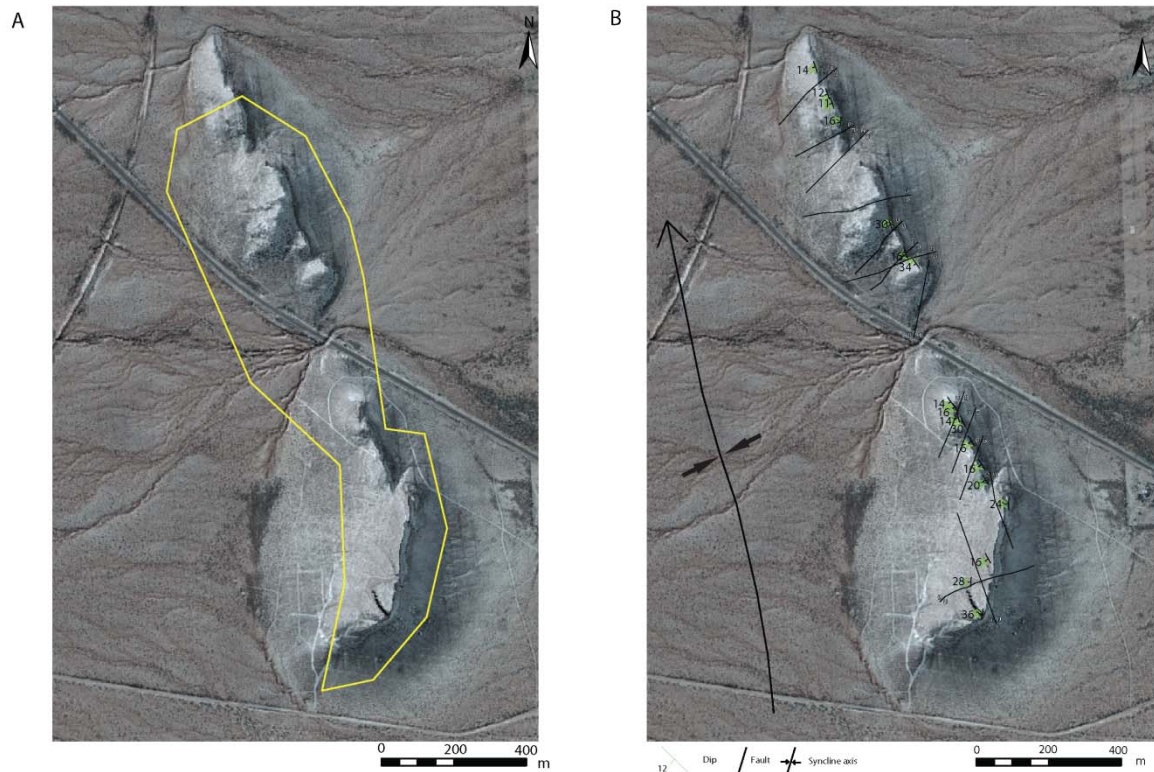


**Figure 38.** A) Orthoimagery map showing lidar data coverage at Paul Spur. B) Orthoimagery map with structural components removed with reconstruction using lidar xyz and intensity data.

near the axis of the syncline at Section A. Additionally, the Paul Spur facies are offset by a number of sub-vertical faults (see Figure 38B).

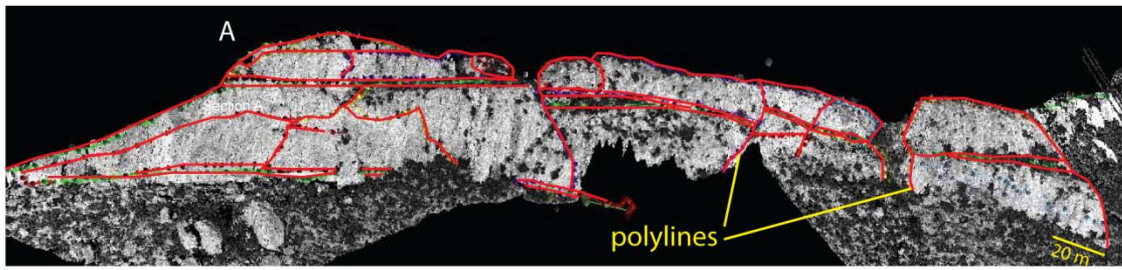
A 2D structural reconstruction of the Paul Spur outcrop included four steps. First, facies boundaries from photomosaic maps, RTK-GPS data and measured section trajectories were mapped on the 3D point cloud dataset in InnovMetric Polyworks (Figure 39A). To account for faulting for future reconstruction, the facies were mapped in discrete polygon sets representing individual fault blocks. Stratigraphic surfaces were extrapolated from Sections A-F to Sections K-Q based on simple geometry and thickness

trends observed at Sections A-F. Second, a two-dimensional view of the facies and fault blocks was created. A z-plane with orientation approximate to NW-SE depositional dip at 165 degrees azimuth provided a surface onto which the facies and fault blocks are projected (Figure 39B). Third, folding was taken out of the patch-reef by rotating the fault blocks around vectors parallel to the x-axis. Three vectors were used to account for varying dips along the syncline limb: one vector (length ~320 m) was used to rotate facies near the syncline axis at Sections A-F with average dips 26.0 degrees (Figure 39C), a second vector (length 262 m) for facies at Sections G-J with average dips 16.0 degrees, and a third vector (length 560 m) for facies at Sections K-Q with average dips 13.8 degrees. Fourth, the rotated fault block traces were exported from Polyworks into Adobe Illustrator for a qualitative vertical offset reconstruction (Figure 39D). An approximate horizontal datum was chosen between Cycle 1 and Cycle 2.

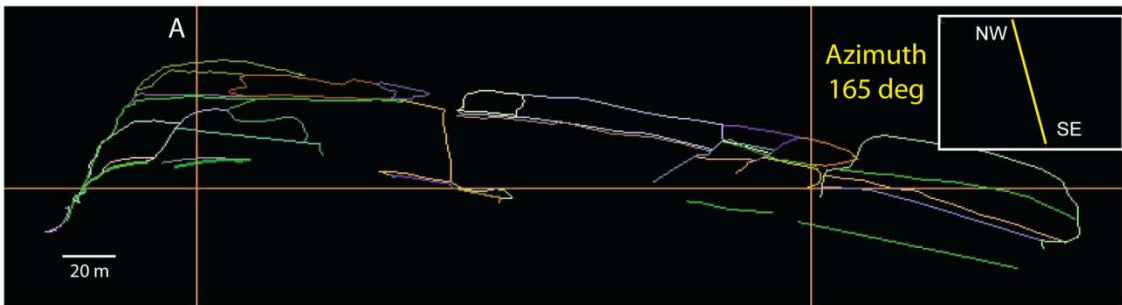
The results of structural restoration are shown in Figure 40. The reconstruction allows for more accurate portrayal of facies thickness and lateral extents at the time of deposition; however, it is important to note that the effects of differential compaction post-burial are not considered in this study. The consequence of dismissing compaction trends is an inaccurate depiction of original depositional topography. For example, it is expected that the echinoid-*Orbitolina*-mollusk grainstones at Sections K-Q are topographically higher than the reef frame facies at Section A (Scott, 1979).

At Sections A-F, significant deformation and high-angle dips from increased folding near the synclinal axis at Section A result in inaccurate facies thickness measurements in the field. For example, in measured section, the *Microsolena*-

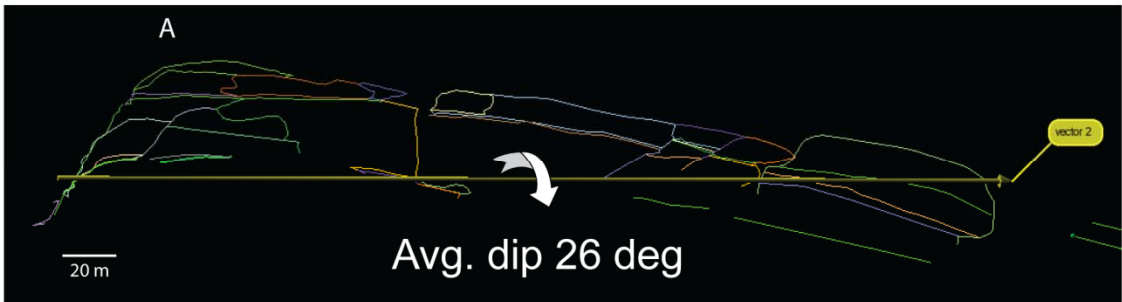
SE NW  
 Step 1: Map facies from photomosaics



Step 2: Snap facies interpretations to 2D plane parallel to depositional dip



Step 3: Remove folding via vector rotation



Step 4: Group fault blocks and remove faulting

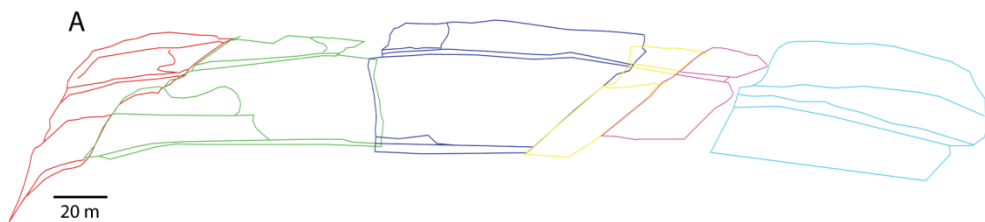


**Figure 39.** Diagrams illustrating the method by which folding and faulting are removed from lidar data in order to determine accurate facies thicknesses and original 2D lateral facies distribution of the Paul Spur patch reef. A data subset for Sections A-F is shown.

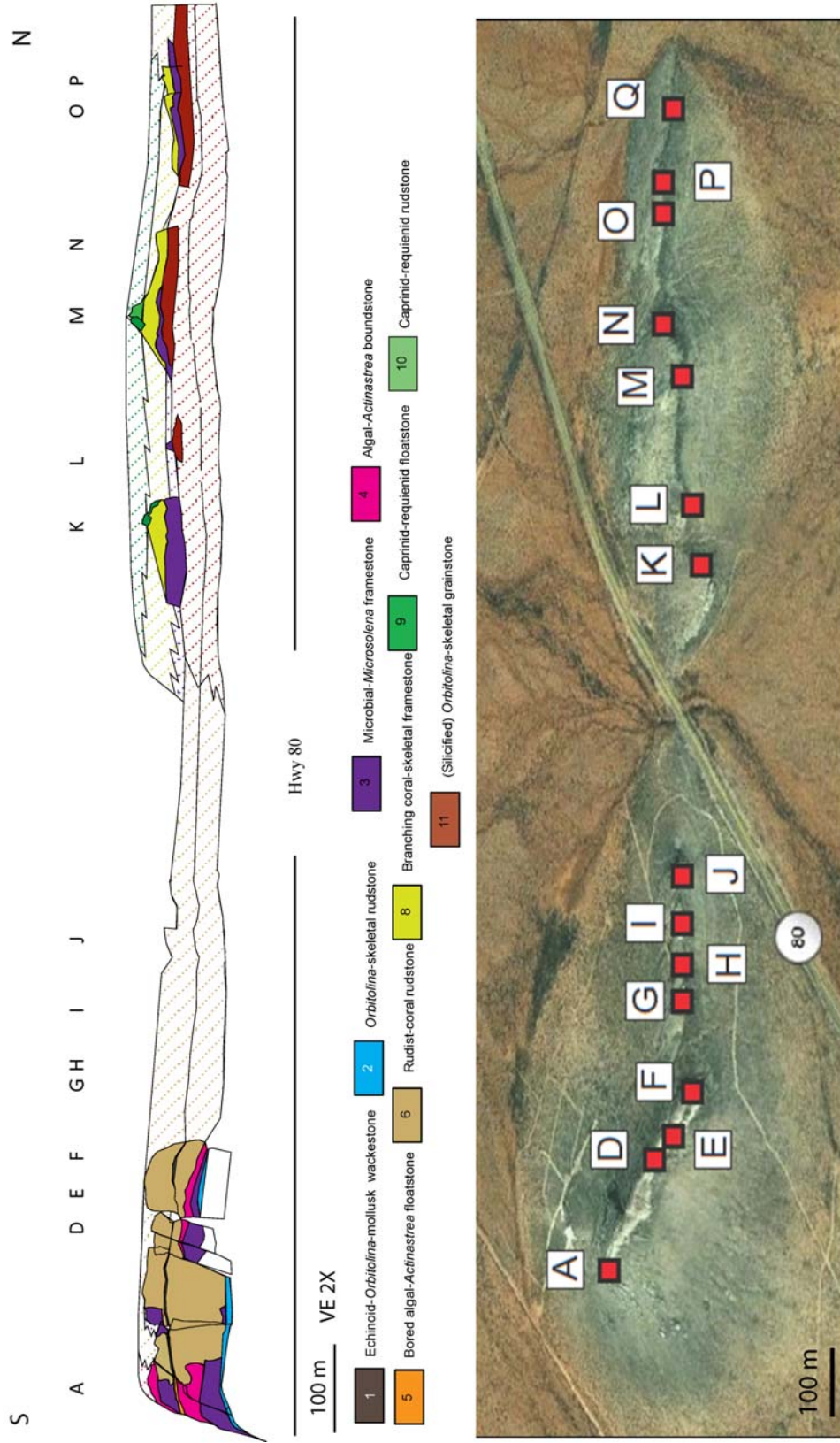


**Figure 40.** 2D facies and structural reconstruction of the Paul Spur reef using lidar and field data compared to structurally deformed outcrop orthoimagery. Solid color represents exposed facies and hatch marks represent inferred facies that are covered by talus or eroded. Folding was removed in PolyWorks by vector rotation and faulting was removed by vertical shifting in Adobe Illustrator. The reef exhibits additional deformation likely from differential compaction; therefore, original depositional topography is not represented by the schematic.

*Actinastrea* vertical facies succession in Cycle 1 measures 20.9 m. Reconstructed thickness is 16.9 m, a difference of ~19%. The average percent error for facies thicknesses in Sections A-F is 29%. Facies located on the synclinal limb at Paul Spur north exhibit less deformation as a result of folding, with dips averaging 13.8 degrees. At Section K, the *Microsolena*-branching coral-rudist floatstone vertical facies succession in measured section is ~9.0 m and is 8.1 m after reconstruction, with 10% inaccuracy. A table summarizing measured and corrected facies thicknesses, dips, angle of correction and percent inaccuracy may be referenced in Table 3. Additionally, the Paul Spur outcrops exhibit varying lateral distributions and are summarized in Table 4. Comparison of these extents will provide a foundation for developing a depositional model.

Echinoid-*Orbitolina*-mollusk wackestone (facies 1) is present along the entire reconstructed 2D profile with a lateral distribution of 1.7 km (see Figure 40). *Orbitolina*-skeletal rudstone (facies 2) is intermittently exposed but is likely continuous for a distance of 320 m from Section A to Section F. Facies 2 is ~1.8 m thick at Section A and thins to the north where it is < 1 m at Section F.

Microbial-*Microsolena* framestone (facies 3) and algal-*Actinastrea* boundstone (facies 4) are prolific at Section A where they form two stacked beds of 16.9 m and 8.1 m, respectively (see Figure 40). These facies thin to the north where they abruptly pinch out at a distance of ~77 m from Section A. Smaller patches of these coral facies are present at Sections D-F where they range from 2.7 to ~4.7 m thick with lateral extents of ~42 m – 123 m. Microbial-*Microsolena* framestone is variably present at Sections K-O. It

Section	Cycle	Facies	Dip (°)	Dip Corr (°)	Meas Thickness (m)	Corrected Thickness (m)	% error	Avg error (%)
A	1	2	36	25	1.6	1.8	10.6	
A	1	3		25	9.1	7.6	16.3	
A	1	4		25	11.8	9.3	21.3	
A	2	5		25	3.2	3.1	4.7	
A	2	3		25	5.6	3.9	30.4	
A	2	4		25	6	4.2	29.7	
A	2	8		25	3.5	2.4	31.4	
A	1-2	6		-	-	28.6	-	
D	1	6	28	25	3.4	2.9	14.7	
D	1	3		25	4.1	2.3	44.1	
D	2	1		25	1.2	1.0	15.0	
D	2	6		25	10.8	7.3	32.6	
E	1	6	16	25	2.8	1.9	32.1	29
E	1	3		25	3	1.8	40.0	
E	1	4		25	2.1	2.9	27.6	
E	2	1		25	1.4	1.0	28.6	
E	2	6		25	16.2	10.4	35.8	
F	1	2	24	25	1.1	-	-	
F	1	6		25	1.2	1.2	0.0	
F*	1	3		25	3	1.4	53.3	
F*	1	4		25	5.1	1.3	73.9	
F	1	6		25	2.4	3.5	31.4	
F	2	1		25	1.4	0.8	42.9	
F	2	6		25	12.8	8.9	30.2	
G*	1	1	20	16	0	7.0	100.0	
G	2	6		16	10.1	9.0	10.8	
H†	1	1	16	16	3.7	8.7	57.6	
H	2	6		16	11.6	8.6	25.9	
I	1	1	14	16	7	4.4	37.1	46
I†	2	6		16	12.7	3.5	72.4	
J	1	1	16	16	7	3.4	51.4	
J	2	6		16	7.3	6.5	11.0	
K	2	11	34	13.8	0.3	-	-	
K	3	3		13.8	5.5	4.9	10.9	
K	3	8		13.8	3.5	3.2	10.0	
K†	3	9		13.8	6.4	1.8	71.9	
L	1	1	16	13.8	11	9.7	11.8	
L	2	11		13.8	7	5.4	23.0	
L	3	3		13.8	2.8	2.3	17.9	
M	2	1	30	13.8	10.5	10.4	1.4	
M	2	11		13.8	4.6	7.5	38.7	
M	3	3		13.8	2.4	2.5	4.0	
M	3	8		13.8	2.5	2.6	3.8	
M	3	10		13.8	6.7	5.3	20.3	
N	2	1	16	13.8	10.2	10.2	0.1	21
N	2	11		13.8	10.2	12.2	16.4	
N	3	3		13.8	1.5	1.3	13.3	
N	3	8		13.8	1.4	1.1	21.4	
O	1	1	11.5	13.8	8.3	7.6	9.0	
O†	2	11		13.8	4.5	1.4	68.7	
O	3	3		13.8	3.2	2.6	18.8	
O	3	8		13.8	4.6	3.0	34.8	
P	1	1	14	13.8	14.8	8.5	42.6	
P	3	6		13.8	6.1	5.5	6.1	
P	3	11		13.8	0.5	-	-	

\* Inaccurate mapping on lidar

† Anomalous inaccuracy in measured section

**Table 3.** Summary of facies thicknesses by sections showing measured and corrected values after structural reconstruction. Average percent error is high near the synclinal axis at Sections A-F compared to the limb at Sections K-Q. An unusually high average at Sections G-J is attributed to inaccurate measured thicknesses and ambiguity of the location of the stratigraphic surfaces.

Cycle	Facies	Section	Lateral distance (m)
1	1	A-P	1700
1	2	A	272.2
1	3	A	71.5
1	3	A-D	42.5
1	3	D-F	123
1	4	A	59.5
1	4	E-F	77
1	6	A-F	287
2	5	A	15.8
2	1	A-F	287
2	3	A	34.1
2	3	A-D	46.9
2	4	A	45.2
2	6	A-F	267.6
2	11	K-P	603.2
3	1	M	62.2
3	3	K-O	556.6?
3	8	K-O	556.6?
3	6	P-O	95.9

**Table 4.** Lateral extents of facies at Paul Spur measured from ground-based lidar interpretations.

is 4.9 m at Section K and exhibits an overall thinning to Section O where it is 2.6 m thick. Discrete patches vary from 47-174 m in lateral extent (see Figure 40) and the total extent is ~556 m. Facies 5 is restricted to Section A and is 3.1 m at Section A. This facies extends 15.8 m to the north where it thins and grades into facies 1 (see Figure 40).

Rudist-coral rudstone (facies 6) comprises the majority of the outcrop between Sections A – F. This facies is 28.6 m thick where grades laterally into facies 3 and 4 near Section A and extends 287 meters to Section F. Facies 6 comprises the architecture at Sections G – J and spans a lateral distance of ~267 m to Highway 80 (see Figure 40). The total lateral extent of facies 6 from north of Section A to Section J is ~555 m. Rudist-coral rudstone forms the major cliff-forming beds at Section P where it is 5.5 m thick and spans a lateral distance of ~96 m to Section O (south).

The following facies are laterally constrained to Sections K-O: *Orbitolina*-skeletal grainstone (facies 11), branching coral-skeletal framestone (facies 8), caprinid-requienid floatstone (facies 9) and caprinid-requienid rudstone (facies 10). The outcrop base at Section K is composed of *Orbitolina*-skeletal grainstone (facies 11) and is assumed to grade laterally across Highway 80 into facies 6 at Sections G – J. This facies transition is inferred (see Figure 40). *Orbitolina*-skeletal grainstone forms the base of the cliff-forming beds at Sections K-Q and is therefore variably exposed; thicknesses range from 5.4 m at Section L to 12.2 m at Section N (see Table 3). Facies 11 exhibits the greatest lateral extent and is present from Section K to Section P for ~603 m. This facies continues past the extents of the lidar data set to Section Q where it dips into the subsurface.

Branching coral-skeletal framestone (facies 8) is present at Sections K-O where it forms patches 2.6-3.2 m thick that are ~111 m in lateral extent. It is possible that this facies was originally laterally continuous (see Figure 40) and that the patchy architecture is a result of faulting observed in outcrop. Caprinid-requienid floatstone and rudstone (facies 9 and 10) comprise the top 1 – 6 m of Sections K – O. A small percentage of these facies are exposed on east face and therefore facies dimensions are based on measured section data and distances measured on GoogleEarth®. Caprinid-requienid floatstone is 2.8 m thick at Section K and extends ~275 m to Section M where it is 4.5 m thick and grades into caprinid-requienid rudstone. Caprinid-requienid rudstone is 5 m thick at Section M and thins to less than 1 m thick at Section O near the silicified grainstone (facies 11) contact. The total lateral extent of facies 10 is difficult to delineate because of

faulting; however, the presence of this facies at Section O suggests continuous lateral extent of ~150 m.

## **DEPOSITIONAL MODEL**

The facies suite observed at the Paul Spur outcrop represents 2D dip-parallel exposure of a multicyclic patch-reef with the following components based on facies distributions from ground-based lidar: 1) southern narrow (~70 m) windward margins with distinct zonation of coral reef frame facies, and 2) laterally extensive (~870 m) leeward margins with north-dipping beds of reef-derived rudstone and grainstone debris facies (Figure 41). Although the exact 3-dimensional extents of the Paul Spur patch-reef are unknown because of limited exposure, it likely exhibited the elongate shape similar to the Maverick Basin patch-reefs (Scott, 1979; Hofling and Scott, 2002; Aconcha, 2008). Overall, the Paul Spur patch-reef was deposited in a relatively moderate-energy open marine environment (Scott, 1979; Warzeski, 1983) similar to the Maverick Basin reefs.

The view to the north at Section A shows the asymmetric stacked windward margins at the Paul Spur patch-reef (Figure 42A) that overlie continuous beds of echinoid-*Orbitolina*-mollusk wackestone. Consistent with Scott's (1979) interpretation, this facies exhibited a relatively flat seafloor topography that is evident where individual beds may be traced laterally near Section A. Original depositional topography of the lower the margin is well-preserved, as bedded flank rudstones and packstones are clearly visible on the southwest side. These beds dip to the southwest at ~23 degrees (Figure 42B) and grade laterally into the windward margin core facies. These core facies include *Orbitolina*-skeletal rudstone shoal (facies 2), microbial-*Microsolena* framestone (facies

S (Windward)

(Leeward) N

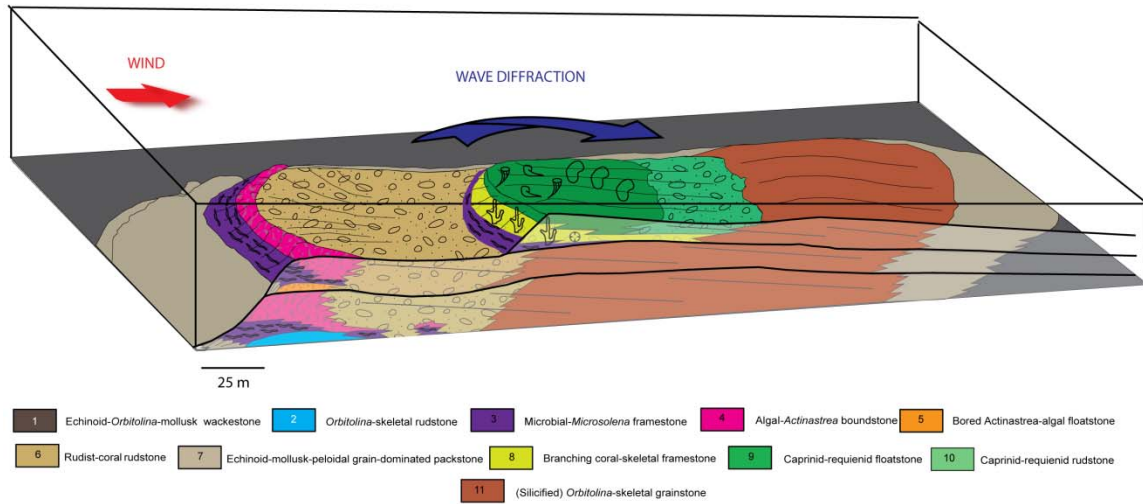


**Figure 41.** Conceptual depositional model of Paul Spur patch reef. The reef exhibits distinct windward asymmetry and it is inferred that dominant wind energy was from the south. Wave diffraction around the reef core (facies 3, 4 and 8) allowed for deposition of debris material on the leeward side of the reef. Reef debris consists of proximal rudist-coral rudstones (facies 6) and distal *Orbitolina*-skeletal grainstones (facies 11), skeletal packstones (facies 7) and caprinid-requienid rudstone (facies 10). The reef is nucleated on top of an *Orbitolina*-skeletal rudstone shoal (facies 2) which in turn overlies the flat seafloor composed of echinoid-*Orbitolina*-mollusk wackestone (facies 1).

3) and algal-*Actinastrea* boundstone (facies 4) reef frame (Figure 43). The reef frame facies exhibit a narrow lateral distribution, as is characteristic of modern windward margins (Brown and Dunne, 1980; Hubbard et al., 1990; Jones, 1994; Hughes, 1998). A third margin at Section K is characterized by a vertical succession of microbial-*Microsolena* framestone (facies 3), branching coral-skeletal framestone (facies 8) and caprinid-requienid floatstone (facies 9) (see Figure 41).

Windward margin development is attributed to reef orientation to prevailing trade winds, dominant ocean currents and tidal currents, where coral growth is dominant in regions facing the strongest current (Ball, 1967; James, 1983) on the windward side.

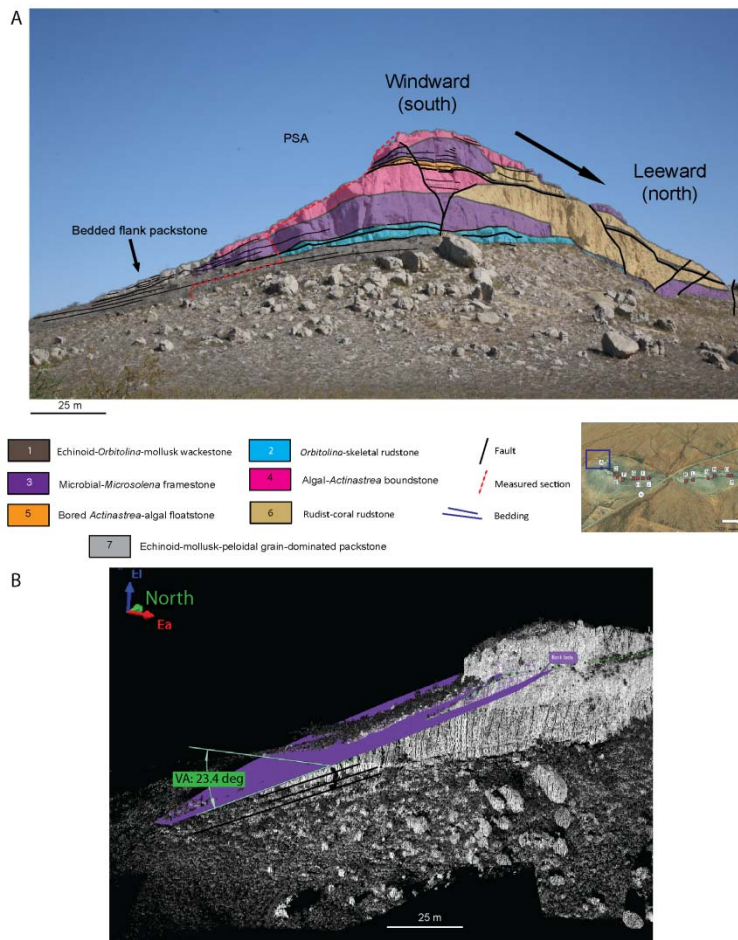


**Figure 42.** A) Facies distribution at the windward margin of the Paul Spur patch-reef. Bedded flank Echinoid-mollusk-peloidal grain-dominated packstones (facies 7) on the southwestern limb and bedded rudstone facies on the leeward margin show that original depositional topography is preserved. The windward margin is characterized by relatively flat seafloor topography composed of laterally continuous echinoid-*Orbitolina*-mollusk wackestone (facies 1) (Scott, 1979), reef nucleus composed of *Orbitolina*-skeletal rudstone (facies 2), narrow lateral distribution of reef frame facies (facies 3 and 4) and laterally extensive rudist-coral rudstone debris facies (facies 6). B) A best-fit plane was superimposed on the dip slope from which the flank bed packstone dip angles of ~23 degrees were calculated.

Aconcha (2008) interpreted windward margins for Lower Glen Rose patch-reefs in the Maverick Basin based on angle of repose analysis from seismic stratal slicing, where the margins were characterized by relatively steep angles in excess of 20 degrees. Aconcha

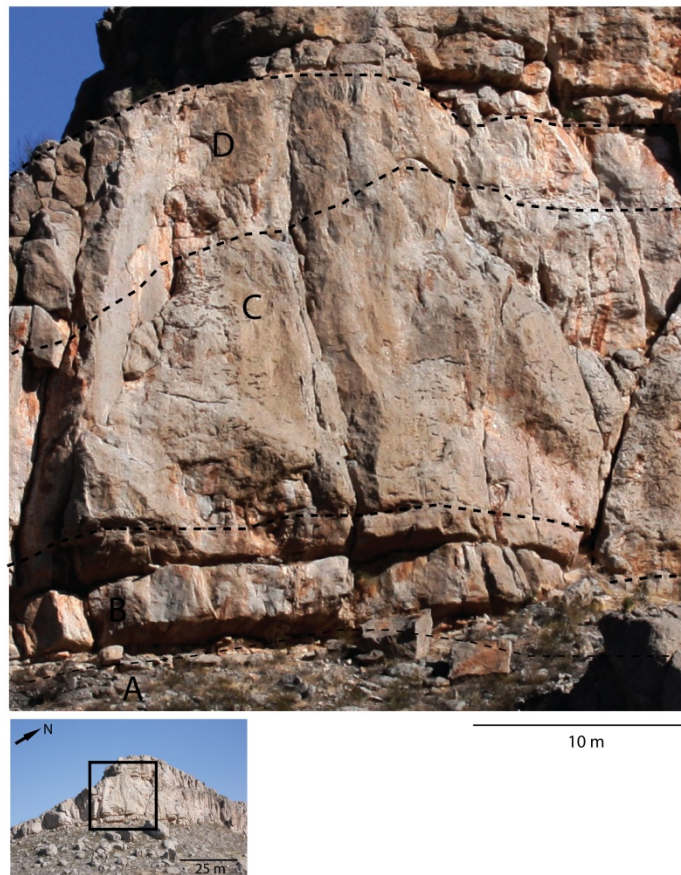


**Figure 43.** Vertical facies succession of Cycle 1 at the southern nose of Paul Spur. A) Basal echinoid-*Orbitolina*-mollusk wackestone is overlain by B) *Orbitolina*-skeletal rudstone (reef nucleus). C) Microbial-*Microsolena* framestone represents the pioneering reef community above the rudstone beds. D) Algal-*Actinastrea* boundstone is the capping reef community. Note that facies are characterized by distinct weathering patterns.

concluded that, based the aforementioned geomorphometric analysis, the Maverick Basin patch-reefs were subject to similar wind and current energies that define analogous patch-reef geometries in the Great Barrier Reef complex and Belize. This conclusion may serve as a sufficient analogy for wind and current processes affecting the Paul Spur reef, where the location of coral frame facies on the southern margin indicates prevailing wave and wind energy is from that direction.

The leeward margins at Paul Spur are characterized by the laterally-extensive reef-derived rudist-coral rudstone (facies 6), rudist rudstone (facies 10) and *Orbitolina*-skeletal grainstone (facies 11) that are present at Sections D-Q. Leeward transport of reef debris facies 6, 10 and 11 is evident from the presence of north-dipping beds within these facies. These beds exhibit lower angle dips than those observed on the windward margin, ~11-15 degrees (Figure 44). Comparatively, the mean angles of repose for leeward margins in the Lower Glen Rose patch-reefs range from 12 to 20 degrees (Aconcha, 2008).

Leeward accumulation of reefal debris is commonly attributed to transport by storm-generated currents (Ball, 1967; Hubbard et. al, 1990); however, the presence of well-sorted grainstone complexes on the leeward side of the Paul Spur patch-reef suggests that a sand belt formed under the influence of consistent wave energy. A modern example of well-developed lee sands is documented in the Belize barrier reef system where reef-derived sands are prograding landward in less than 2 m of water for a distance of 500 m (Gischler and Lomando, 1999). Leeward transport is attributed to dissipating wind-induced mean wave energy from the east-northeast over the windward margin of the laterally continuous barrier system (Purdy et al., 2003). This type of wave-induced leeward transport of sands is also prevalent on modern patch-reef systems such as those located near Anegada, British Virgin Islands (Brown and Dunne, 1980). These reefs are subject to moderately strong wind-induced wave energy from the east-northeast, moderate ocean currents from the northeast and low-amplitude north-south directed tidal energy that allows for the development of well-sorted coarse sands on the south-

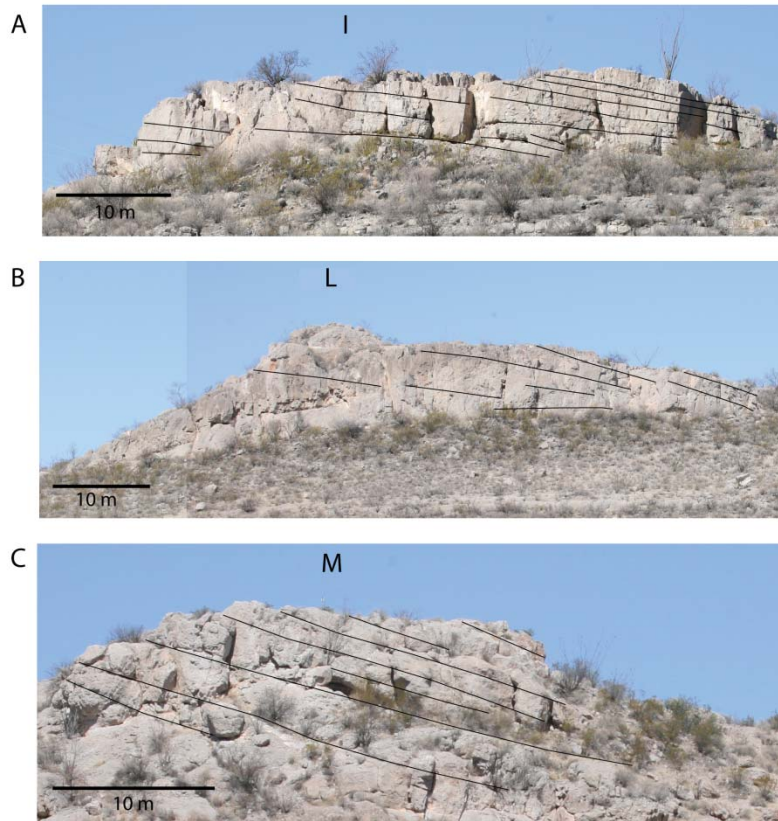


**Figure 44.** The leeward margin at Paul Spur is characterized by low-angle dipping beds of reef-derived debris. A) Rudist-coral rudstone (facies 6) forms well-defined beds that dip ~11 degrees at Section I, B) *Orbitolina*-skeletal grainstone shoals (facies 11) show faint dips ~12-17 degrees at Section L, C) Caprinid-requienid rudstone (facies 10) beds dip up to 15 degrees at Section M. All debris beds dip to the north and suggest landward transport and infilling processes similar to those observed in the Belize shelf.

southwest sides of the patch-reefs. Extensive leeward propagation of carbonate sand is observed on the reef island of Zirku, United Arab Emirates (Figure 45). This reef windward-leeward geomorphology may be analogous to that of the Paul Spur patch-reef.

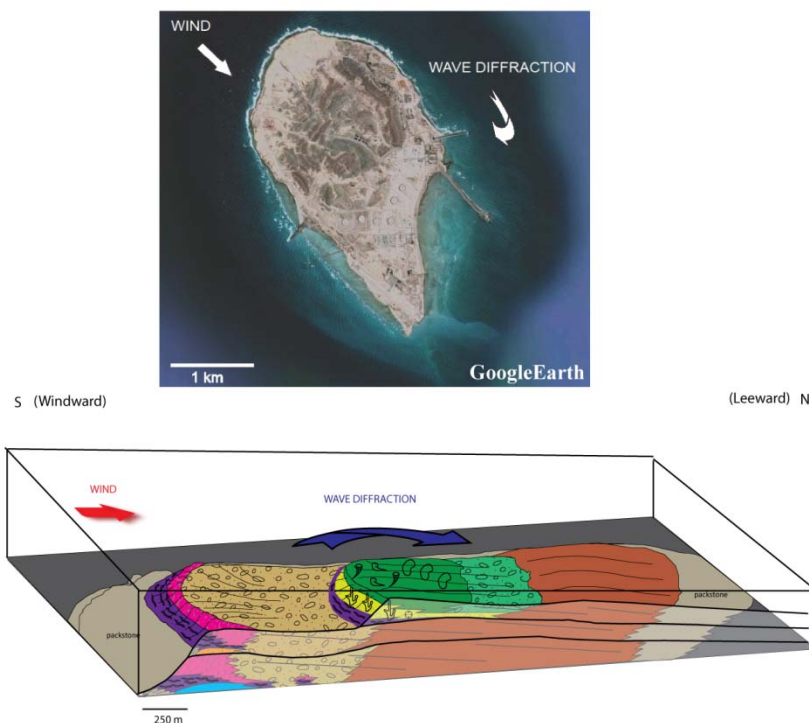


**Figure 45.** Depositional processes associated with the landward progradation of reef-debris facies at Paul Spur compared to a modern analog in the Persian Gulf.

### STRATIGRAPHIC SUCCESSION AND DEPOSITIONAL HISTORY

The Paul Spur patch-reef is multicyclic and is comprised of three shallowing-upward cycles: Cycle 1 spans Sections A-F, Cycle 2 spans Sections A-Q, and Cycle 3 spans Sections K-P (Figure 46). Overall, the three cycles exhibit an aggradational to retrogradational trend. Cycle tops were delineated by the position of indicator facies and sedimentary structures within vertical facies relationships.

Three indicator facies are present at the Paul Spur patch-reef and have specific stratigraphic importance in terms of decreasing and increasing accommodation: 1) Echinoid-*Orbitolina*-mollusk wackestone, 2) Bored algal-*Actinastrea* floatstone and 3)

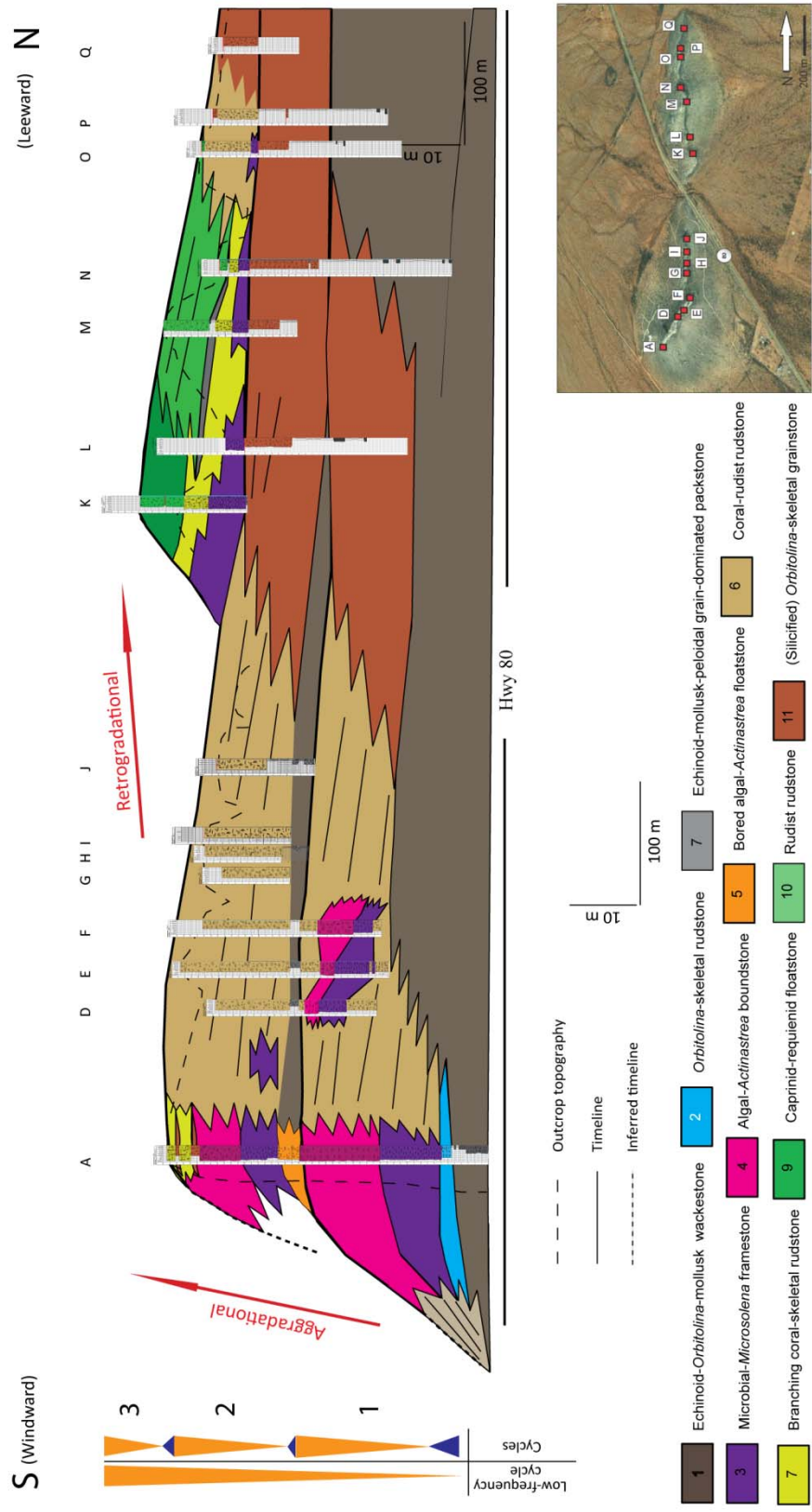


Figure 46. Schematic stratigraphic architecture of the Paul Spur patch-reef. The reef is comprised of three aggradational to retrogradational cycles. Cycles 1 and 2 exhibit aggradational stacking indicated by stacked reef-frame facies at Section A. Cycles 2 and 3 are present on the northern outcrop and exhibit retrogradational stacking where deep-water microbial-*Microsolena* framestone facies overlies shallow-water *Orbitolina*-skeletal grainstone shoal facies. Outcrop topography is indicated by the dashed line and original depositional topography of the patch-reef is not depicted in the schematic.

*Orbitolina*-skeletal grainstone. As mentioned in the facies descriptions above, echinoid-*Orbitolina*-mollusk wackestone is indicative of an open subtidal depositional environment below storm wave-base and may be used as a proxy for maximum accommodation (flooding) settings within the ramp interior (Scott, 1979; Vilas et al., 1995; Aconcha, 2008). This flooding indicator may be traced north of Section A to Section F where it delineates Cycle 1 from Cycle 2 (see Figure 46). This facies grades laterally to the south into bored algal-*Actinastrea* floatstone at Section A, which is interpreted to be a marine hardground. Boring of carbonate facies is characteristic of submarine hardground surfaces (Shinn, 1969; Wilson, 1975, p. 296). Hardgrounds are indicators of low carbonate productivity (Stearn and Scoffin, 1977) that may be associated with rapid local sea-level rise (Kendall and Schlager, 1981).

*Orbitolina*-skeletal grainstone is an important indicator facies that reflects a low-accommodation setting and represents the shallowest water facies at Paul Spur. It is composed of well-sorted skeletal and peloidal grains and no mud, which indicates a shallow agitated setting above fair-weather wave base (Wilson, 1975, p. 65). As is documented in modern settings such as the Belize barrier reef system, these wave-agitated shoal environments may develop in only a few centimeters to meters of water (Gischler and Lomando, 1999).

Cycle 1 initiated on transgressive echinoid-*Orbitolina*-mollusk wackestones (facies 1) that formed the flat open-marine sea-floor sediments of the Lower Mural Limestone (Scott, 1979) (see Figure 46). Transgression continued where reworked flat-shaped *Orbitolina* and skeletal debris formed the laterally discontinuous *Orbitolina*-

rudist-coral rudstone (facies 2) shoals upon which the pioneering microbial-*Microsolena* framestone (facies 3) community nucleated. Discrete patches of *Microsolena* are observed at Paul Spur south between Sections A and Section D (see Figure 24). Growth of framestone facies propagated into shallow water at the south margin where algal-*Actinastrea* boundstone facies (facies 4) became dominant. Rudist-coral rudstone (facies 6) debris facies were shed leeward of the reef frame where they were likely reworked into high-energy *Orbitolina*-skeletal grainstone shoals (facies 11) above fair-weather wave base.

Deposition of framestone facies at the windward margin was briefly terminated, as indicated by the presence bored algal-*Actinastrea* floatstone (facies 5) at Section A that formed concomitant to deposition of open ramp echinoid-*Orbitolina*-mollusk wackestone (facies 1) above rudist-coral rudstone debris facies at Sections D-F. These events mark flooding of the margin and the initiation of Cycle 2 deposition. Cycle 2 framestone facies were deposited in the same vertical succession as those in Cycle 1 (Figure 46). The algal-*Actinastrea* boundstones of Cycle 2 reached a “keep up” phase where capping *Orbitolina*-skeletal grainstones indicate growth above fair-weather wave base. Syndepositional fractures likely formed within the boundstone as a result of early marine lithification (see Figure 27). On a large scale, fracturing is common in aggradational reef margins and is driven by stresses associated with gravitational instability of the margin (Frost and Kerans, 2010). The grainstone-filled fractures at Paul Spur may therefore be indicators of a low-accommodation setting where patch-reef growth outpaced sea-level rise. On the leeward margin, the rudist-coral rudstone debris

facies of Cycle 2 were deposited to the north of the reef frame at Sections D – J while wave-reworked *Orbitolina*-skeletal grainstone shoals were deposited at Sections L – P.

Cycle 3 was initiated by a second flooding event in which the deep-water pioneering microbial-*Microsolena* framestone (facies 2) was deposited. Significant backstepping occurred where these reef frame facies were deposited on top of *Orbitolina*-skeletal grainstone shoal facies of Cycle 2 (see Figure 46). Capping caprinid-requienid floatstone colonies became the dominant reef-building organisms at the top of Cycle 3. Although the top of Cycle 3 is likely missing at the Paul Spur reef, it is possible that this cycle shallows into bedded ramp-interior carbonates such as those observed at the Grassy Hill locality to the north. A similar patch-reef located ~30 miles east of Paul Spur exhibits this vertical facies succession (Hartshorne, 1989).

Cycle stacking patterns reflect varying trends in sea-level change in marine environments (Mitchum and Van Wagoner, 1991) and have been documented in many Cretaceous carbonate settings, including those in central and south Texas (Lehmann et al., 2000; Mancini and Puckett, 2005). The three cycles observed at Paul Spur may be described in terms of overall stacking patterns based on outcrop geometry, facies offset, and physical bounding surfaces where observed. Cycles 1 and 2 exhibit aggradational stacking, as these cycles are arranged vertically with no significant backstepping. Although the presence of echinoid-*Orbitolina*-mollusk wackestone and coeval bored algal-*Actinastrea* floatstone indicates minor flooding between Cycles 1 and 2, this flooding event was not significant enough to drive reef production in a landward direction. Aggradational stacking is best observed in the reef facies at Section A (Figure

47). Cycle 2 and 3 exhibit a retrogradational, or a landward-stepping cycle stacking trend. Retrogradational stacking is based on facies offset observed at Sections L – M, where shallow-water *Orbitolina*-skeletal grainstones are overlain by deeper water pioneering microbial-*Microsolena* framestone (Figure 48).

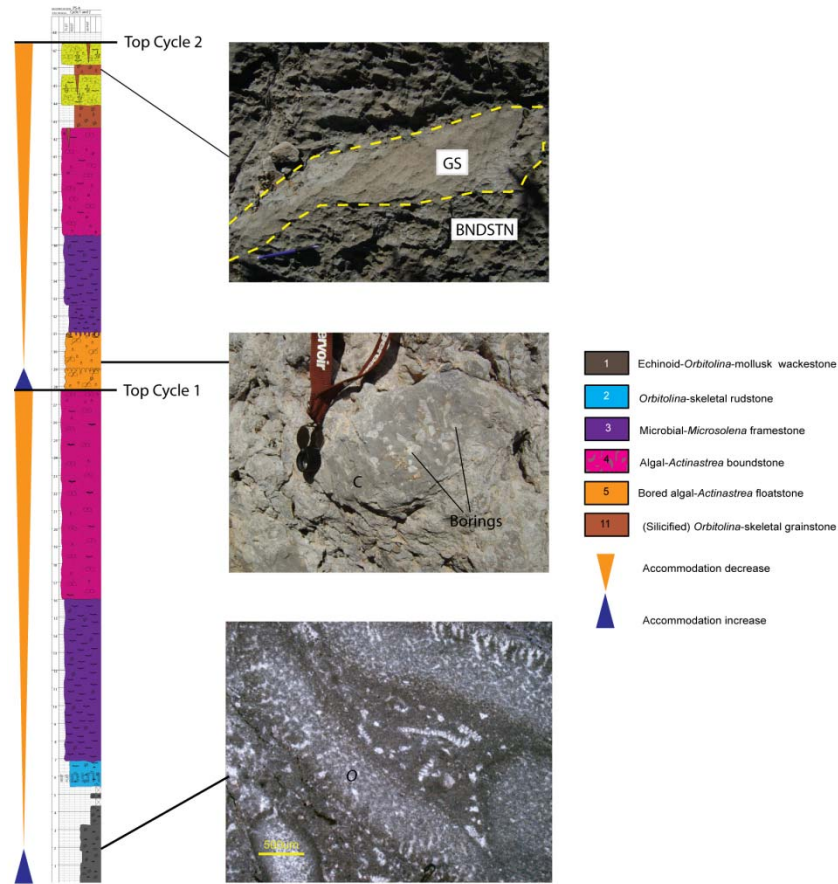


**Figure 47.** Vertical facies succession of reef-frame facies at the windward margin (Section A) showing indicator facies used for stratigraphic interpretation. Echinoid-*Orbitolina*-mollusk wackestone (facies 1) indicates a deep-water setting relative to the reef facies. Upward shallowing is observed in the vertical succession from *Orbitolina*-skeletal rudstone shoal nucleus, pioneering *Microsolena*-microbial framestone reef facies and *Actinastrea*-algal boundstone facies, which represents the shallowest water setting. The presence of extensively bored fragments of *Actinastrea* corals above facies 4 indicates a depositional hiatus (Stearn and Scoffin, 1977) that is likely associated with flooding conditions. A second shallowing succession is observed where grainstone-filled syndepositional fractures indicate reef growth into fair-weather wave base.

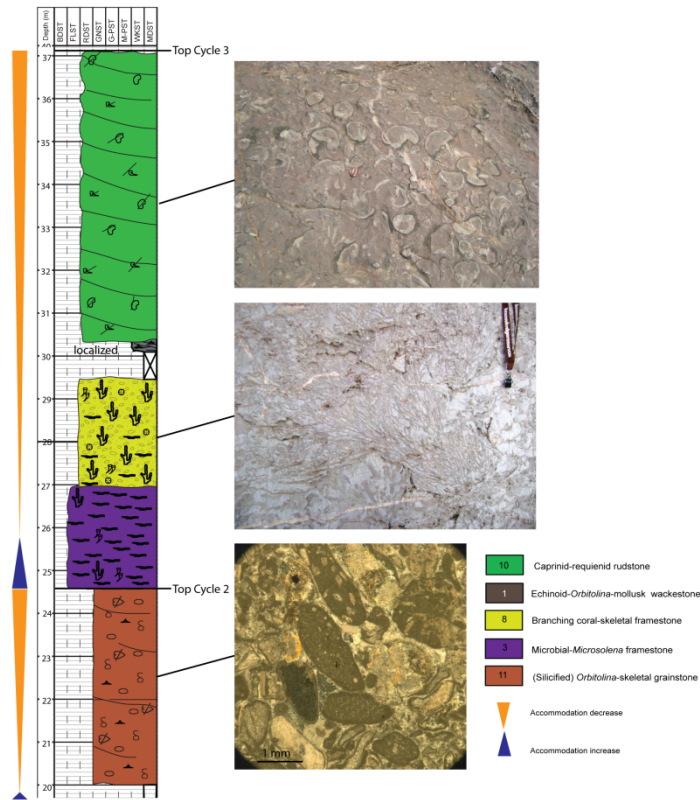


**Figure 48.** Vertical facies succession of *Orbitolina*-skeletal shoal grainstones of Cycle 2 and reef-frame facies of Cycle 3 at Section M. Upward shallowing is observed from echinoid-*Orbitolina*-mollusk wackestone (not shown) to *Orbitolina*-skeletal grainstone in Cycle 2. Increase accommodation is observed in Cycle 3 where a thin bed of echinoid-*Orbitolina*-mollusk wackestone indicates a minor flooding event similar to that observed between Cycle 1 and Cycle 2 at Paul Spur south. Upward shallowing in Cycle 3 is indicated by the presence of capping caprinid-requienid floatstone.

## STRATIGRAPHIC FRAMEWORK

A proposed stratigraphic framework for the Paul Spur patch-reef and associated ramp interior bedded carbonates at Grassy Hill is depicted in Figure 49A. The outcrops at Paul Spur are interpreted to form a low-relief transgressive margin with initial flooding marked by the deposition of continuous basal echinoid-*Orbitolina*-mollusk wackestone. This margin formed by deposition of Cycles 1 and 2 at Paul Spur during an aggradational

phase; at Grassy Hill this phase is marked by the deposition of well-bedded and non-cyclic packstones. Maximum transgression onto the shelf is indicated by landward-stepping of coral framestone facies within the Paul Spur Cycle 3 with small-scale (~6 m) patch-reef development in the northern-most (landward) extent of the ramp interior facies at Grassy Hill. Overall, Cycles 1 through 3 at Grassy Hill and Paul Spur are contained in a transgressive systems tract, with a turnaround into regressive facies marked by the deposition of caprinid-requienid floatstones at Paul Spur and miliolid-peloid wackestones at Grassy Hill at the top of Cycle 3. A fourth cycle at Grassy Hill comprised of miliolid-peloid wackestones, lime mudstones and siliciclastic sandstones forms a highstand systems tract and marks the initial regression of the paleo-shoreline and progradation of the shelf margin into the Sonora, Mexico area (Figure 49B).

In the northern Sonora area, Gonzalez-Leon et al. (2007) subdivided the Mural Limestone into three third-order depositional cycles (see Figure 3), the second of which is patch-reef prone and contains the Aptian-Albian boundary. Although these cycles are not presently correlated to southern Arizona, it is likely that the Mural Limestone patch-reef outcrops and associated basal facies in this study are contained within the late transgressive systems tract (TST) and early highstand systems tract (HST) of the Cycle 2 Tuape Shale and Los Coyotes members (Glen R1 cycle of Scott et al. (2007) in Texas), as they too span the Aptian-Albian boundary (Scott, 1979).



## **5. Discussion**

### **STRATIGRAPHIC SETTING**

As mentioned above, the cycles identified at Paul Spur and Grassy Hill are likely contained within the late TST-HST legs of a third-order depositional sequence that includes the Tuape Shale and Los Coyotes members of Mural Limestone deposits in the Sonora, Mexico area; however, this statement cannot be confirmed without well-constrained biostratigraphy or stable isotope data. Correlation results from Sonora, Mexico to south Texas (Gonzalez-Leon et al., 2007) concluded that the Tuape Shale-Los Coyotes third-order sequence is time-equivalent to the Hensel-Glen Rose 1 cycle of Scott et al. (2007). Correlation from Scott et al. (2007) to the sequence framework of Loucks and Kerans (2003) in which the Maverick Basin patch-reefs are contained is unclear. It is possible that Scott's cycle correlates to the third-order Lower Glen Rose Sequence 7 of Loucks and Kerans (2003), although the Aptian-Albian boundary in that study is placed much lower in the section within the Cow Creek Limestone.

### **STRATIGRAPHIC DRIVERS**

The reef evolution observed at Paul Spur is similar to that documented by Aconcha (2008) for the Maverick Basin patch-reefs in Texas. Aconcha (2008) concluded that patch-reefs accumulated in three stages primarily within the transgressive systems tract (TST) of the third-order depositional Sequence 7 of Loucks and Kerans (2003). Aconcha (2008) also concluded that the Maverick Basin reefs exhibit a capping regressive unit that is representative of highstand conditions. An important implication of

the similar depositional histories of the Paul Spur and Maverick Basin patch-reefs is that eustasy was the main driver for stratigraphy on the Comanche Shelf and Chihuahua Trough; eustatic controls on carbonate ramp evolution have been documented for both areas (Lawton et al., 2003; Loucks and Kerans, 2003).

Although eustasy has been documented as the main stratigraphic driver for the Mural Limestone (Bilodeau, 1982; Warzeski, 1983; Scott and Warzeski, 1993; Lawton et al. 2003), it is important to consider the impact of fluctuating environmental conditions that were common during Lower Cretaceous time. Changes in reef ecosystems during Lower Cretaceous time associated with climate change, nutrient shifts, oxygen, turbidity and habitat are well documented and the causes of each are generally linked to one another (Scott, 1995; Hofling and Scott, 2002; Dupraz and Strasser, 2002; Gotz et al 2005; Pomar et al., 2005). These changes may have further implications for reef evolution and stratigraphy in humid subtropical climates such as the Bisbee Basin where siliciclastic influx is present in varying degrees and may be driven by coastal processes (i.e. avulsion) that are independent of sea-level change.

For example, increase of siliciclastic run-off into marine environments is postulated to cause an increase in nutrient supply in reef environments (Hallock and Schlager, 1986; Insalaco, 1995; Tomas et al., 2008). The presence of siliciclastics during Mural deposition may therefore have significant effects on reef growth and cycle development at the Paul Spur patch-reef, as there is a distinct change from the nutrient tolerant microsolenid-dominated communities (Dupraz and Strasser, 2002) in Cycles 1 and 2 to diverse branching coral communities in Cycle 3 that require a clear, shallow and

nutrient-poor marine environment (Hallock and Schlager, 1986). Diversification of these coral types in Cycle 3 at Paul Spur may simply indicate a shift in siliciclastic sediment input into the area rather than a shallowing event associated with the transition to a sea-level highstand. Whatever the case, cyclicity development at Paul Spur was likely driven by a combination of eustasy and environmental factors.

### **IMPLICATIONS FOR RESERVOIR CHARACTERIZATION**

In the Maverick Basin reefs, primary porosity up to 13% exists in reef boundstone and flank facies with enhanced permeability up to 33 mD from fractures (Aconcha, 2008). The majority of gas and gas condensate production from these patch-reefs are from this facies (Loucks and Kerans, 2003). Reef detrital facies composed of peloid-skeletal rudstone to grainstone contain < 5% porosity (Aconcha, 2008), which is attributed to early marine cementation by bladed Mg-calcite cement (Loucks and Kerans, 2003); however, original porosity was estimated to be up to 45% (Loucks and Kerans, 2003). No significant backreef grainstone complex has been documented for the Maverick Basin reefs.

The Paul Spur patch-reef frame facies exhibit no primary porosity, which is attributed to occlusion of frame facies by lime mud in microbial-*Microsolena* and significant encrustation of corals by *Lithocodium/Bacinella* in algal-*Actinastrea* boundstone. Although small fractures exist, they are occluded with equant calcite spar. Reef facies at Paul Spur are therefore poor analogs for reservoir potential in the Maverick Basin patch-reef play; however, evidence for well-developed porosity in the patch-reef is found in partially-silicified back-reef *Orbitolina*-skeletal grainstone shoals. These

grainstones were analyzed for porosity and permeability from plugs drilled from 10 hand samples. Results from the analysis show that present porosity and permeability are negligible ( $< 2\%$  and  $< 0.1$  mD, respectively). In thin section, however, grainstones show poorly-developed early marine cements and significant primary pore space, although much of the primary porosity has been occluded with a later generation of calcite spar (see Figure 32C). Furthermore, some grains have been leached and replaced with euhedral quartz (see Figure 32D) which suggests that there was enough porosity and permeability for silica-bearing fluids to propagate through the grainstones. The most important implications for porosity development in back-reef grainstones at Paul Spur are 1) under different diagenetic conditions, grainstones may have been a suitable target for hydrocarbon accumulation and 2) reservoir volume for laterally extensive grainstone bodies is potentially greater than that of narrowly-distributed reef boundstones.

## **6. Conclusions**

The Mural Limestone of southeastern Arizona is representative of a ramp interior setting with complex facies architecture and varying degrees of cyclicity. Small mud-dominated coral-algal buildups (~5 m thick) and tabular biostromes (1.5 to 4 m thick) consisting of caprinid-requienid floatstones are common in the bedded ramp interior carbonates at the Grassy Hill locality. Coral-algal patch-reefs are associated with peloidal-foraminifer-mollusk-skeletal mud-dominated packstones in a shallow subtidal setting. Relatively thick caprinid-requienid floatstones are up to 4 m thick and are prolific above coral-algal patch-reef facies at Section GHE2. Thin 1.5 m thick caprinid-requienid floatstones are associated with restricted lagoon peloid-miliolid wackestones. Some

caprinid-rudist buildups thrived in higher energy settings where they are associated with *Orbitolina*-skeletal grainstone. Localized *Orbitolina*-rich skeletal grainstones are associated with tidal channel lag, are likely laterally discontinuous and are non-porous.

Overall, the facies at Grassy Hill exhibit poor cyclicity. Three large-scale cycles were identified; cycle tops were picked on top of thin beds of miliolid wackestone, which are the shallowest marine facies in the study area.

In the outcrops at the Paul Spur locality, Mural facies consist of a 10 to 35 m thick patch-reef with four distinct reef communities: microbial-*Microsolena* framestone, algal-*Actinastrea* boundstone, branching coral-skeletal framestone and caprinid-requienid floatstone. Reef-flank facies consist of rudist-coral rudstone debris and backreef *Orbitolina*-skeletal grainstone shoals. Echinoid-*Orbitolina*-mollusk wackestone represents the deeper, low-energy environment below fair-weather wave base.

Three aggradational to retrogradational cycles of reef growth are evident. Retrogradational stacking is consistent with that of time-equivalent Lower Glen Rose patch-reefs in the Maverick Basin of Texas, which suggests a eustatic driver for stratigraphic architecture along the Bisbee/Comanche shelf. Reef and backreef shoal facies exhibit poor porosity and permeability in outcrop. Petrographic analysis of backreef grainstones shows that primary porosity may have been present based on the lack of well-developed marine rim cements and deposition of euhedral quartz, respectively.

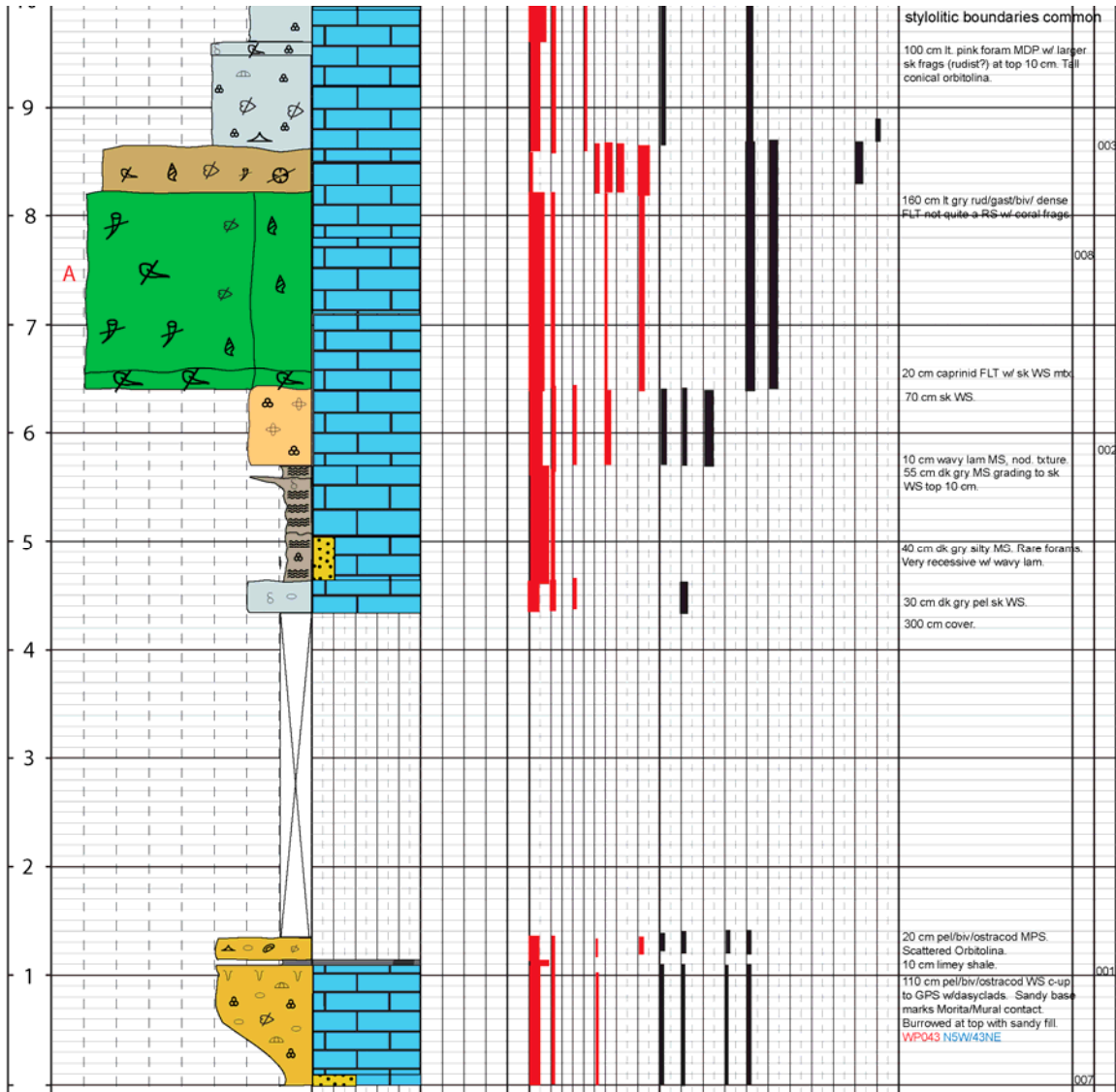
Furthermore, new insights from this study show that laterally extensive grain-rich reservoir-prone facies are dominant on the leeward side of mud-rich reef buildups, which

suggests that the backreef shoal facies may be suitable reservoir target similar to capping shoal facies in the Maverick Basin reefs.

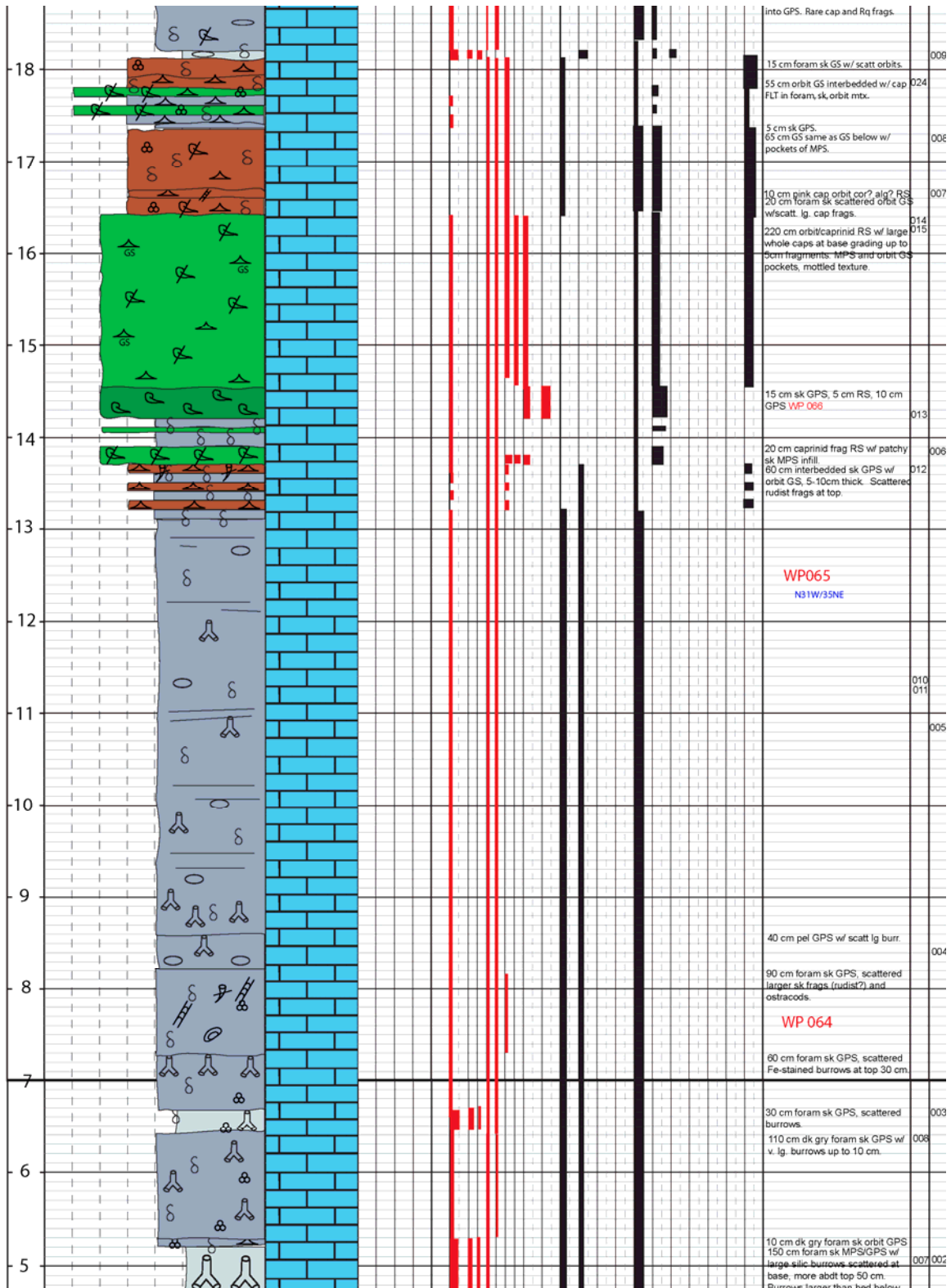
## **Appendix A: Measured section data**

Measured section data include six sections from the Grassy Hill locality and fifteen sections from the Paul Spur locality. Each section contains coded facies as described in the main document, mineralogy, allochem percentages, grain sizes and additional field observations. These data were collected between June of 2009 and January of 2010.



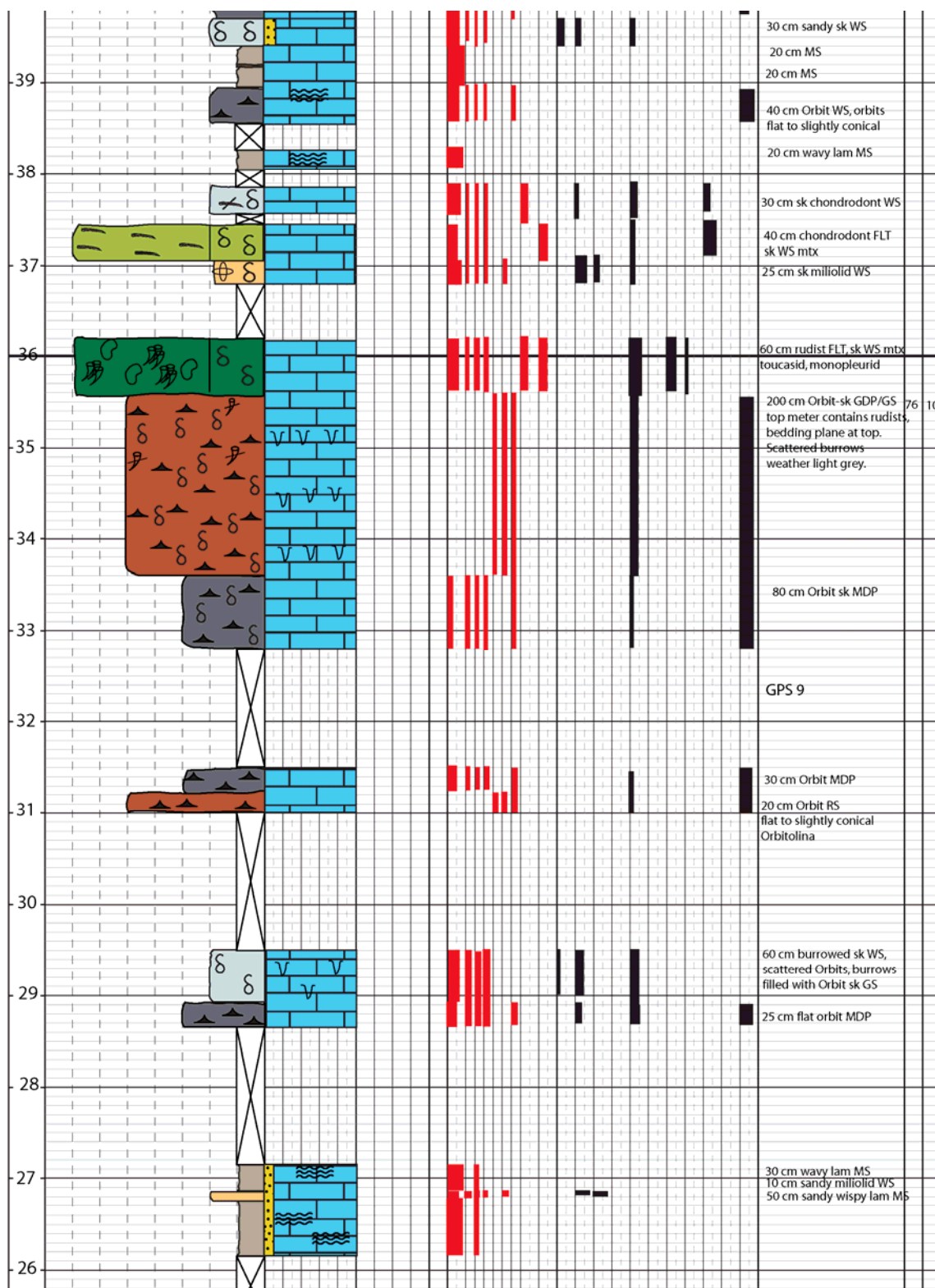


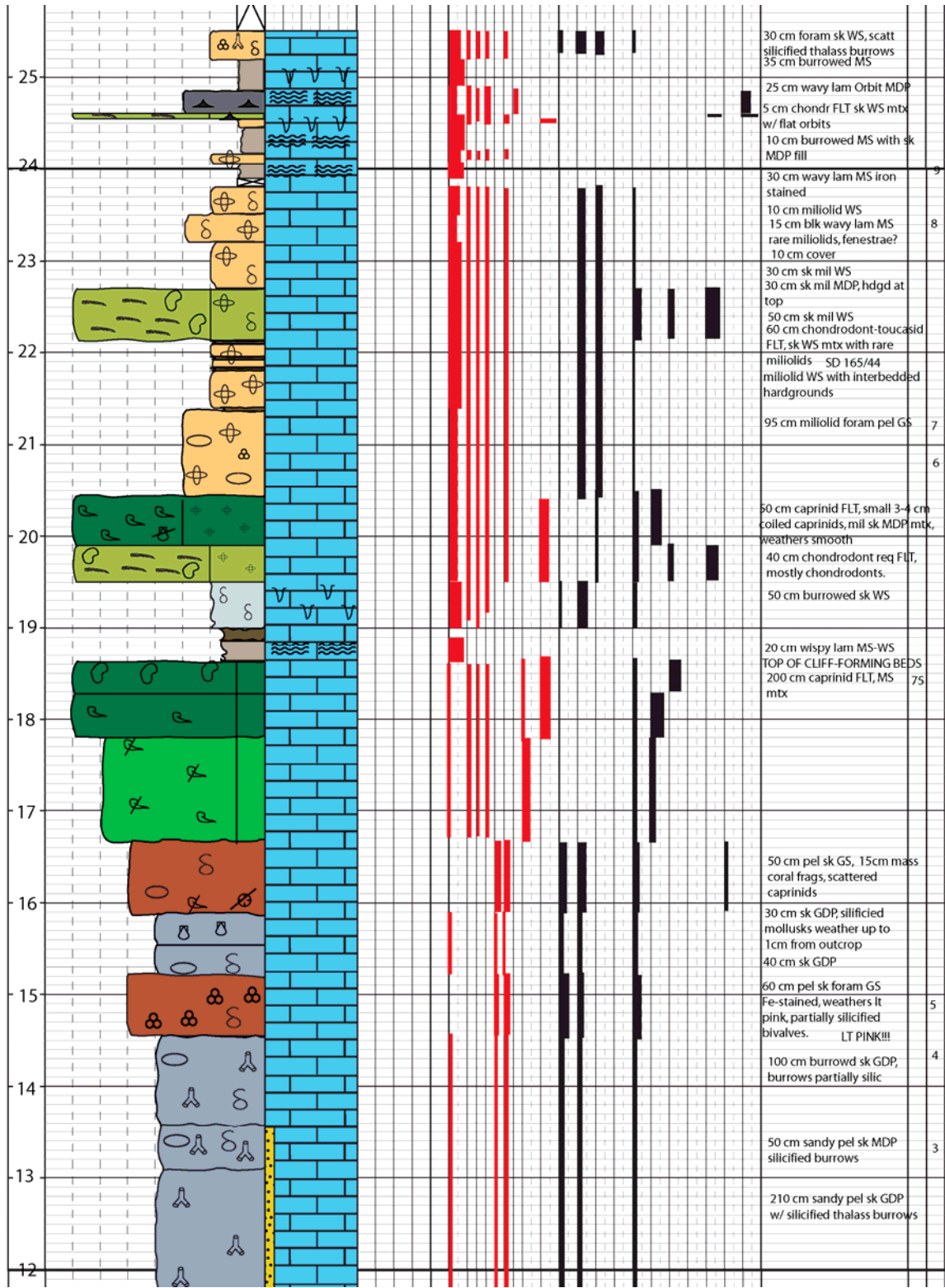


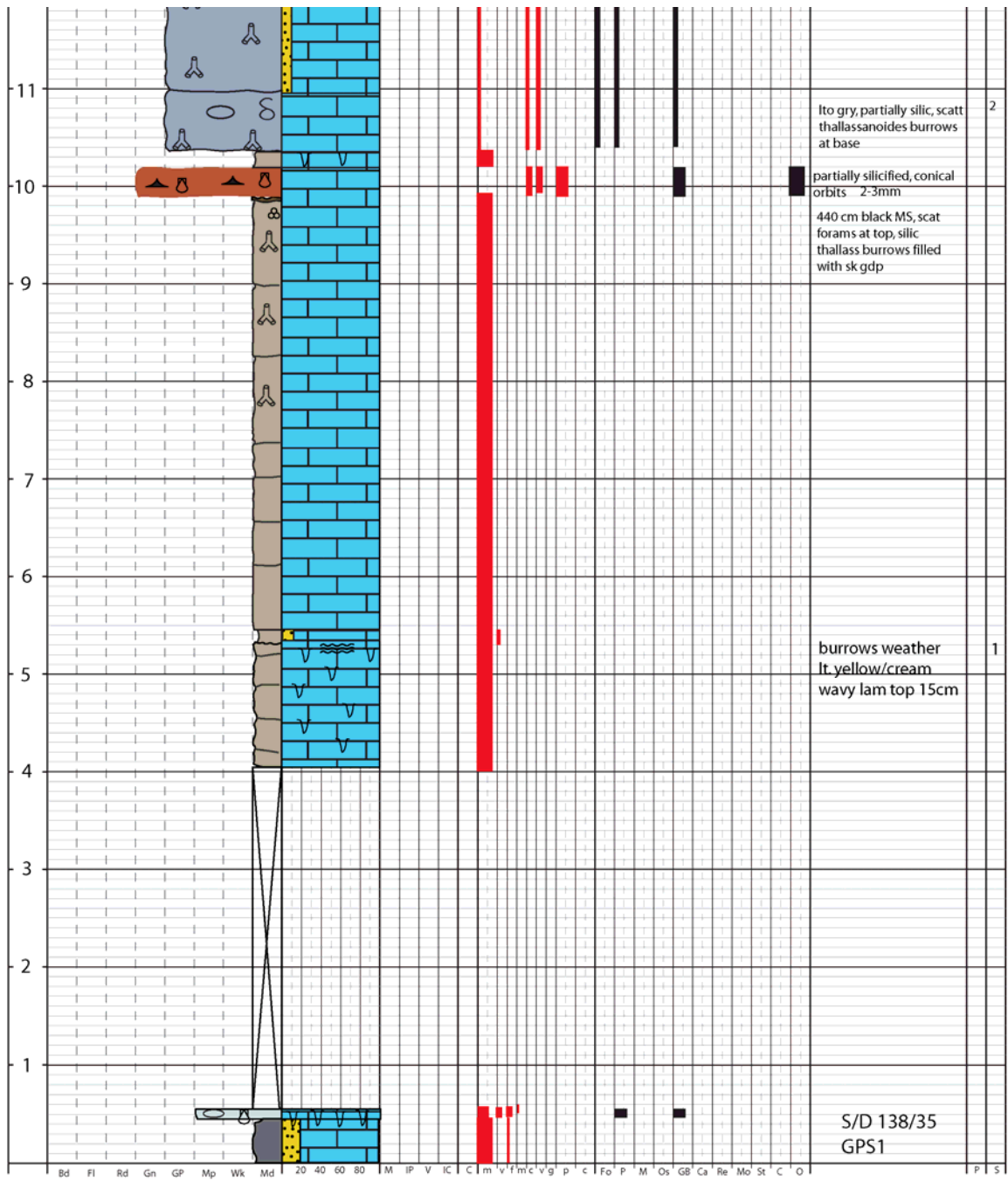




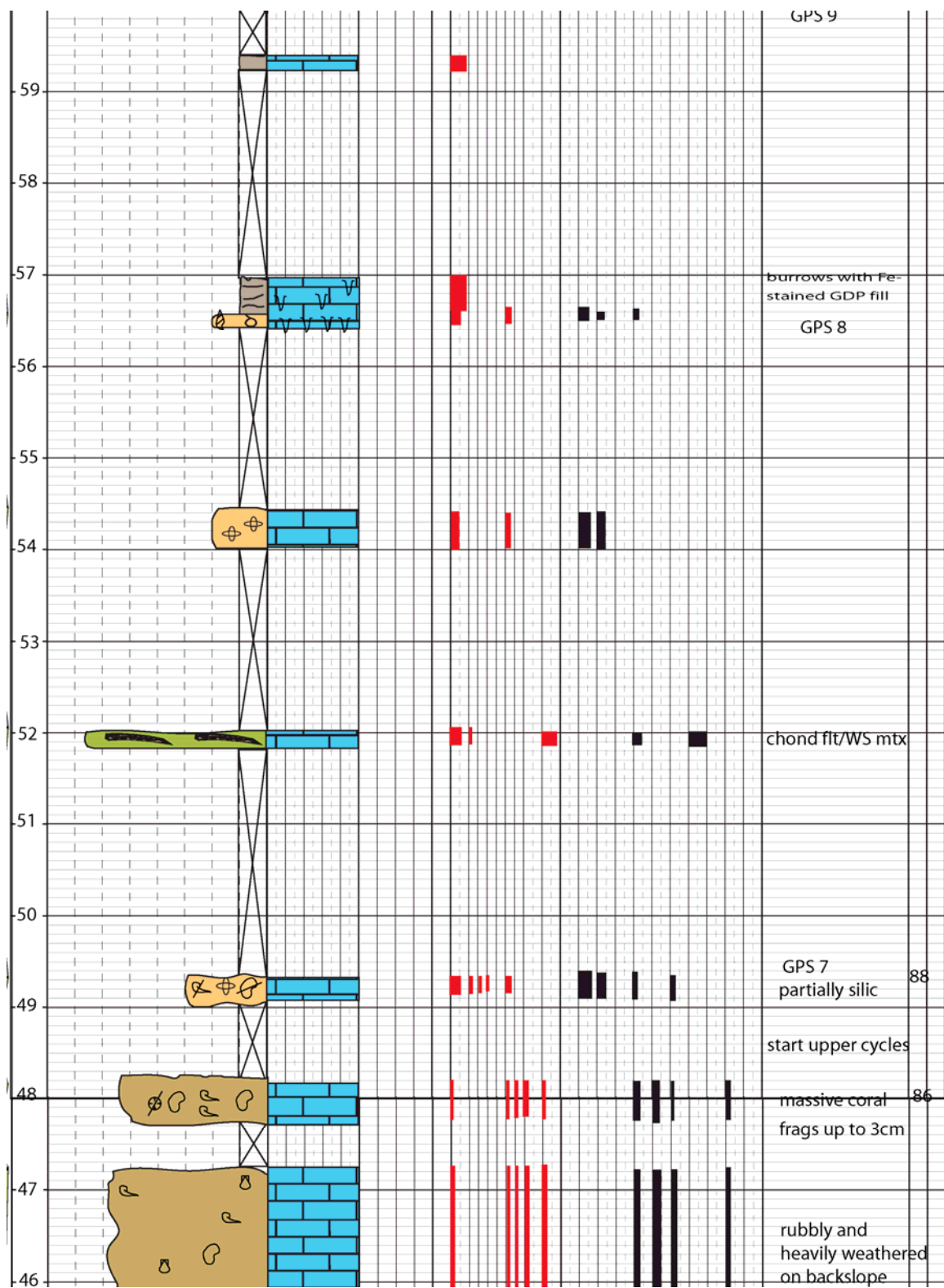


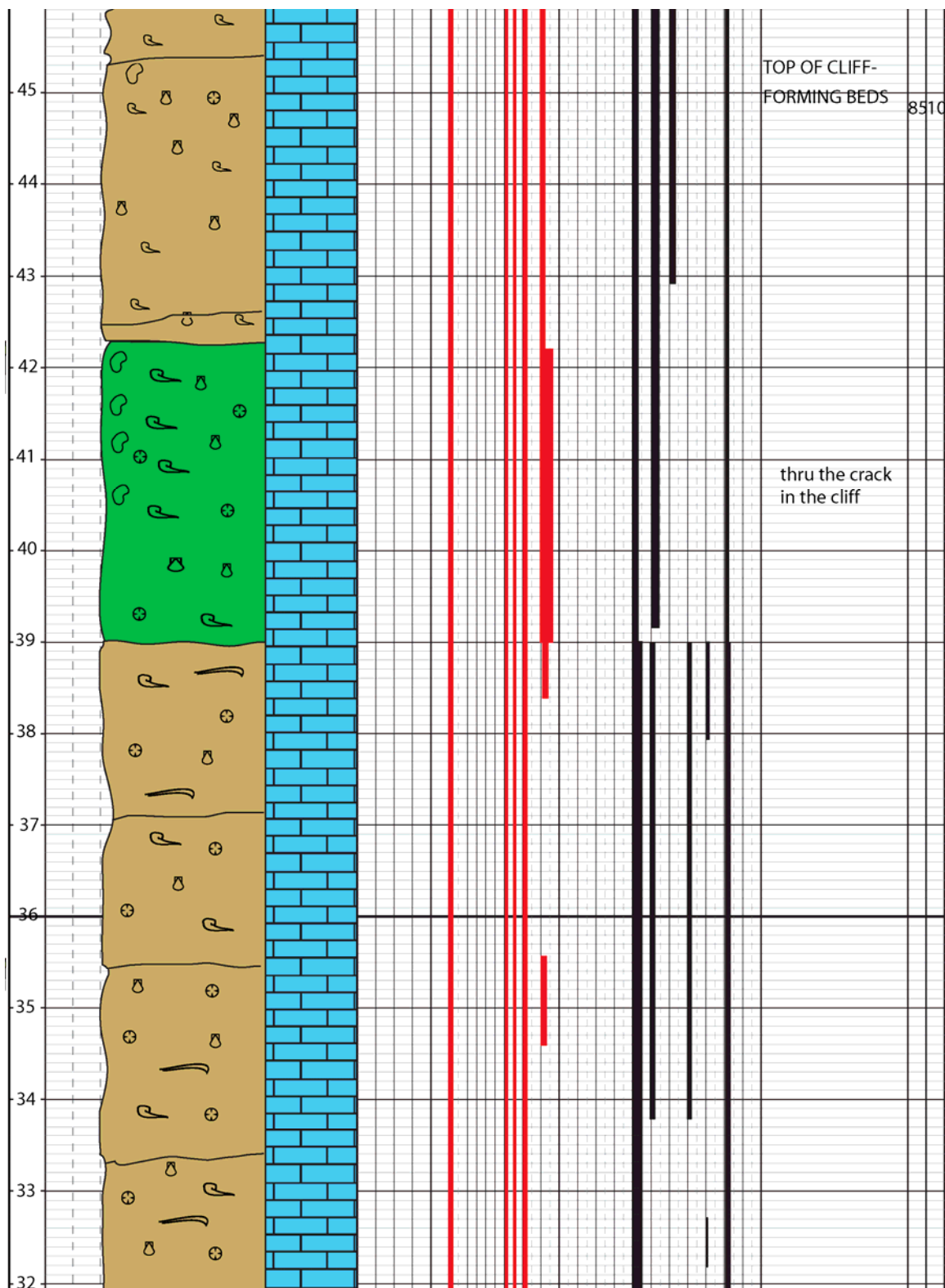


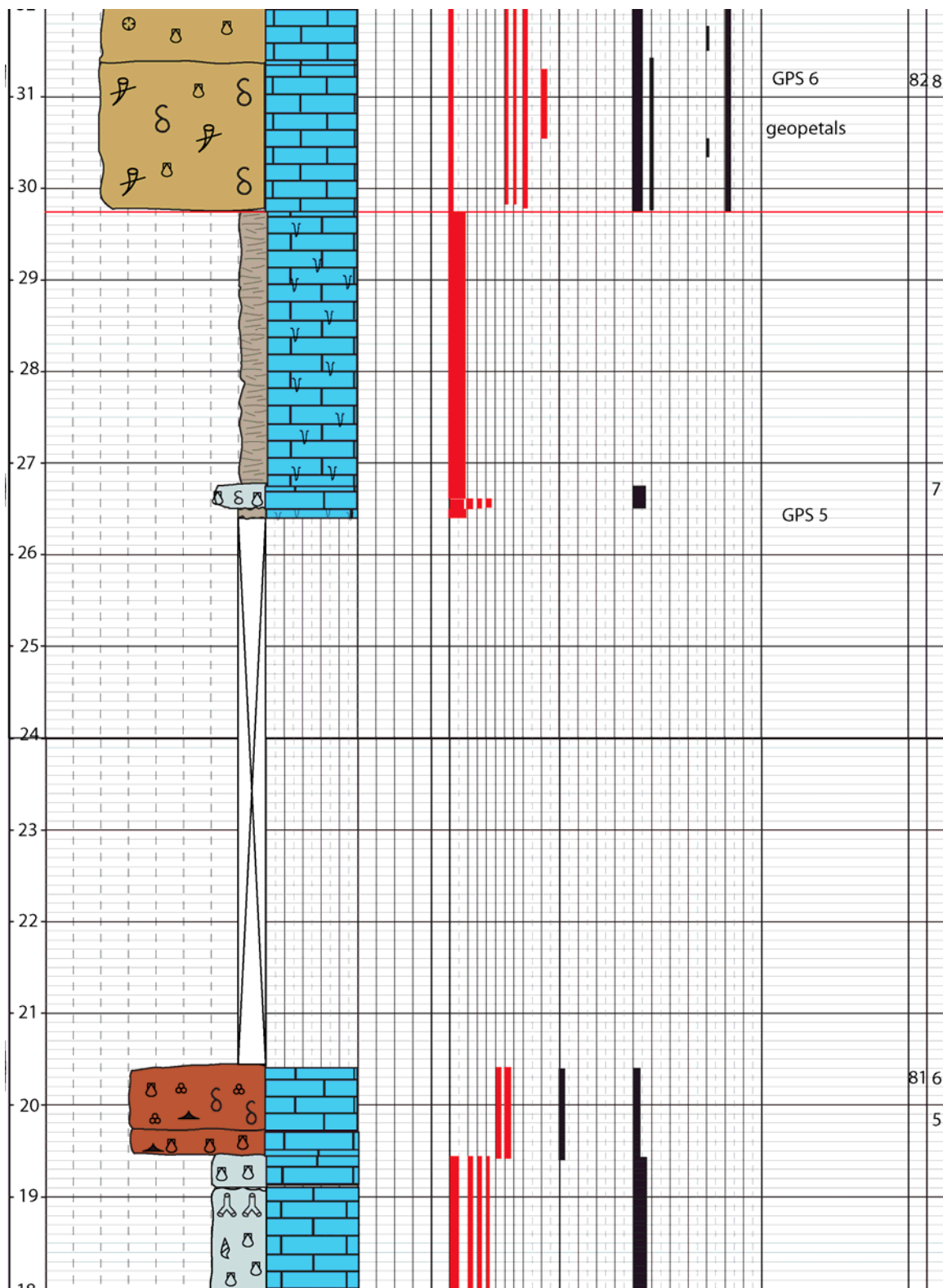


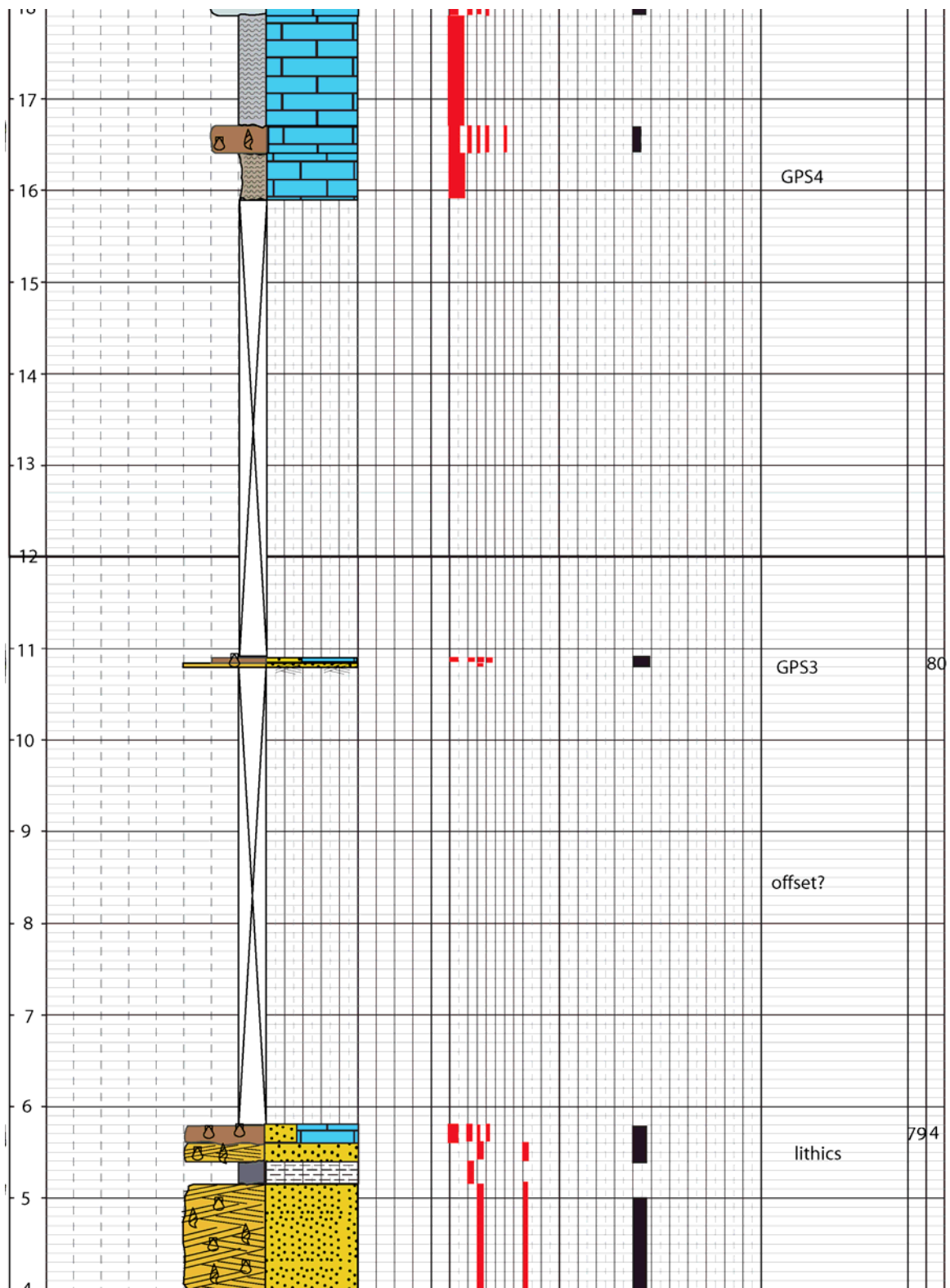


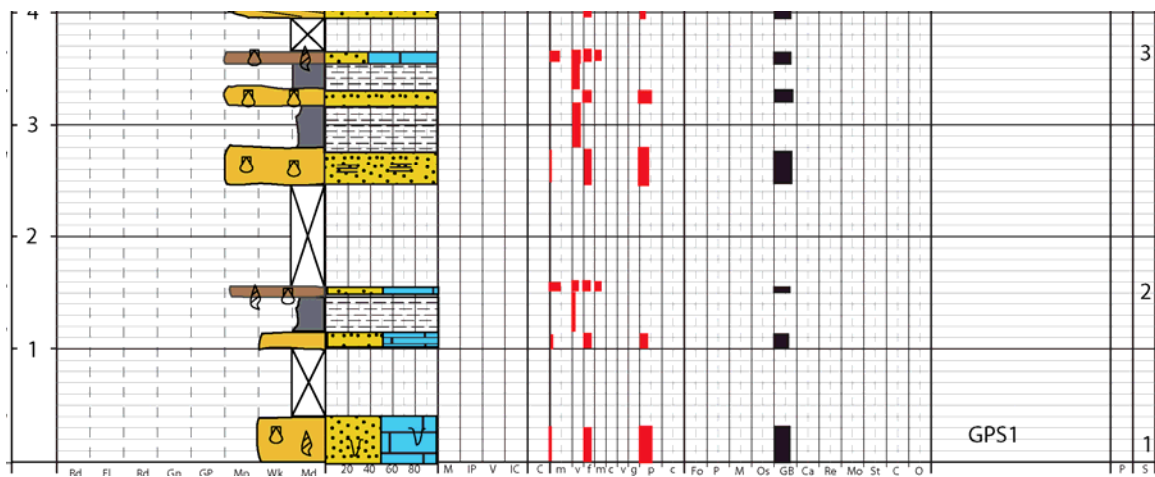




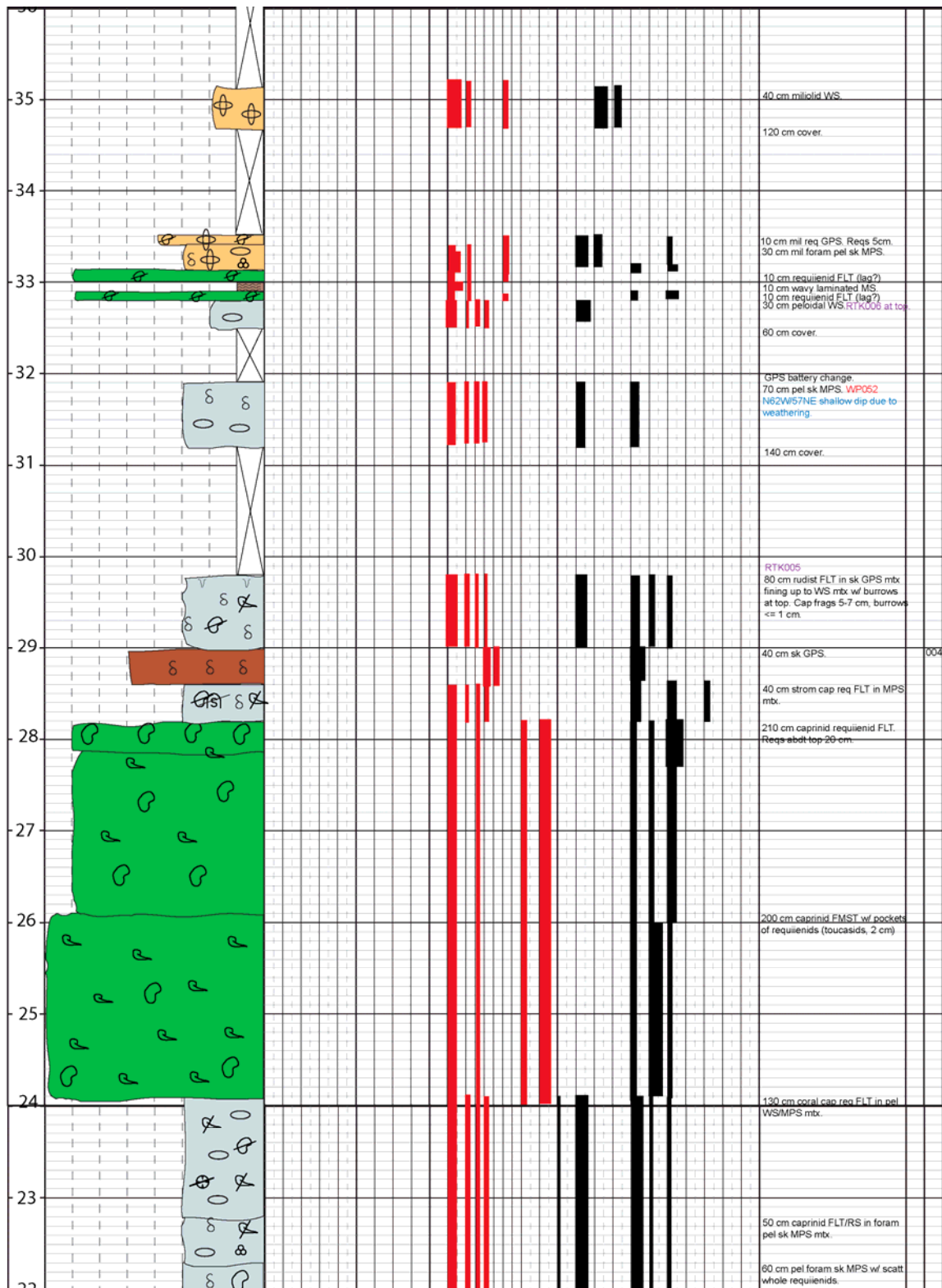




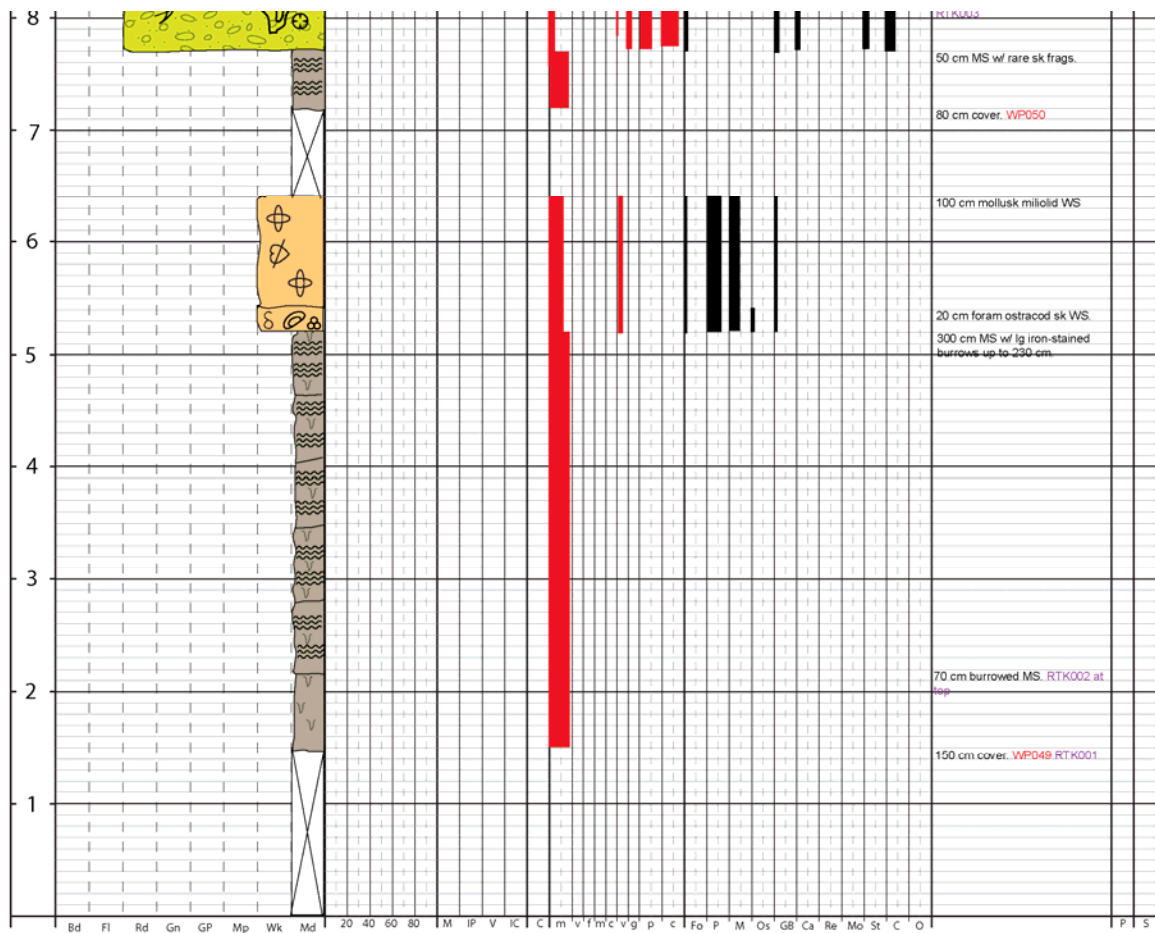




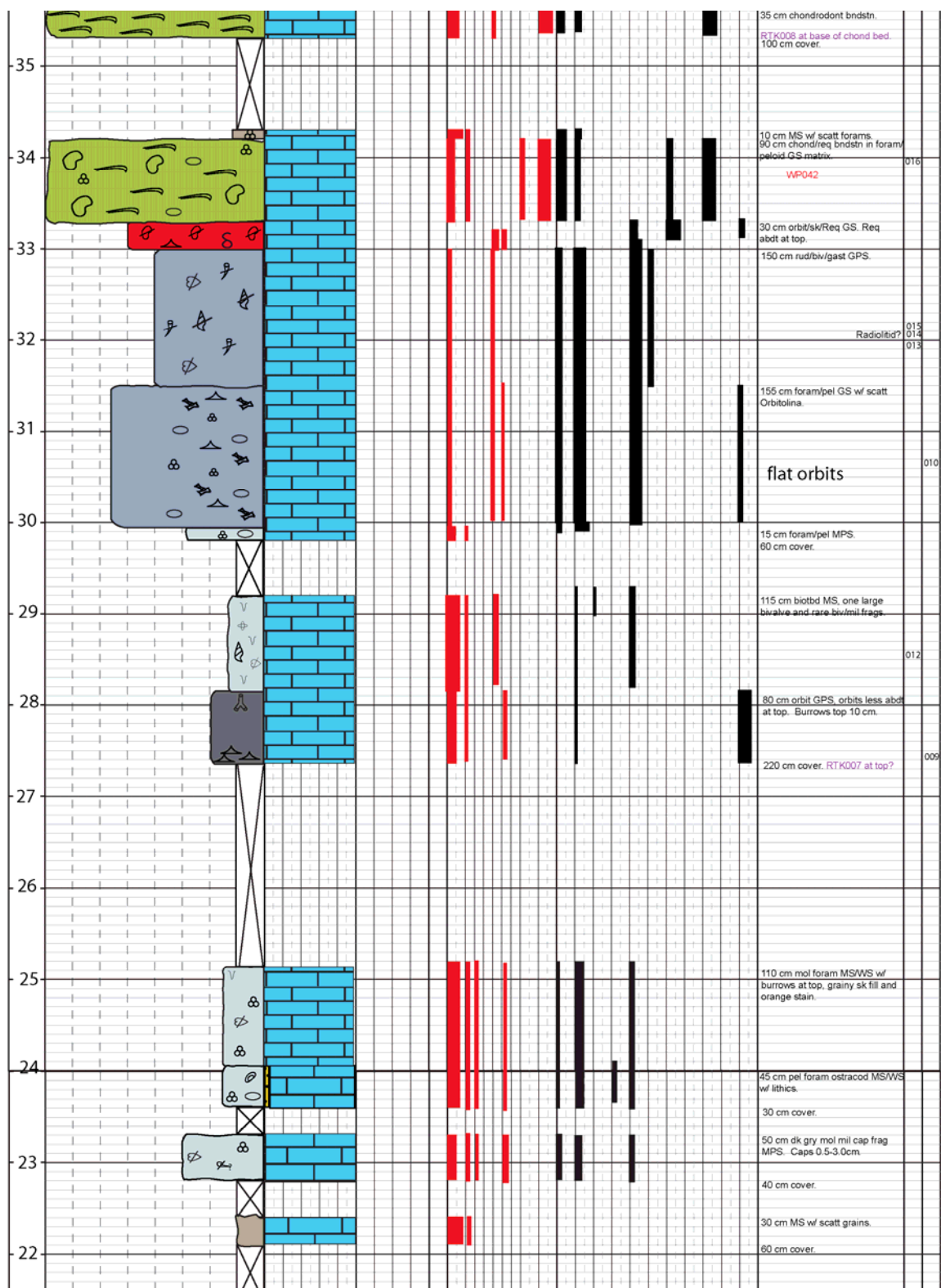


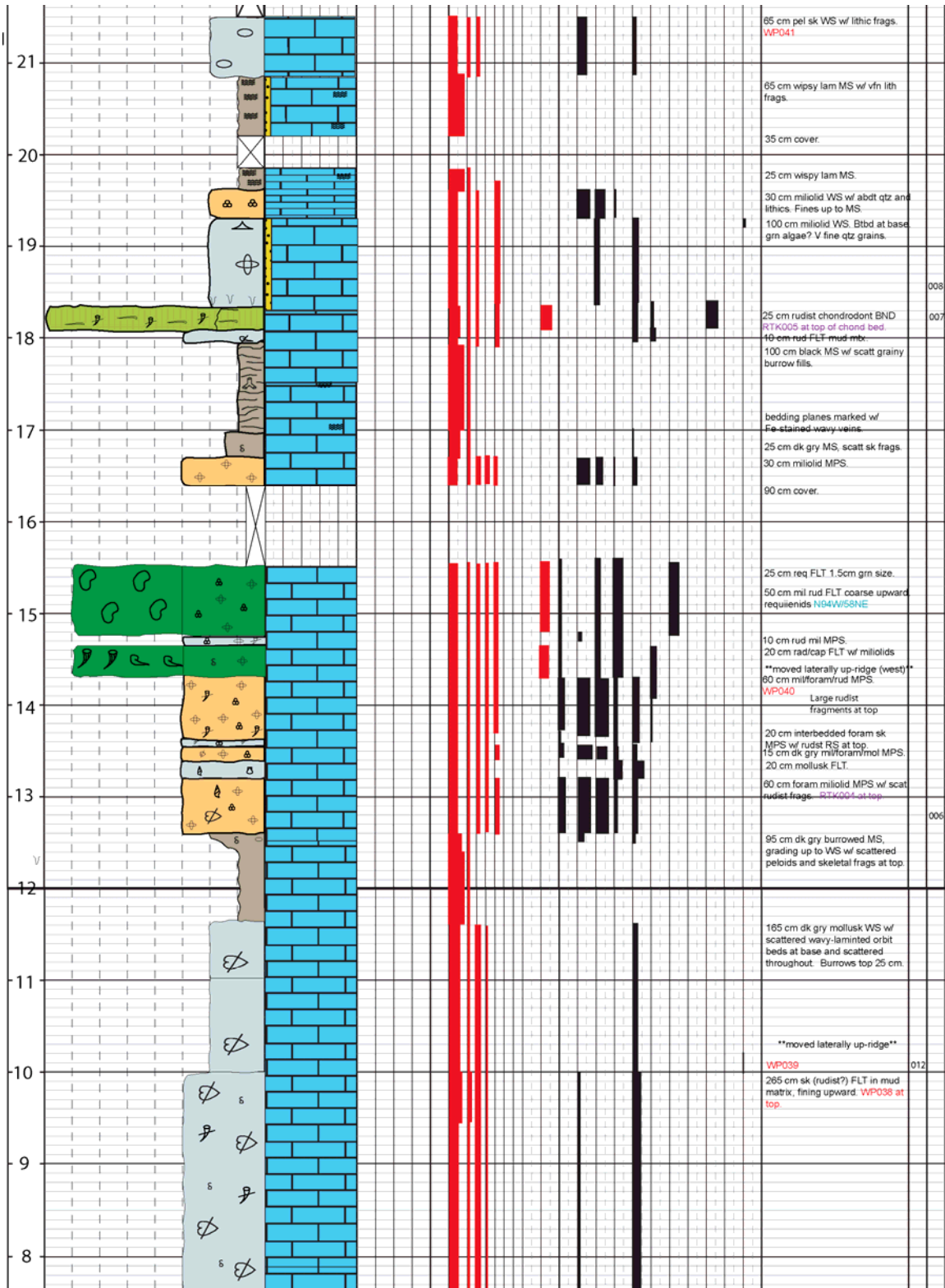






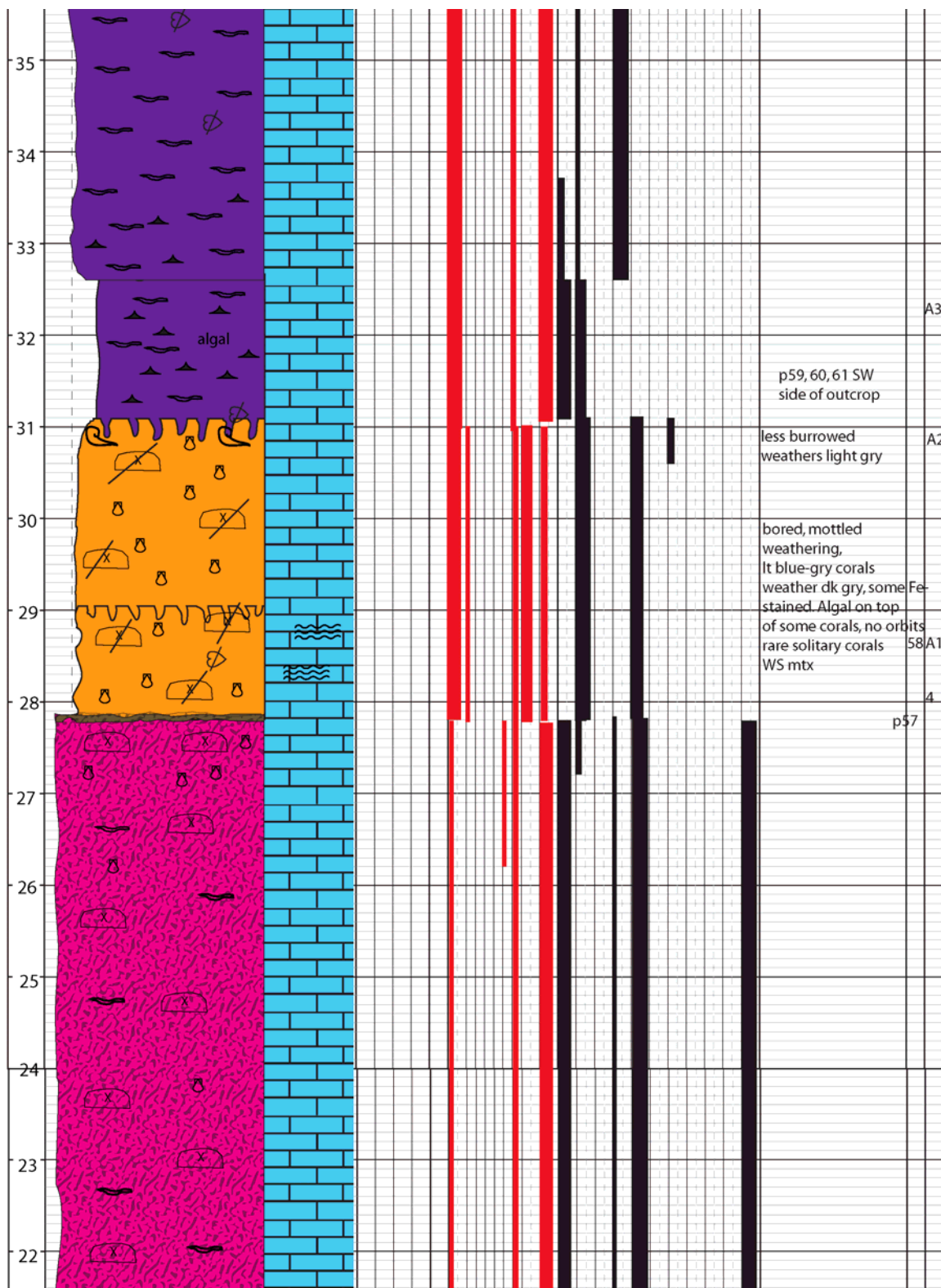


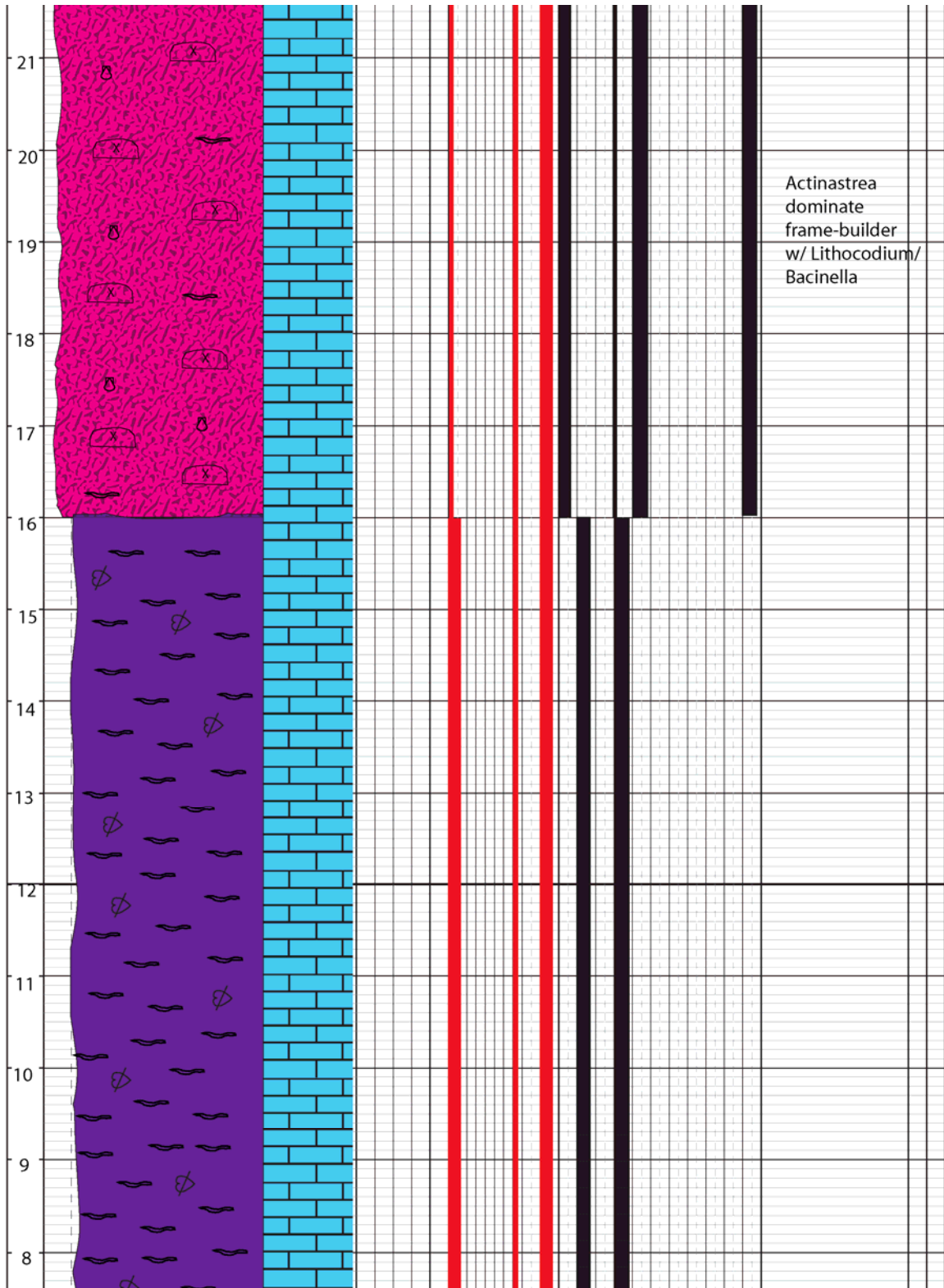


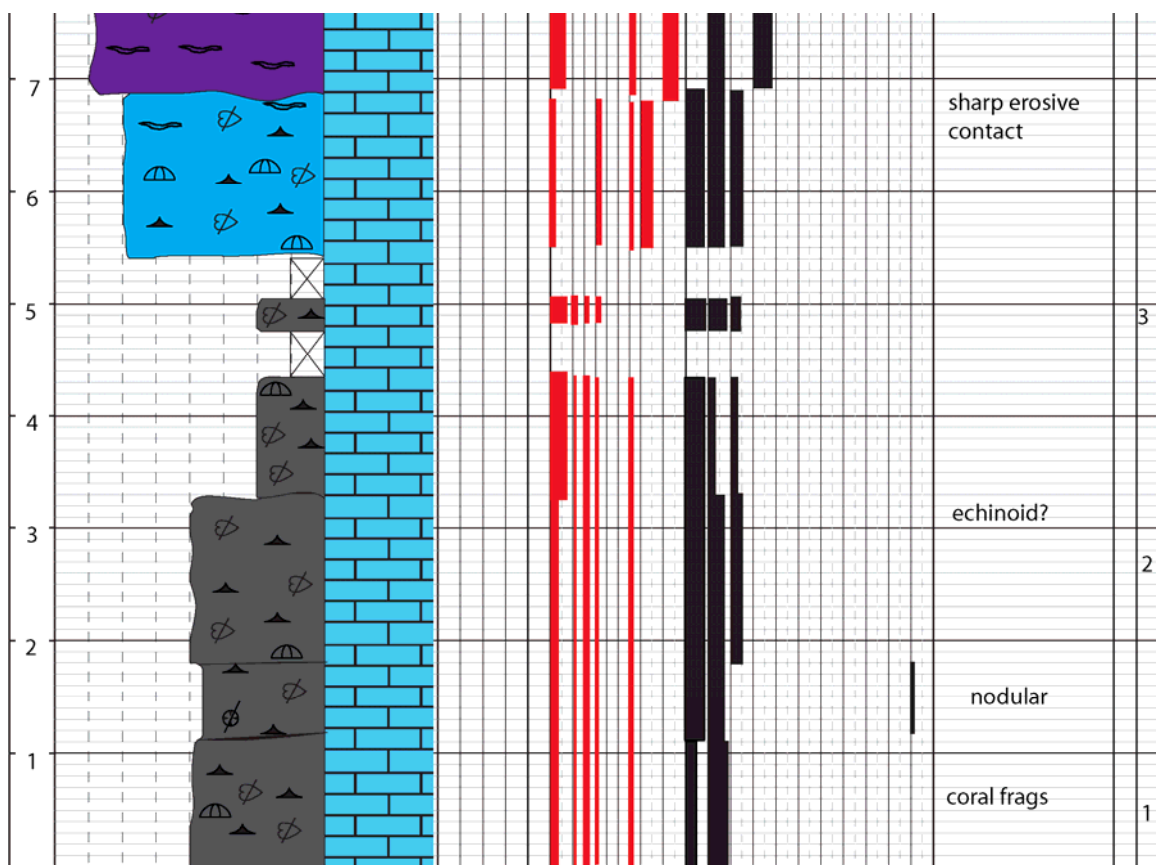












MEASURED SECTION: PS-D (DBSG6B)

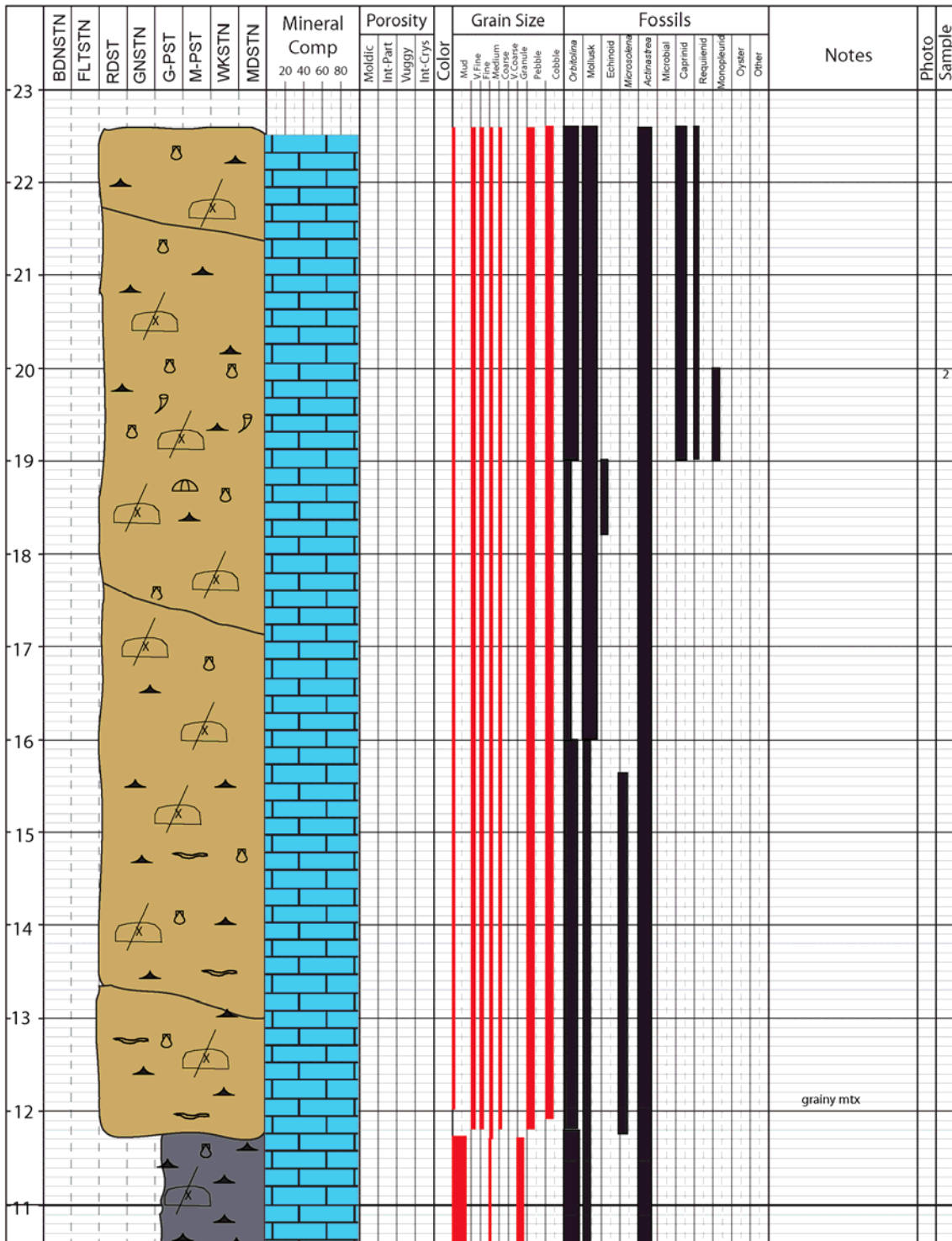
LOCATION: Paul Spur south, south end of northern nose of main outcrop

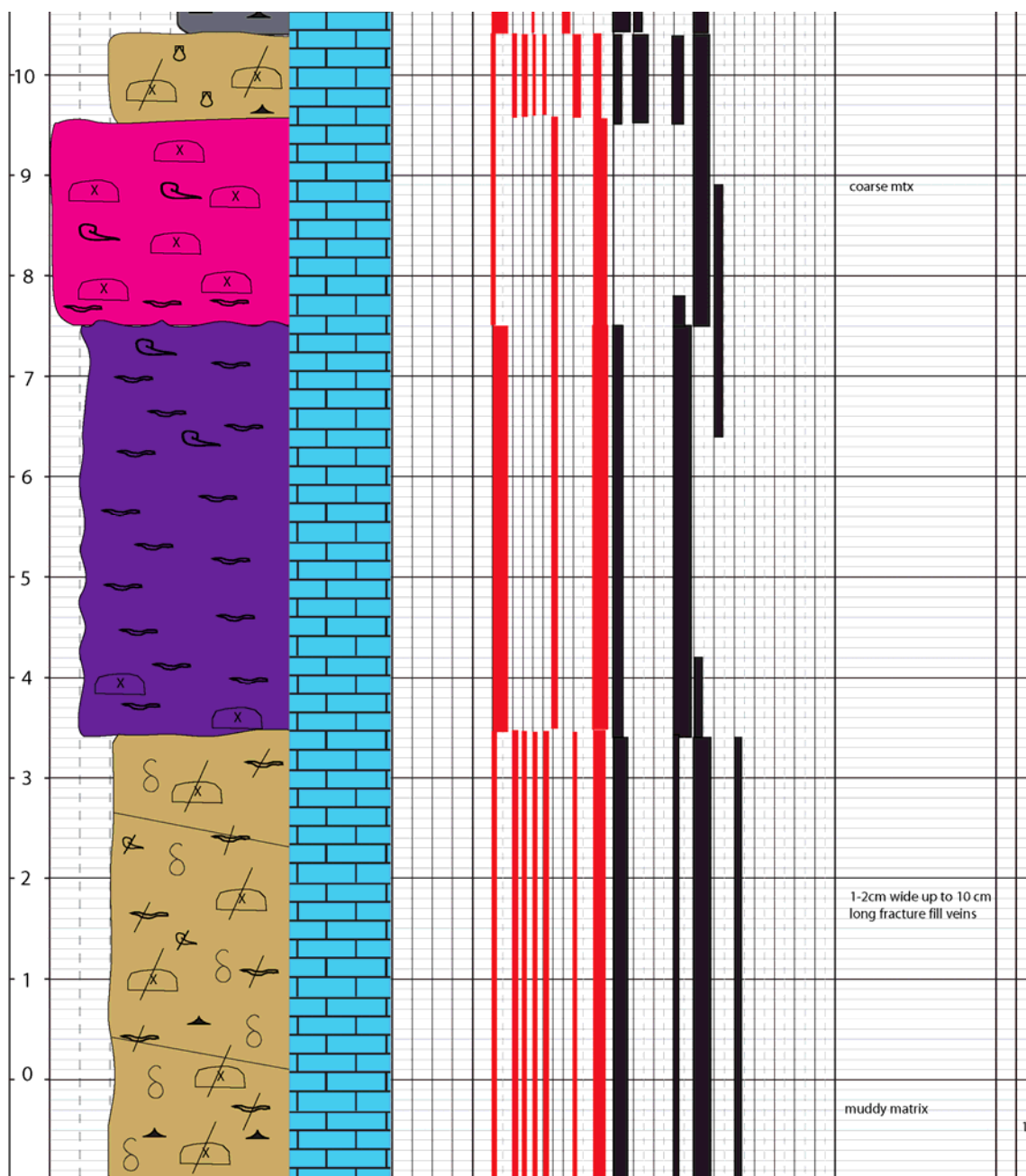
SHEET:

STRAT INTERVAL: Cycle 1,2

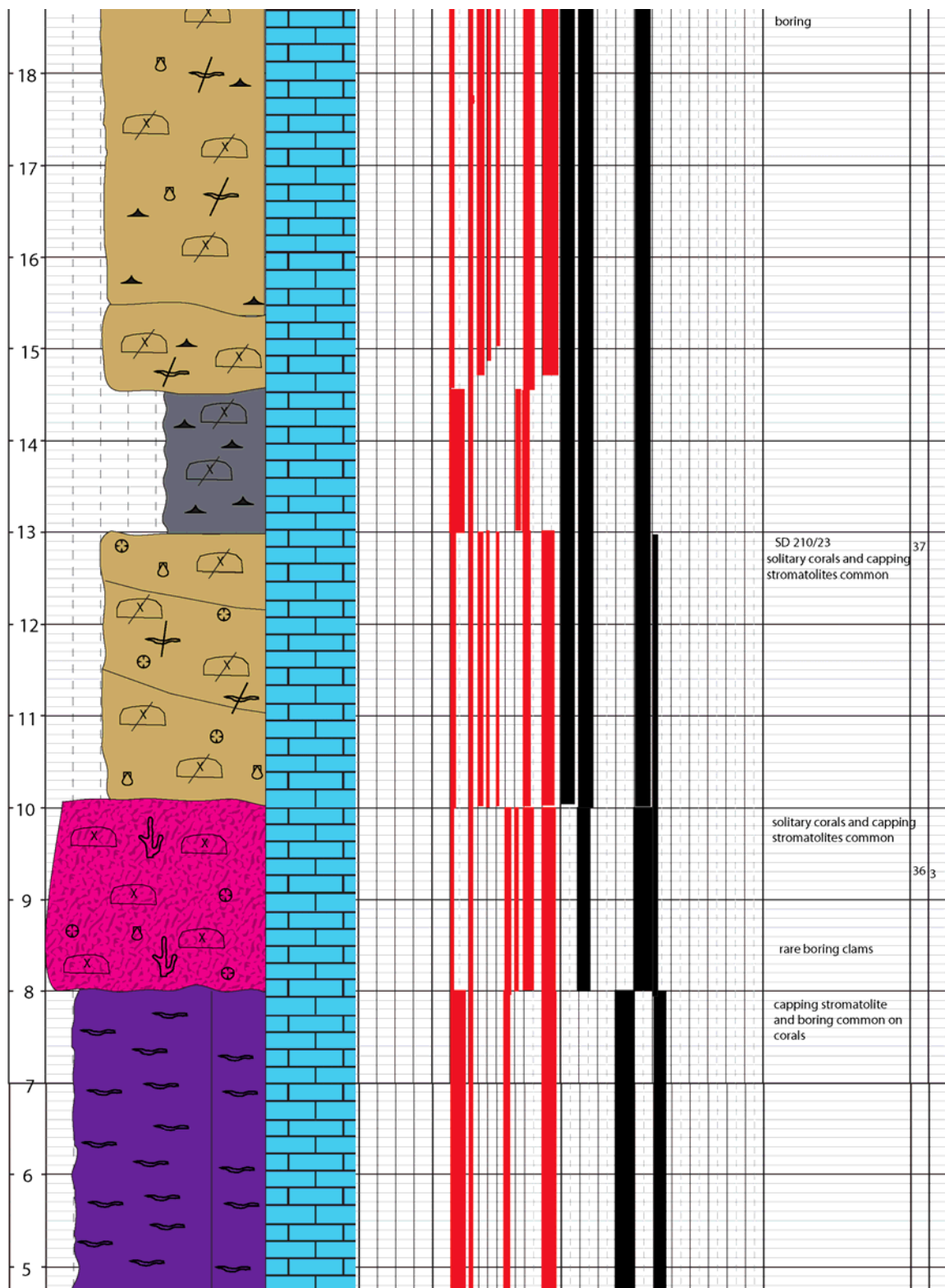
LOGGED BY: RCC

DATE: November 2009



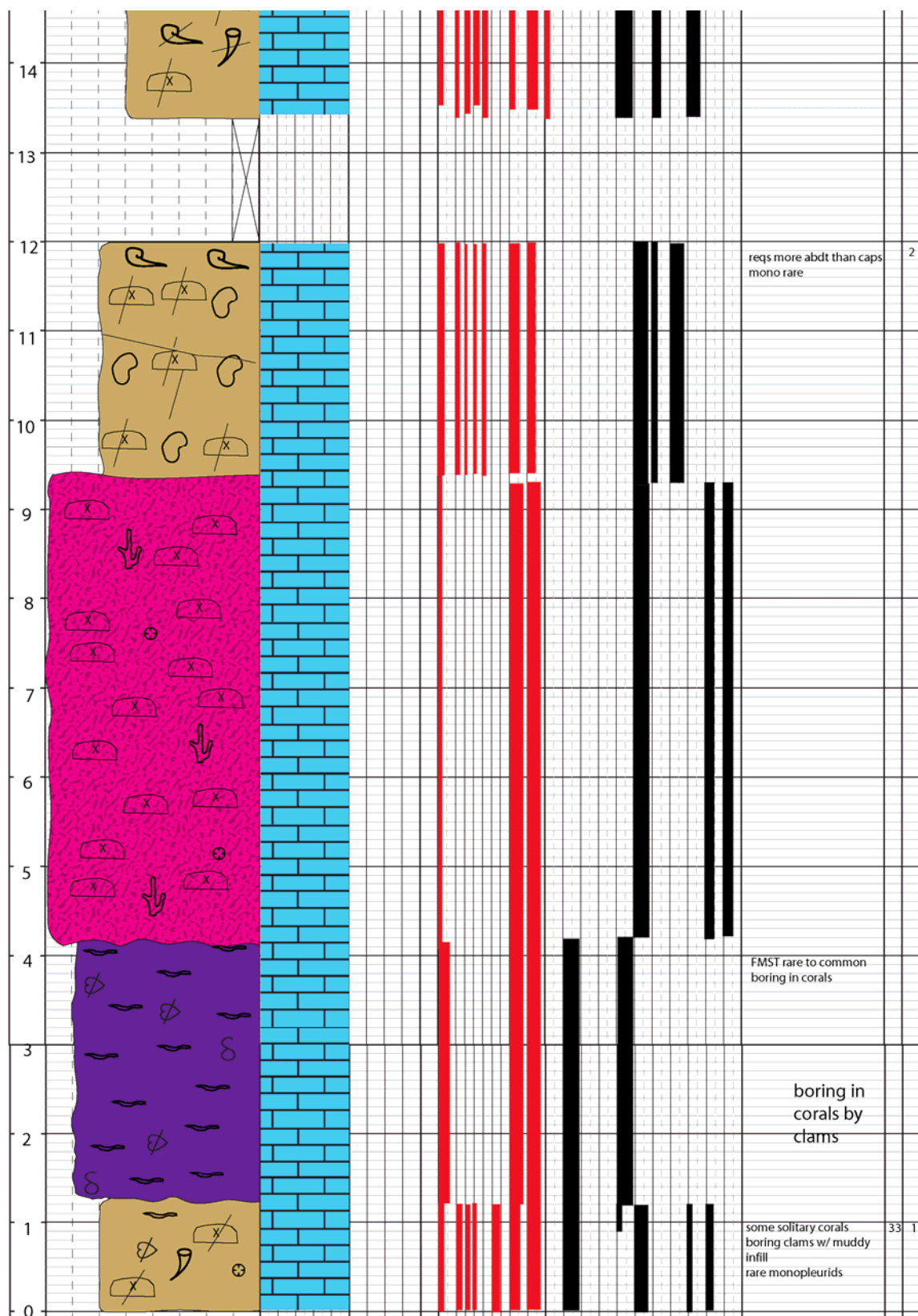






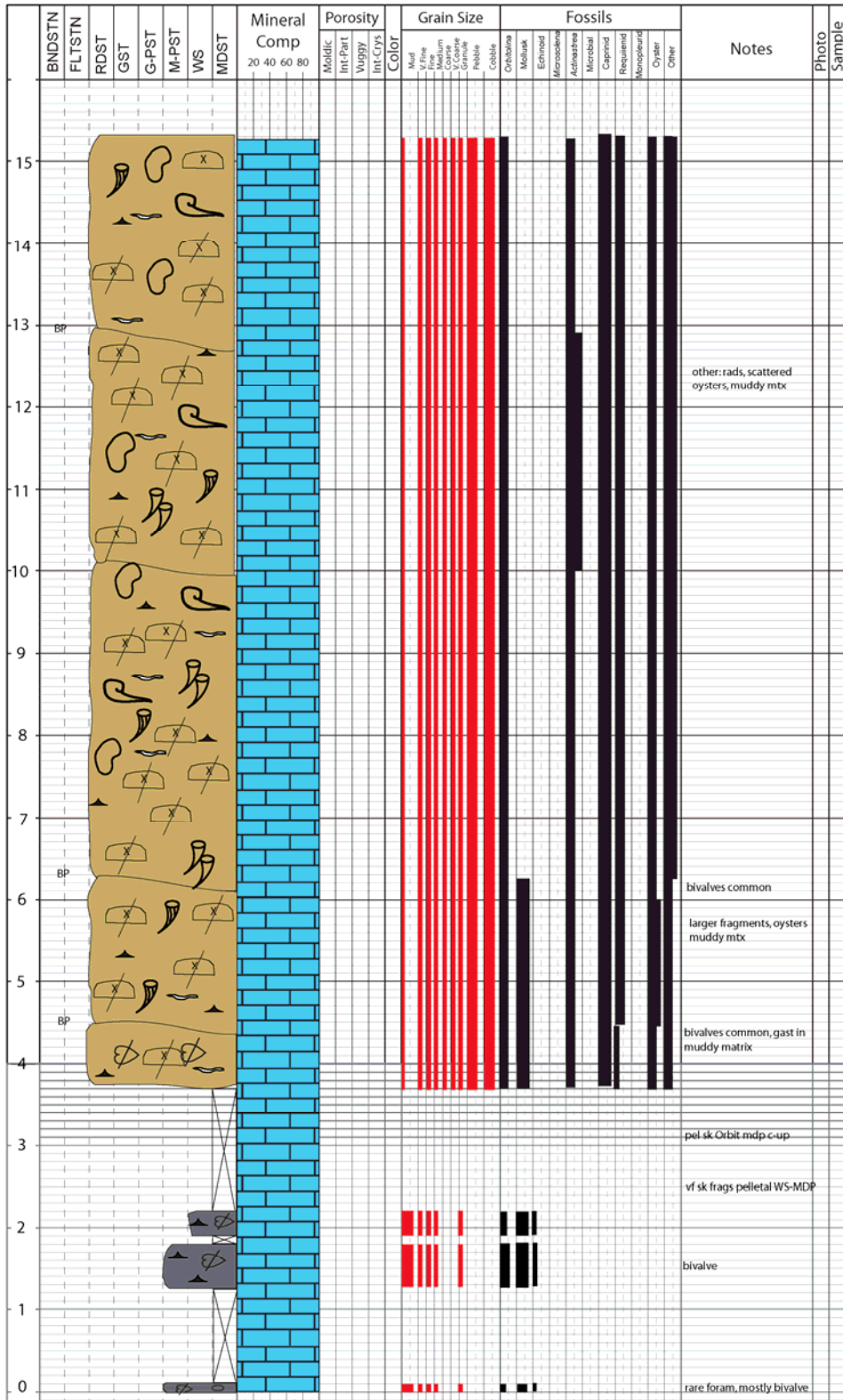








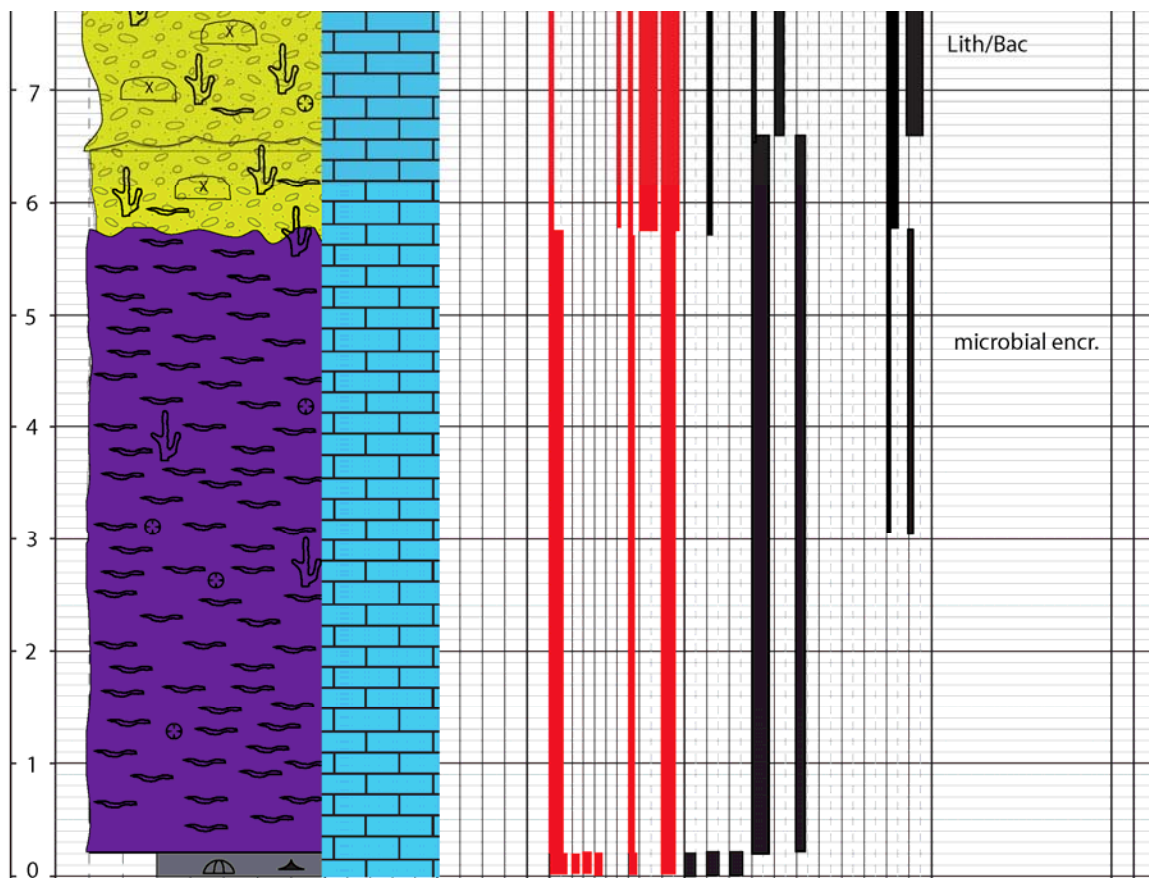
MEASURED SECTION: PSH LOCATION: Paul Spur (South) Cycle 2 SHEET:  
 STRAT INTERVAL: 0-15m LOGGED BY: REA DATE: Nov. 2009



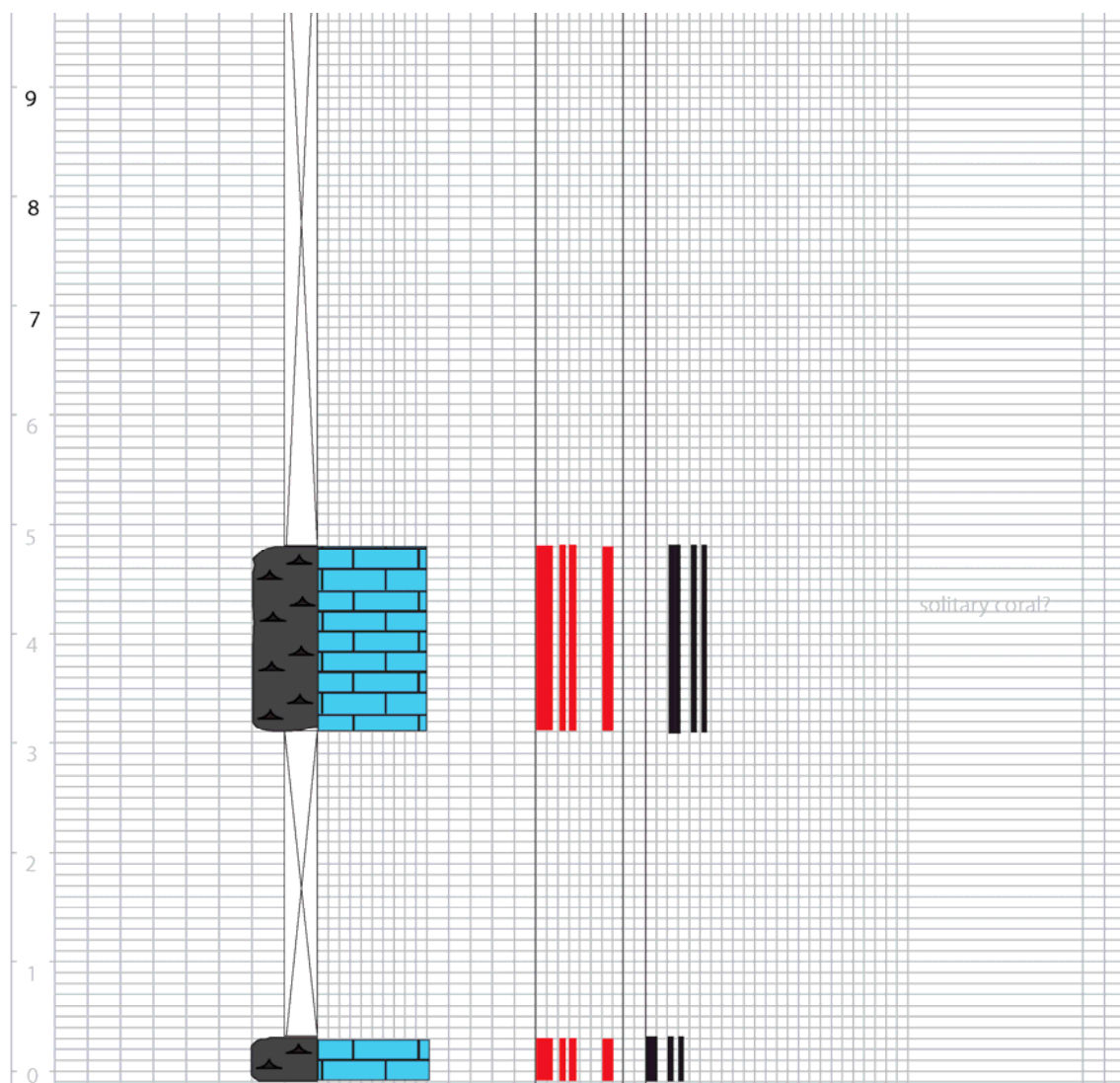




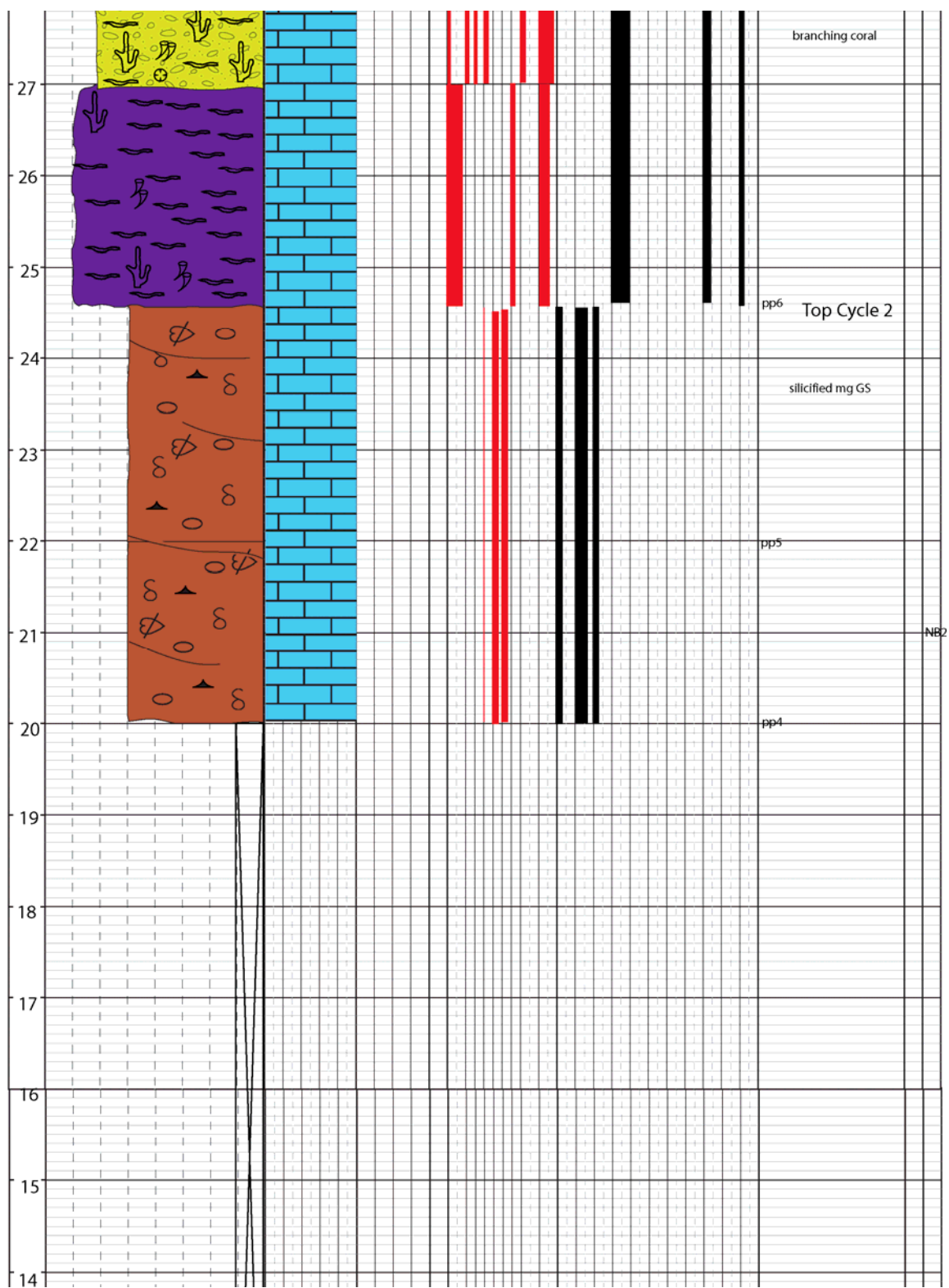


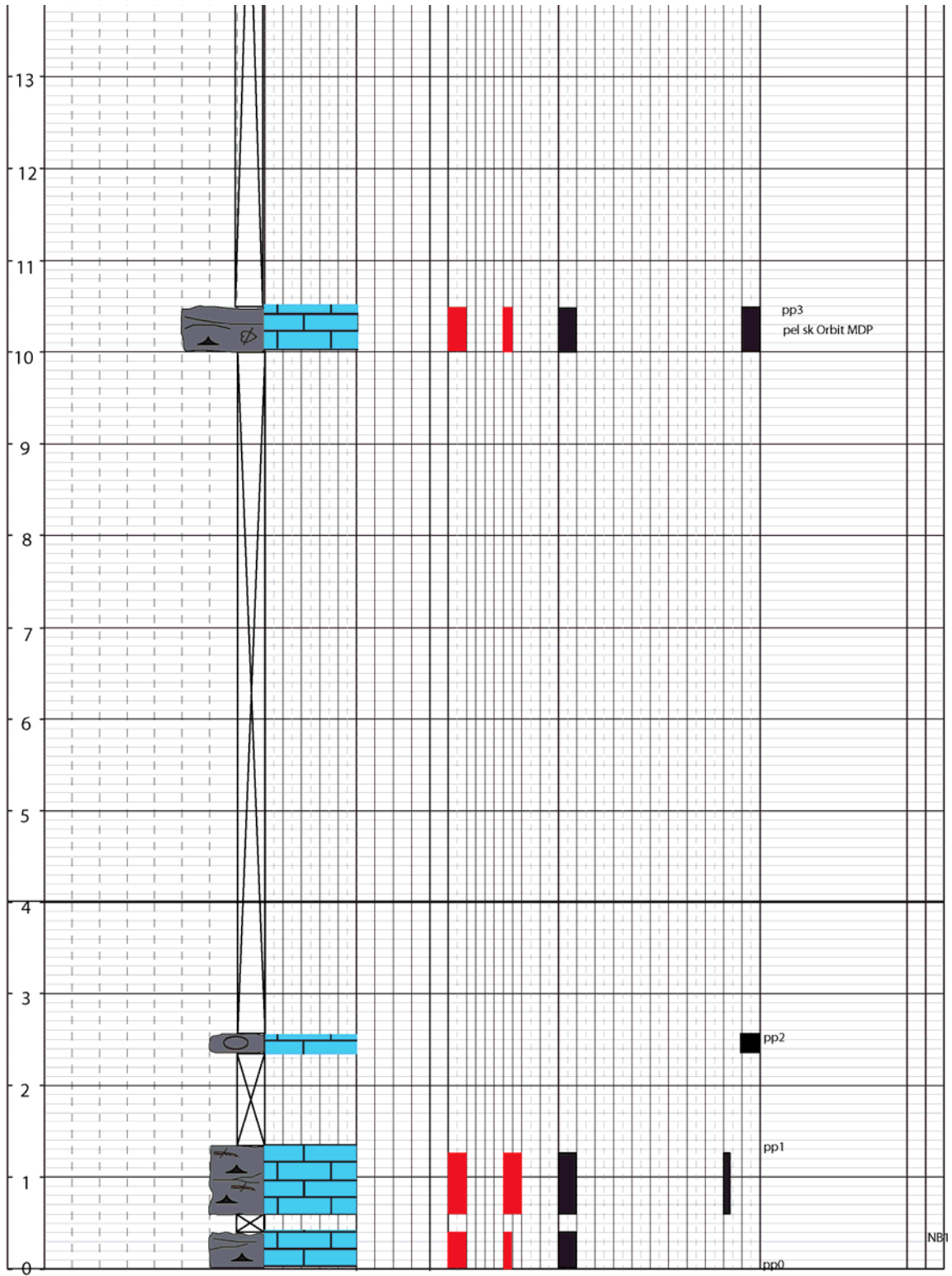




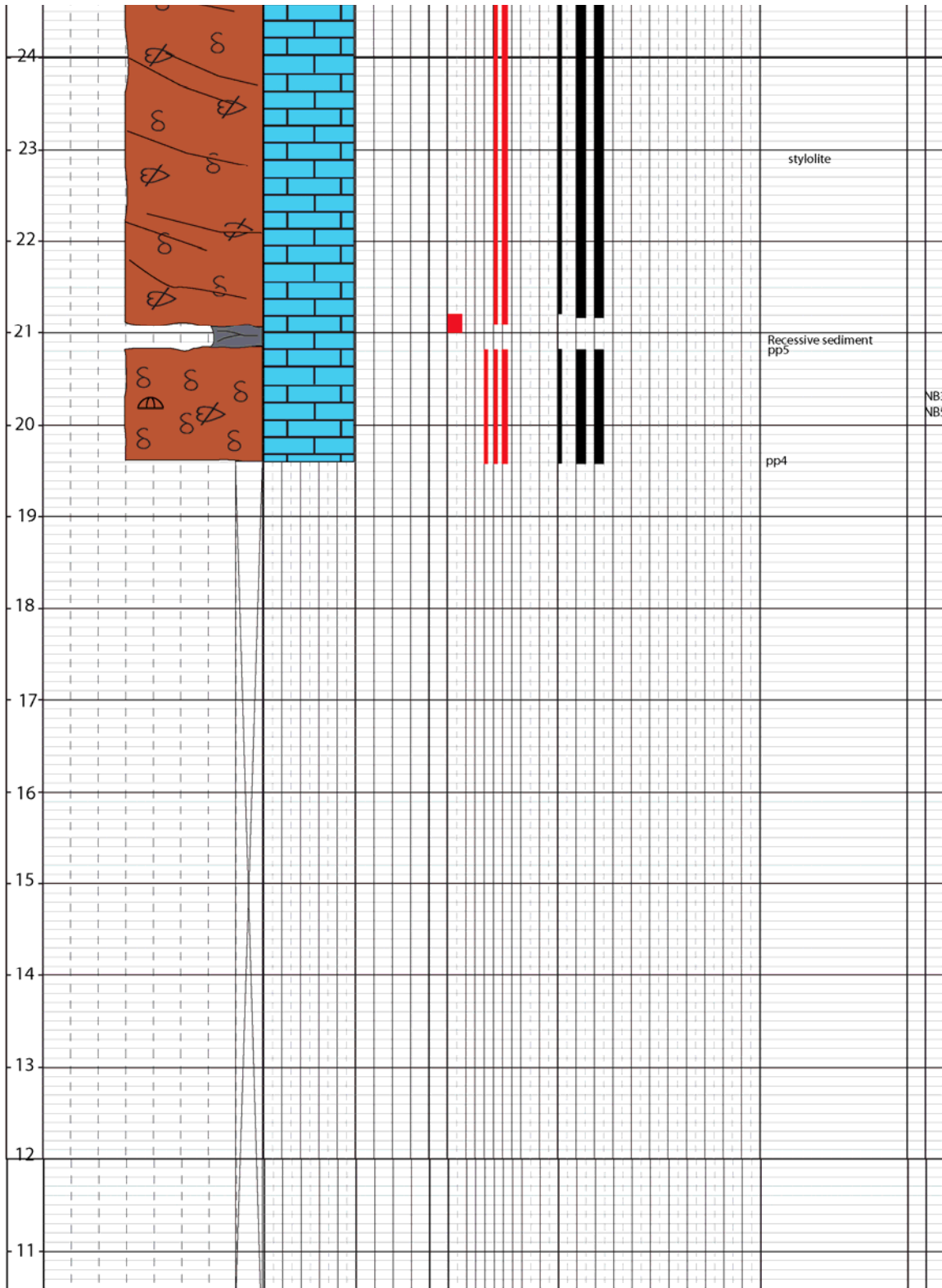


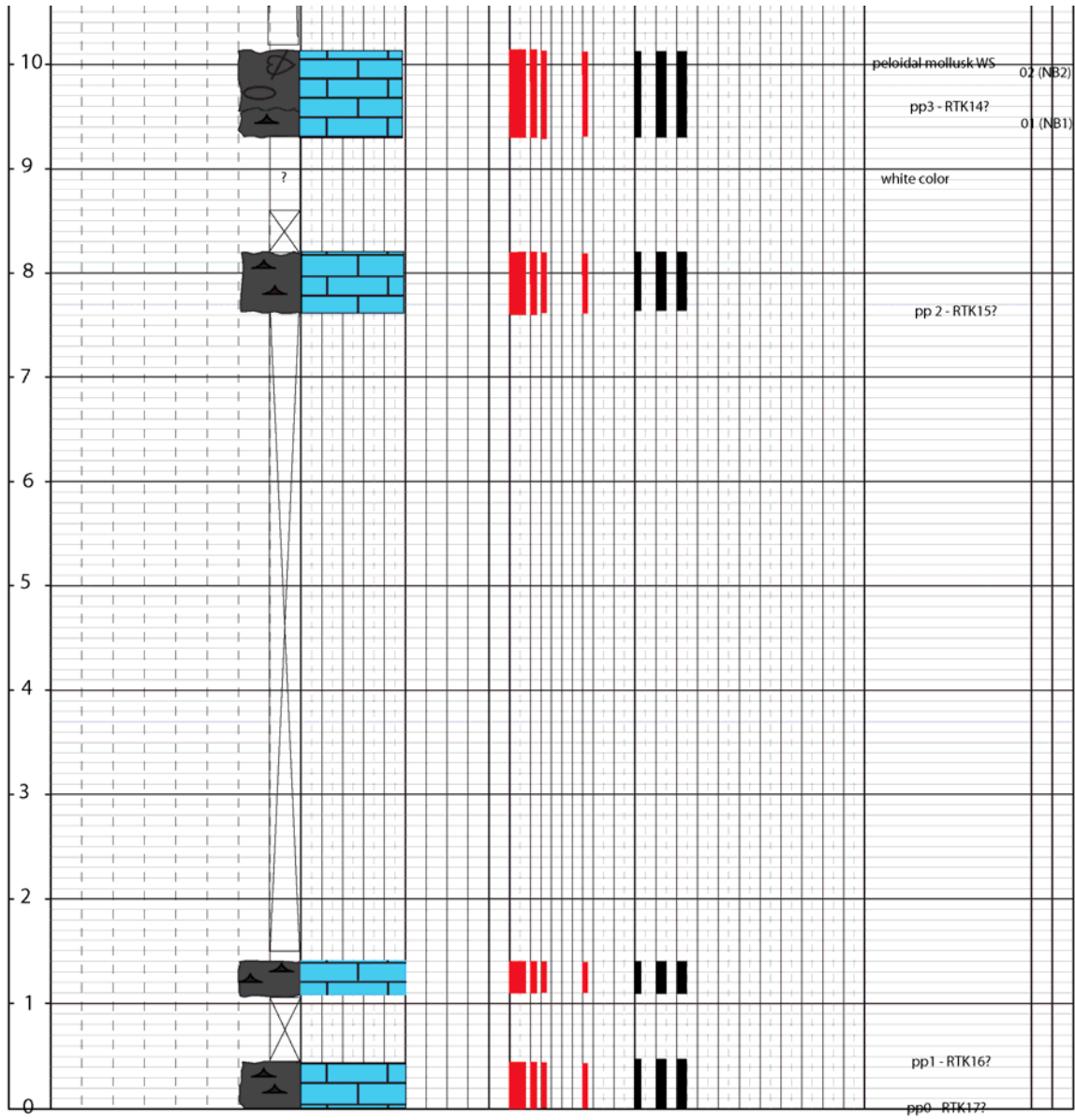












MEASURED SECTION: PS-O

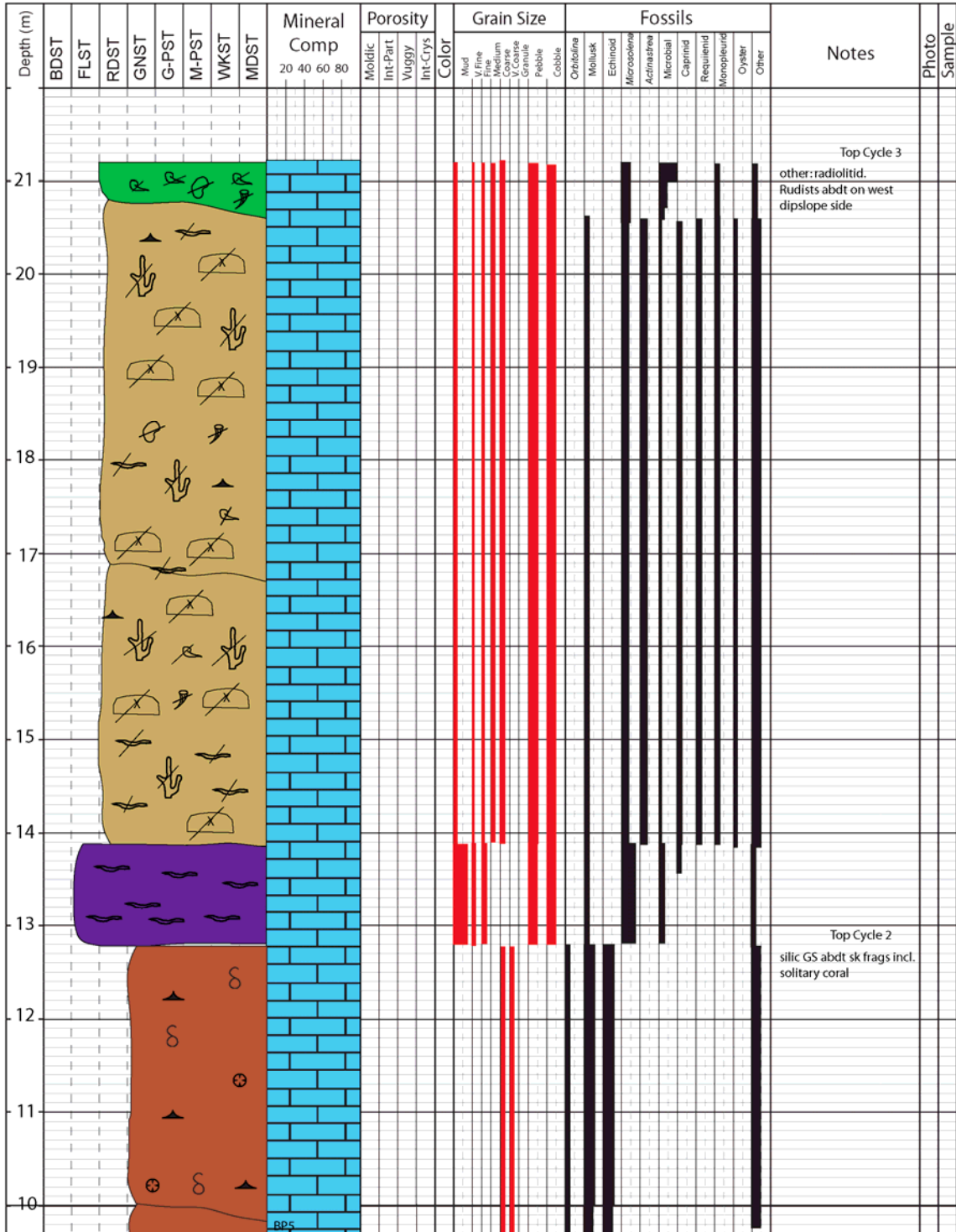
LOCATION: Paul Spur North (North3 #3)

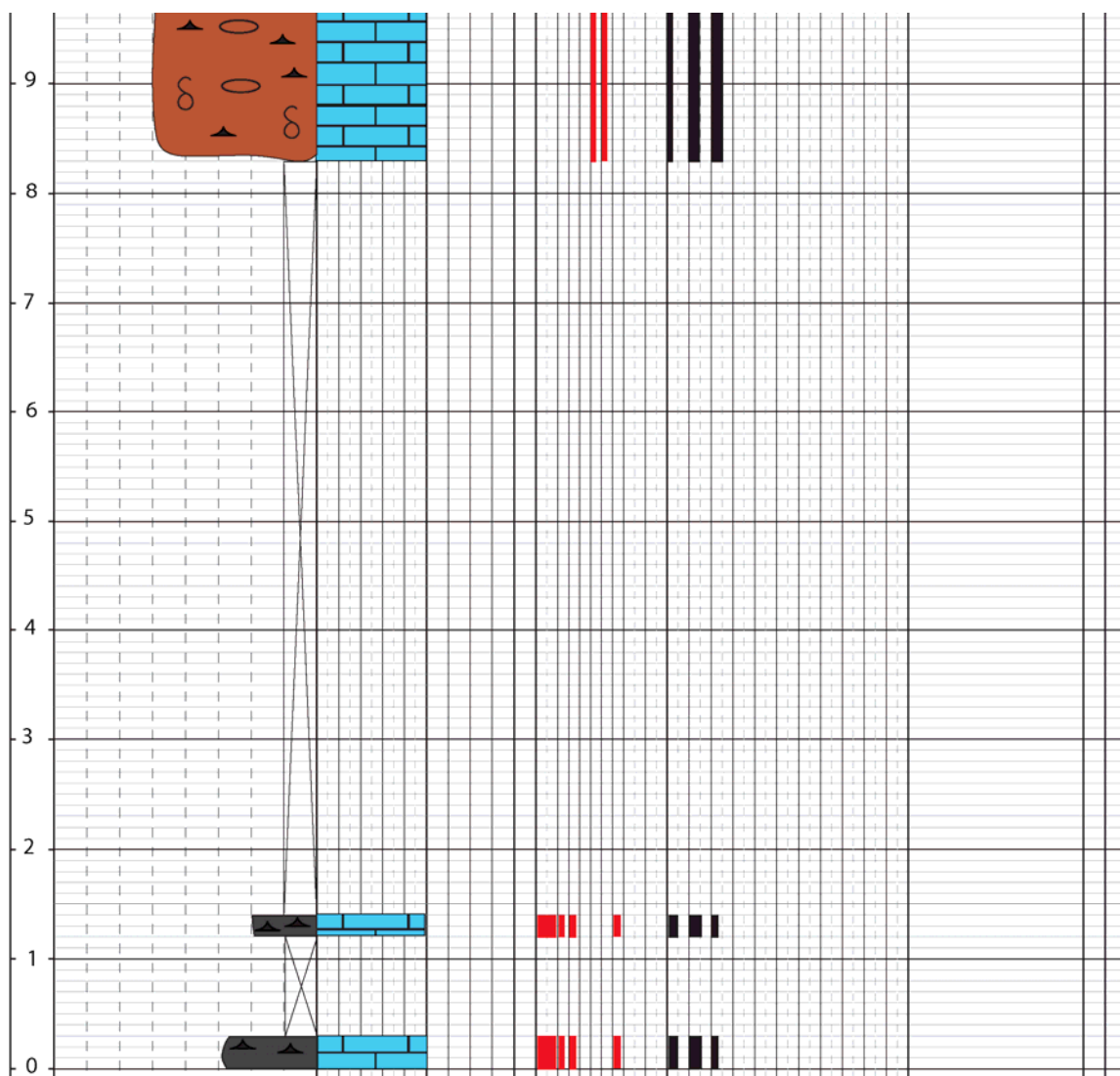
SHEET:

STRAT INTERVAL: Cycle 2,3

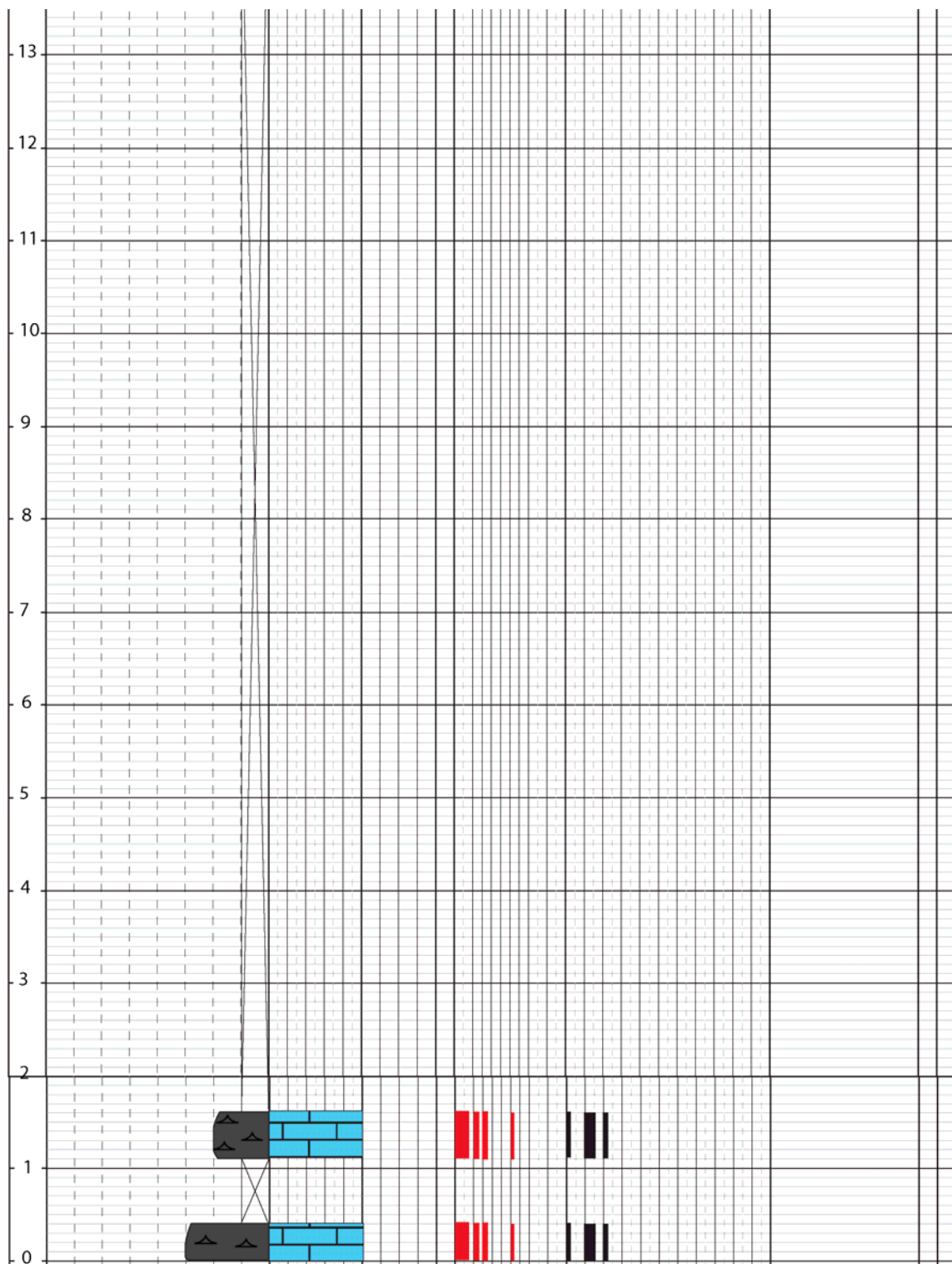
LOGGED BY: SS

DATE: Nov. 2009











## References

- Aconcha, E. S., 2008, Integrated core, well log, and seismic interpretation of Albian patch reefs in the Maverick Basin, SW Texas: Master's thesis, The University of Texas at Austin, 97 p.
- Alsharan, A. S., 1995, Facies variation, diagenesis, and exploration potential of the Cretaceous rudist-bearing carbonates of the Arabian Gulf: AAPG Bulletin v. 79 no. 4, p. 531-550.
- Baines, G. B. K., Beveridge, P. K., Maragos, J. E., 1974, Storms and island building at Funafuti Atoll, Ellice Islands, Proc. 2nd International Coral Reef Symposium #2, p. 485-496.
- Ball, M. M., 1967, Sand bodies of Florida and the Bahamas: Journal of Sedimentary Petrology, v. 37, no. 2, p. 556-591.
- Bebout, D. G., and Loucks, R. G., 1974, Stuart City trend Lower Cretaceous, South Texas, a carbonate shelf-margin model for hydrocarbon exploration: The University of Texas at Austin, Bureau of Economic Geology Report of Investigations, no. 78, 181 p.
- Bellian, J. A., Kerans, Charles, and Jennette, D. C., 2005, Digital outcrop models: applications of terrestrial scanning lidar technology in stratigraphic modeling: Journal of Sedimentary Research, v. 75, no. 2, p. 166-176.
- Bilodeau, W. L., Tectonic models for Early Cretaceous rifting in southeastern Arizona: Geology, v. 10, no. 9, p. 466-470.
- Boggs, S., 2006, Principles of Sedimentology and Stratigraphy: Upper Saddle River, Pearson Prentice Hall, 662 p.
- Bonnaffe, Florence, Jennette, Dave, and Andrews, John, 2007, A method for acquiring and processing ground-based lidar data in difficult-to-access outcrops for use in three-dimensional, virtual-reality models: Geosphere, v. 3, no. 6, p. 501-510.
- Brown, B. E. and Dunne, R. P., 1980, Environmental controls of patch-reef growth and development: Marine Biology, v. 56, no. 1, p. 85-96.
- Buitron, B. E., Carrillo, M., del Carmen, M., Aguilera, N., 1995, A middle Albian biota (algae, foraminifera and gastropoda) from Ahuacatlan, State of Queretaro, Mexico: Revista Mexicana de Ciencias Geologicas, v. 12, no. 2, p. 145-156.

- Burchette, T. P., and Britton, S. R., 1985, Carbonate facies analysis in the exploration for hydrocarbons: a case-study from the Cretaceous of the Middle East: Geological Society of London, Special Publications, v. 18, p. 311-338.
- Dupraz, C., and Strasser, A., 2002, Nutritional models in coral-microbialite reefs (Jurassic, Oxfordian, Switzerland): evolution of trophic structure as a response to environmental change: *Palaios*, v. 17, p. 449-471.
- Enos, P., 1974, Reefs, platforms and basins of Middle Cretaceous in northeast Mexico: *AAPG Bulletin*, v. 58, no. 5, p. 800-809.
- Enos, P., 1983, Chapter 6: Shelf environment, in Scholle, P. A., Bebout, D. G., and Moore, C. H., 1983, Carbonate Depositional Environments: AAPG Memoir No. 33, p. 298-343.
- Flügel, E., 2004, *Microfacies of Carbonate Rocks*, Berlin, Springer-Verlag, 976 p.
- Frost, E. L., III, and Kerans, Charles, 2010, Controls on syndepositional fracture patterns, Devonian reef complexes, Canning Basin, western Australia: *Journal of Structural Geology* (available online).
- Fursich, F. T., 1993, Paleocology and evolution of Mesozoic salinity-controlled benthic macroinvertebrate associations: *Lethaia*, v. 25, issue 4, p. 327-346.
- Gischler, E., and Lomando, A. J., 1999, Recent sedimentary facies of isolated carbonate platforms, Belize-Yucatan system, central America: *Journal of Sedimentary Research*, v. 69, no. 3, p. 747-763.
- Gonzalez-Leon, C. M., Scott, R. W., Loser, H., Lawton, T. F., Robert, E., and Valencia, V. A., 2007, Upper Aptian-lower Albian Mural formation: stratigraphy, biostratigraphy and depositional cycles on the Sonoran shelf, northern Mexico: *Cretaceous Research*, v. 29, pp. 249-266.
- Gotz, S., Loser, H., and Schmid, D. U., Reef development on a deepening platform: two Early Cretaceous coralline patch reefs (Cati, Llacova Formation, Eastern Spain) compared: *Cretaceous Research*, v. 26, p. 854-881.
- Hallock, P., and Schlager, W., 1986, Nutrient excess and the demise of coral reefs and carbonate platforms: *Palaios*, v. 1, p. 389-398.
- Hamdan, A. R. A., and Alsharhan, A. S., 1991, Palaeoenvironments and palaeocology of the rudists in the Shuaiba Formation (Aptian) United Arab Emirates: *Journal of African Earth Sciences*, v. 12, no. 4, p. 569-581.

- Hartshorne, P. M., 1989, Facies architecture of a Lower Cretaceous coral-rudist patch reef, Arizona: *Cretaceous Research*, v. 10, p. 311-336.
- Hayes, P. T., 1970, Mesozoic Stratigraphy of the Mule and Huachuca Mountains, Geol. Survey Prof. Paper 688-B, 42 p.
- Hillgartner, H., van Buchem, F. S. P., Gaumet, F., Razin, P., Pittet, B., Grottsch, J., Droste, H., 2003, The Barremian-Aptian evolution of the Eastern Arabian carbonate platform margin (Northern Oman), *Journal of Sedimentary Geology*, v. 73, no. 5, p. 756-773.
- Hofling, R., and Scott, R. W., 2002, Early and mid-Cretaceous buildups, in *Phanerozoic Reef Patterns* (Eds. Kiessling, W., Flugel, W., and Golonka, J.): SEPM Special Publication No. 72, p. 521-548.
- Hubbard, D. K., Miller, A. I., and Scaturro, D., 1990, Production and cycling of calcium carbonate in a shelf-edge reef system (St. Croix, U.S. Virgin Islands): Applications to the nature of reef systems in the fossil record: *Journal of Sedimentary Petrology*, v. 60., no. 3, p. 335-360.
- Hughes, T. P., 1999, Off-reef transport of coral fragments at Lizard Island, Australia: *Marine Geology*, v. 157, p. 1-6.
- Immenhauser, A., and Scott, R. W., 2002, An estimate of Albian sea-level amplitudes and its implication for the duration of stratigraphic hiatuses: *Sedimentary Geology*, v. 152, p. 19-28.
- Insalaco, E., 1996, Upper Jurassic microsolenid biostromes of northern and central Europe: facies and depositional environment: *Palaios*, v. 121, p. 169-194.
- James, N. P., 1983, Chapter 8: Reef environment, in Scholle, P. A., Bebout, D. G., and Moore, C. H., 1983, *Carbonate Depositional Environments*: AAPG Memoir No. 33, p. 346-462.
- Janson, Xavier, Kerans, Charles, Bellian, J. A., and Fitchen, William, 2007, Three-dimensional geological and synthetic seismic model of Early Permian redeposited basinal carbonate deposits, Victorio Canyon, west Texas: *AAPG Bulletin*, v. 91, p. 1405-1436.
- Jones, M. R., 1995, The Torres Reefs, North Queensland, Australia – strong tidal flows a modern control on their growth: *Coral Reefs*, v. 14, p. 63-69.
- Kendall, C. G., and Schlager, W., 1981, Carbonates and relative changes in sea level: *Marine Geology*, v. 44, p. 181-212.

- Kerans, Charles, 2002, Styles of rudist buildup development along the northern margin of the Maverick Basin, Pecos River Canyon, Southwest Texas: Gulf Coast Association of Geological Societies Transactions, v. 52, p. 501-516.
- Kerans, Charles, Zahm, L., Wang, F., Wright, W., and Fu, Q., 2008, Sequence framework and facies architecture of a Cretaceous Carbonate Ramp: Late Albian of the Pecos River, West Texas: Field Trip Guidebook, Bureau of Economic Geology, The University of Texas at Austin.
- Lawton, T. F., Gonzalez-leon, C. M., Lucas, S. G., and Scott, R. W., 2003, Stratigraphy and sedimentology of the upper Aptian-Albian Mural Limestone (Bisbee Group) in northern Sonora, Mexico: Cretaceous Research, v. 25, p. 43-60.
- Lehmann, C., Osleger, D. A., and Montanez, I., 2000, Sequence stratigraphy of Lower Cretaceous (Barremian-Albian) carbonate platforms of northeastern Mexico: Regional and global correlations: Journal of Sedimentary Research, v. 70, no. 2, p. 373-391.
- Loucks, R. G., 1977, Porosity development and distribution in shoal-water carbonate complexes: subsurface Pearsall Formation (Lower Cretaceous), South Texas, in Bebout, D. G., and Loucks, R. G., eds., Cretaceous carbonates of Texas and Mexico: applications to subsurface exploration: Texas Bureau of Economic Geology Report of Investigation 89, Austin, p. 169-181.
- Loucks R. G., and Kerans, Charles, 2003, Lower Cretaceous Glen Rose 'patch reef' reservoir in the Chittim Field, Maverick County, south Texas: Transactions - Gulf Coast Association of Geological Societies, v. 53, pp.490-503.
- Lozo, F. E., 1949, Stratigraphic relations of Fredericksburg limestones, North-Central Texas, in Guidebook, Seventeenth Annual Field Trip, Cretaceous of Austin, Texas Area: Shreveport Geol. Soc., p. 85-91.
- Mancini, E. M., and Puckett, 2005, Jurassic and Cretaceous transgressive-regressive (T-R) cycles, Northern Gulf of Mexico, USA: Stratigraphy, v. 2, no. 1, p. 31-48.
- Mitchum, R. M., and Van Wagoner, J. C., 1991, High-frequency sequences and their stacking patterns: sequence-stratigraphic evidence of high-frequency eustatic cycles: Sedimentary Geology, v. 70, no. 2-4, p. 131-147, 153-160.
- Osleger, D., 1991, Subtidal carbonate cycles: Implications for allocyclic vs. autocyclic controls, Geology, v. 19, no. 19, p. 917-920.
- Perkins, B. F., 1974, Paleoecology of a rudist reef complex in the Comanche Cretaceous Glen Rose Limestone of central Texas: Geoscience and Man, v. 8, p. 131-174.

- Phelps, R. M., Kerans, Charles, Scott, S. Z., Janson, Xavier, and Bellian, J. A., 2009  
Three-dimensional modeling and sequence stratigraphy of a carbonate ramp-to-shelf transition, Permian Upper San Andres Formation: *Sedimentology*, v. 55, no. 6, p. 1777-1813.
- Pomar, L., Gili, E., Obrador, A., and Ward, W. C., 2005, Facies architecture and high-resolution sequence stratigraphy of an Upper Cretaceous platform margin succession, southern central Pyrenees, Spain: *Sedimentary Geology*, V., 175, p. 339-365.
- Purdy, E. G., Gischler, E., and Lomando, A. J., The Belize margin revisited. 2. Origin of Holocene antecedent topography, *International Journal of earth Science*, v. 92, p. 552-572.
- Ransome, F. L., 1904, The geology and ore deposits of the Bisbee Quadrangle, Arizona: U.S. Geol. Survey, Professional Paper #21, 167 p.
- Read, J. F., 1995, Overview of carbonate platform sequences, cycle stratigraphy and reservoirs in greenhouse and icehouse worlds, in Read, J. F., Kerans, C., Weber, L. J., Sarg, J. F., and Wright F. W., Milankovitch sea level changes, cycles and reservoirs on carbonate platforms in greenhouse and icehouse worlds: SEPM Short Course Notes No. 35, p. 1-102.
- Rigby, J. K., and Scott, R. W., Sponges from the Lower Cretaceous Mural Limestone in Arizona and northern Mexico: *Journal of Paleontology*, v. 55, no. 3, p. 552-562.
- Rose, P. R., 1972, Edwards Group, surface and subsurface, central Texas: The University of Texas at Austin, Bureau of Economic Geology Report of Investigations No. 52, 48 p.
- Ross, D. J., and Skelton, P. W., 1993, Rudist formations of the Cretaceous: a palaeoecological, sedimentological and stratigraphical review, in Wright, V. P. (Ed.), *Sedimentology Review*, Cambridge, Blackwell Scientific Publications, 152 p.
- Schmid, D. U., and Leinfelder, R. R., 1996, Jurassic Lithocodium aggregation Troglotella incrustans foraminiferal consortium: *Paleontology*, v. 39, no. 1, p. 21-52.
- Scoffin, T. P., 1993, The geological effects of hurricanes on coral reefs and the interpretation of storm deposits, *Coral Reefs*, v. 12, p. 203-222.
- Scott, R. J., 2004, The Maverick Basin: New Technology-New Success: Gulf Coast Association of Geological Societies Transactions, v. 54, p. 603-620

- Scott, R. W., 1979, Depositional model of early Cretaceous coral-algal-rudist reefs, Arizona: *The American Association of Petroleum Geologists Bulletin*, v. 63, no. 7, pp. 1108-1127.
- Scott, R. W., 1987, Stratigraphy and correlation of the Cretaceous Mural Limestone, Arizona and Sonora. In: Dickinson, W.R., Klute, M.F. (Eds.), *Mesozoic Rocks of southern Arizona and adjacent areas: Arizona Geological Society, Digest 18*, pp. 335-363.
- Scott, R. W., 1995, Global environmental controls on Cretaceous reefal ecosystems: *Palaeogeography, Palaeoclimatology, Palaeoecology*, v. 119, p. 187-199.
- Scott, R. W., and Kidson, 1977, Lower Cretaceous depositional systems, West Texas, in Bebout, D. G., and Loucks, R. G., eds., *Cretaceous carbonates of Texas and Mexico: applications to subsurface exploration: Texas Bureau of Economic Geology Report of Investigation 89*, Austin, p. 169-181.
- Scott, R. W., and Warzeski, E. R., 1993, An Aptian-Albian shelf ramp, Arizona and Sonora: *The American Association of Petroleum Geologists Memoir*, v. 56, pp. 71-79.
- Scott, R. W., Fernandez-Mendiola, P. A., Gili, E., and Simo, A., 1990, Persistence of coral –rudist reefs into the Late Cretaceous, *Palaios*, v. 5, p. 98-110.
- Scott, R. W., Molineaux, A., Loser, H., and Mancini, E. A., 2007, Lower Albian sequence stratigraphy and coral buildups: Glen Rose Formation, Texas, U.S.A., in Scott, R. W. (Ed.), *Cretaceous rudists and carbonate platforms, environmental feedback*, SEPM Special Publication No. 87, p. 181-191.
- Shinn, E. A., 1969, Submarine lithification of Holocene carbonate sediments in the Persian Gulf: *Journal of Sedimentology*, v. 12, issue 1-2, p. 109-144.
- Shinn, E. A., 1975, Coral Reef recovery in Florida and the Persian Gulf: *Environmental Geology*, v. 1, p. 241-254.
- Stearn, C. W., and Scoffin, T. P., 1977, Carbonate budget of a fringing reef, Barbados: *Proc. Third International Coral Reef Symposium*, v. 2, p. 471-477.
- Stoyanow, A., 1949, Lower Cretaceous stratigraphy in southeastern Arizona: *Geological Society of American Memoir No. 38*, 169 p.
- Tomas, S., Loser, H., and Salas, R., 2008, Low-light and nutrient-rich coral assemblages in an Upper Aptian carbonate platform of the southern Maestrat Basin (Iberian Chain, eastern Spain): *Cretaceous Research*, v. 29, p. 509-534.

- Vail, P. R., Mitchum Jr., R. M., Todd, R. G., Widmier, J. M, Thompson III, S., Sangree, J. B, and Bubb, J. N., 1977, Seismic stratigraphy and global changes of seal level, in Payton, C. E. (Ed.), Seismic stratigraphy-applications to hydrocarbon exploration: American Association of Petroleum Geologists Memoir 26, p. 49-205.
- Vilas, L., Masse, J. P., and Arias, C., 1995, Orbitolina episodes in carbonate platform evolution: the early Aptian model from SE Spain: *Palaeo*, v. 119, p. 35-45.
- Warzeski, E. R., 1983, Facies patterns and diagenesis of a lower Cretaceous carbonate shelf: northeastern Sonora and southeastern Arizona: PhD dissertation, State University of New York, Binghamton, 401 p.
- Warzeski, E. R., 1987, Revised stratigraphy of the Mural Limestone: A lower Cretaceous carbonate shelf in Arizona and Sonora, in: Dickinson, W.R., Klute, M.F. (Eds.), Mesozoic Rocks of southern Arizona and adjacent areas: Arizona Geological Society, Digest 18, pp. 335-363.
- Wilson, J. L., 1975, Carbonate Facies in Geologic History, New York, Springer-Verlag, 471 p.
- Wilson, J. L, and Jones, C., 1983, Chapter 7: Middle shelf environment, in Scholle, P. A., Bebout, D. G., and Moore, C. H., 1983, Carbonate Depositional Environments: AAPG Memoir No. 33, p. 298-343.

## **Vita**

Rachel E. Aisner came to the University of Texas at Austin in August 2008 after working for five years as a geologic technician with a small independent oil company in Midland, Texas. She holds a B.A. in mathematics from Smith College and became interested in the geologic sciences after volunteering with WTGS, PBS-SEPM and SWS-AAPG. Through classes, workshops and meetings she developed an interest in invertebrate paleontology and carbonate sequence stratigraphy. She subsequently pursued a M.S. at the Jackson School of Geosciences under the supervision of Dr. Charles Kerans.

E-mail: [raisner@gmail.com](mailto:raisner@gmail.com)

This thesis was typed by the author.